STIC-ILL

From: Arthur, Lisa
Sent: Wednesday, November 17, 1999 9:00 AM
To: STIC-ILL
Subject: REFERENCES FOR 08/647,311

Please provide a copy of the following:

1. bohlander et al. GENOMICS (1992) 13: 1322-1324.
2. kAMB ET AL. NATURE GENETICS 8:22-26 (september 1994)
3. Nobori et al. CANCER RES. 1991 51: 3193-3197.
4. Nobori et al. CANCER RES. 1993 53: 1098-1101
5. Nobori et al. NATURE 1994 368:753-756.
6. Porterfield et al. SOMATIC CELL AND MOLECULAR GENETICS 20(5): 391-400 (1994).
7. Cheng et al. CANCER RES. 54:I 5547-5551 (NOVEMBER 1994).
8. dREYLING ET AL. CANCER RES (March 1995) 55: 984-988
9. Olopade et al. PNAS (1995) 92: 6489-6493.

Thanks

[CANCER RESEARCH 54, 5547–5551, November 1, 1994]

C5

Advances in Brief

p16 Alterations and Deletion Mapping of 9p21–p22 in Malignant Mesothelioma[1]

Jin Quan Cheng, Suresh C. Jhanwar, Walter M. Klein, Daphne W. Bell, Wen-Ching Lee, Deborah A. Altomare, Tsutomu Nobori, Olufunmilayo I. Olopade, Alan J. Buckler, and Joseph R. Testa[2]

Department of Medical Oncology, Fox Chase Cancer Center, Philadelphia, Pennsylvania 19111 [J. Q. C., W. M. K., D. W. B., W-C. L., D. A. A., J. R. T.]; Department of Pathology, Memorial Sloan-Kettering Cancer Center, New York, New York 10021 [S. C. J.]; Department of Medicine, University of California, San Diego, La Jolla, California 92093 [T. N.]; Department of Medicine, University of Chicago, Chicago, Illinois 60637 [O. I. O.]; and Molecular and Neurological Unit, Massachusetts General Hospital, Charlestown, Massachusetts 02129 [A. J. B.]

Abstract

To determine whether *p16* is altered in human malignant mesothelioma (MM), molecular analysis of multiple 9p loci was performed on 40 cell lines and 23 primary tumors from 42 MM patients. We identified homozygous deletions of *p16* in 34 (85%) cell lines and a point mutation in 1 line. Down-regulation of *p16* was observed in 4 of the remaining cell lines, 1 of which displayed a DNA rearrangement of *p16*. Homozygous deletions of *p16* were identified in 5 of 23 (22%) primary tumors; no mutations or rearrangements were found in these specimens. Four cell lines displayed a single homozygous deletion proximal to or distal to *p16*; 4 others had 2 nonoverlapping deletions, one involving *p16* and the other involving a region proximal to this locus. These data indicate that alterations of *p16* are a common occurrence in MM cell lines and, to a lesser extent, in primary tumors. Furthermore, deletions of 9p21–p22 outside of the *p16* locus may reflect the involvement of other putative tumor suppressor genes that could also contribute to the pathogenesis of some MMs.

Introduction

In contrast to oncogenes, TSGs[3] function as negative regulators of cell growth. Accumulating evidence indicates that alterations of TSGs represent predominant pathogenetic events in a number of human malignancies (1). Thus far, more than a dozen TSGs have been mapped and/or cloned through the study of cancer families and tumors. For example, linkage analysis of melanoma families initially pointed to chromosome region 9p13–p22 as the site of a familial melanoma gene(s) (2). Other studies have demonstrated that homozygous deletions of chromosome 9p21–p22 are common in leukemia, melanoma, glioma, lung cancer, MM, head and neck tumors, and bladder carcinomas, suggesting that a critical TSG(s) resides in this region (3–9).

Recently, a gene (*p16/MTS1/CDK4* inhibitor), which was originally cloned using the two-hybrid system in a search for proteins that interact with *CDK4* (10), emerged as a candidate 9p21–p22 TSG when it was found to be homozygously deleted at high frequency in cell lines from many different types of cancer (11, 12). In addition, mutations of *p16* have been observed in some melanoma cell lines and primary esophageal squamous cell carcinomas (11–13).

Functionally, the p16 protein product can bind to and inhibit CDK4, one of several CDKs with the activity that drives cells through the cell cycle and into cell division (10). It is known that all of the CDKs must be activated by cyclins, and several lines of evidence indicate that one of the cyclin partners of CDK4, cyclin D1, can behave as an oncogene (14). These findings suggest that normal control of cell division requires a regulatory balance between cyclin activators of CDKs and inhibitory proteins such as p16, p21, and p27. Alterations leading to overactivity of the CDKs, whether excessive cyclin production or loss of inhibition by proteins such as p16, release cells from the normal constraints of cell division. Such uncontrolled division is characteristic of cancer cells.

Human MMs frequently display multiple chromosomal changes, particularly losses or structural rearrangements of 1p, 3p, 6q, 9p, and 22 (15–17). We demonstrated previously that homozygous deletions of 9p21–p22 are a common occurrence in MM, and we defined the location of a TSG(s) to a region between *IFNA* and *D9S171* (5), a region of approximately 2–3 megabases. In this paper, we report various *p16* alterations, including deletions, rearrangement, mutation, and down-regulation, in 39 of 40 MM cell lines. In addition, homozygous deletions were detected in primary tumor specimens from 5 of 23 MM patients. Among 21 matched tumors/cell line pairs, homozygous deletions were identified in all 21 cell lines as compared to 5 tumor specimens. In some cell lines, we have found additional homozygous deletions outside the *p16* locus, which could reflect extensive rearrangement in this region or the possible involvement of other putative TSGs.

Materials and Methods

Tumor Specimens and Cell Lines. Criteria for the diagnosis of MM were in accordance with established guidelines (18). Approximately 60% of all patients included in this study had a known history of exposure to asbestos (17).[4] All 23 primary MM tumor specimens were obtained from patients who underwent surgery at Memorial Sloan-Kettering Cancer Center, and each sample contained at least 70% tumor cells as was confirmed by an experienced pathologist. Thirty-nine cell lines were established from surgically explanted primary MMs obtained at Memorial Sloan-Kettering Cancer Center or Fox Chase Cancer Center. The methods for establishing these cell lines have been described (19). The remaining cell line, HMESO-1, established by Reale *et al.* (20), was obtained from Dr. Steven M. Keller.

Southern and Northern Analyses. Genomic DNAs from 40 tumor cell lines and 23 frozen tissues from 42 MM patients were purified by proteinase K digestion, extracted with phenol/chloroform, and precipitated by ethanol. Tumor tissues/tumor cell line pairs were available in 21 cases. Digested DNA, after careful spectrophotometric measurement of DNA concentration, was fractionated by 0.8% agarose gel electrophoresis and transferred to nylon membranes for Southern blot analysis (Gene Screen Plus; DuPont New Eng-

Received 8/16/94; accepted 9/29/94.

The costs of publication of this article were defrayed in part by the payment of page charges. This article must therefore be hereby marked *advertisement* in accordance with 18 U.S.C. Section 1734 solely to indicate this fact.

[1] Supported in part by National Cancer Institute Grants CA-45745 and CA-06927, by a gift from the International Association of Heat and Frost Insulators & Asbestos Workers Local No. 14, and by an appropriation from the Commonwealth of Pennsylvania. J. Q. C. and W. C. L. are, respectively, a Special Fellow and a Fellow of the Leukemia Society of America.

[2] To whom requests for reprints should be addressed, at Fox Chase Cancer Center, Department of Medical Oncology, 7701 Burholme Avenue, Philadelphia, PA 19111.

[3] The abbreviations used are: TSGs, tumor suppressor genes; MM, malignant mesothelioma; CDK, cyclin-dependent kinase; PCR, polymerase chain reaction; *IFNA*, interferon α gene cluster locus; *D9S171* and *MDS59*, loci of two arbitrary 9p21–p22 DNA segments; *GAPDH*, glyceraldehyde-3-phosphate dehydrogenase gene; *STS*, sequence tagged site; *MTAP*, methylthioadenosinephospborylase locus; cDNA, complementary DNA; YAC, yeast artificial chromosomes; SSCP, single-strand conformational polymorphism; *IFNA1*, α_1-interferon.

[4] Jhanwar, S., Chen, Q., Cheng, J. Q., Lu, Y. Y., Zakowski, M., and Testa, J. R., manuscript in preparation.

land Nuclear, Boston, MA). For Northern blot analysis, 20 μg of total RNA were separated on a 1% agarose/2.2 M formaldehyde gel and blotted onto Magna NT membrane filters (Micron Separations). The membranes were hybridized overnight with ^{32}P-labeled probes and washed at high stringency. Gene dosage analysis of autoradiograms was performed as described previously (5).

Reverse Transcriptase-Polymerase Chain Reaction. Total cellular RNA was obtained by a one-step guanidinium isothiocyanate-phenol-chloroform extraction procedure (21). For cDNA synthesis, 3 μg of total RNA were denatured by heating at 70°C for 10 min in 12 μl of diethyl pyrocarbonate-treated water, in the presence of 20 pmol of oligo(dT)$_{16}$ primer (22). After chilling on ice for 2 min, single-stranded cDNA was synthesized by incubating the denatured RNA in a 20-μl solution containing 200 units of SuperScript (GIBCO BRL), 1 × reverse transcriptase buffer [50 mM KCl, 20 mM Tris-HCl (pH 8.4), and 2.5 mM $MgCl_2$], 10 mM dithiothreitol, and 0.4 mM deoxynucleotide triphosphate for 1 h at 42°C. The reaction was terminated by heating at 95°C for 2 min and followed by quenching on ice. Two μl of the resulting single-stranded cDNA were used to separately amplify *p16* and *GAPDH*, which was used as a loading control, by PCR with a MiniCycler (MJ Research, Boston, MA). The following conditions were used for amplification of *p16*: 94°C for 1 min, 56°C for 1 min, and 72°C for 1.5 min for 35 cycles; after the final cycle, the reaction was maintained at 72°C for 10 min. For *GAPDH*, the same PCR conditions were used except that the annealing temperature was 55°C. The resulting PCR products were electrophoresed on a 1.8% agarose gel. The primers used for *p16* were: sense 5′-ATGGAGCCTTCGGCTGACT-3′ and antisense 5′-GAGCCTCTCTGGTTCTTTCA-3′.

DNA Probes and Deletion Analysis. The DNA probe used for Southern hybridizations was a *p16* cDNA clone (kindly provided by Dr. David Beach). Primer information for markers *IFNA1* and *D9S171* were obtained from the human Genome Data Base. *MDS59* was originally isolated from a 9p21–p22 region-specific microdissection library (23). The markers *4C6S1* (*STS1*) and *17H8S1* (*STS2*) were derived from YACs containing *D9S171*, whereas *20E4* (*STS3*) and *6C2B1* (*STS4*) were obtained from YACs containing *IFNA1*.

PCR analysis was performed for each of the 3 exons of the *p16* gene and for other chromosome 9p21–p22 loci. Purified DNA (50–100 ng) were amplified in a 25-μl solution containing 0.5 μM concentrations of each primer, 100 μM of each deoxynucleotide triphosphate, and 1.0 unit of Taq polymerase (Perkin-Elmer, Branchburg, NJ). In addition, 5% dimethyl sulfoxide was used in the amplification of each *p16* exon (11). PCR was performed in an MJ Research PTC-100 Programmable Thermal Controller with 0.1 μg of DNA in a total volume of 25 μl. Thirty-five cycles of amplification were carried out with TaqI DNA polymerase (Cetus, Norwalk, CT) and consisted of 1 min at 94°C, 1 min at 58°C, and 1 min at 72°C. The PCR products were analyzed by electrophoresis in 2.0% agarose gels. Primer sequences of *p16* were: exon 1, 5′-GGAGGAAGAAAGAGGAGGG-3′ and 5′-ACTTCGTCCTCCAGAGTCG-3′; exon 2, 5′-TCTGACCATTCTGTTCTCTC-3′ and 5′-CTCAGCTTTGGAAGCTCTCA-3′; and exon 3, 5′-GGATGTTCCACACATCTTTG-3′ and 5′-ATGAAAACTACGAAAGCGGG-3′.

SSCP Analysis. SSCP analysis was carried out on DNA from 23 primary tumor specimens. PCR was carried out as described above with the exception of adding 0.1 μl [α-^{32}P]dCTP to the reaction for SSCP analysis. Following amplification, PCR products were diluted 1:10 with 0.1% SDS/10 mM EDTA. A 3-μl sample of the diluted reaction was then mixed with 3 μl of gel-loading dye (United States Biochemical Corp.). Samples were heat denatured at 94°C for 2 min and chilled on ice, and 3 μl were loaded onto a 6% polyacrylamide gel containing 10% glycerol. Gels were electrophoresed at 5 W of constant power for 18 h at room temperature, using 0.5 × Tris-borate-EDTA buffer. After electrophoresis, the gels were dried and subjected to autoradiography.

Sequence Analysis. PCR products of each *p16* exon were cloned into the pGEM-T vector (Promega, Madison, WI). The inserts were sequenced according to the dideoxy chain termination method using double-stranded recombinant plasmids as a template and T7 and SP6 as primer sites. Reaction products were electrophoresed on 6% polyacrylamide/8 M urea/0.1 M Tris-borate (pH 8.0)/2 mM EDTA gels. After electrophoresis, the gels were transferred to blotting paper, dried, and subjected to autoradiography. For each sample, at least 2 clones were sequenced.

Results

Homozygous Deletions of *p16* and Other Loci in 9p21–22. Homozygous deletions were identified by conventional PCR analysis in the 40 MM cell lines and by both Southern blotting and PCR analyses in the 23 primary tumor specimens. Homozygous deletions of *p16* were identified in 34 (85%) cell lines. The deletions could be categorized as those involving the entire gene, only exon 1, and both exons 2 and 3 (Fig. 1). Complete deletion of *p16* occurred in 30 cell lines (75%), of which 6 showed deletions of *p16* but not of any other 9p21–p22 locus examined. Two cell lines, HMESO-1 and M126, had deletions of exon 1 but retained exons 2 and 3. Two other lines, M155 and M363, had deletions of exons 2 and 3 but not of exon 1. Among 21 cell lines/primary tumor pairs, homozygous deletions of *p16* were detected in all 21 cell lines but in only 5 primary tumor specimens. No differences were observed between the 5 patients with and the 18 without *p16* deletions with regard to clinical features or history of asbestos exposure.

The frequencies of homozygous losses of the remaining markers surrounding *p16* in the 40 MM cell lines are shown in Fig. 2. Our deletion mapping analysis and additional mapping data from YACs suggest that the most likely physical order of these markers is 9pter-*IFNA1-STS4-STS3-p16-MDS59-STS2-STS1-D9S171*-9cen.

Interestingly, one cell line (M263) without a *p16* deletion sustained a homozygous deletion of *STS2* but retained all other 9p21–p22 loci tested. Moreover, four lines (HMESO-1, M363, M140, and M160) having a *p16* deletion also had a second, nonoverlapping region of homozygous loss involving a 200–400-kilobase region between *STS2* and *STS1* or *D9S171*; this region is ~1 megabase proximal to *p16*. Of significance, an intervening marker, *MDS59* (~600 kilobases proximal to *p16*, and distal to *STS2*) was retained in 3 of these 5 cases. In the remaining 2 cell lines, *STS2* was present, whereas *STS1* and *D9S171* were deleted, respectively (Fig. 2).

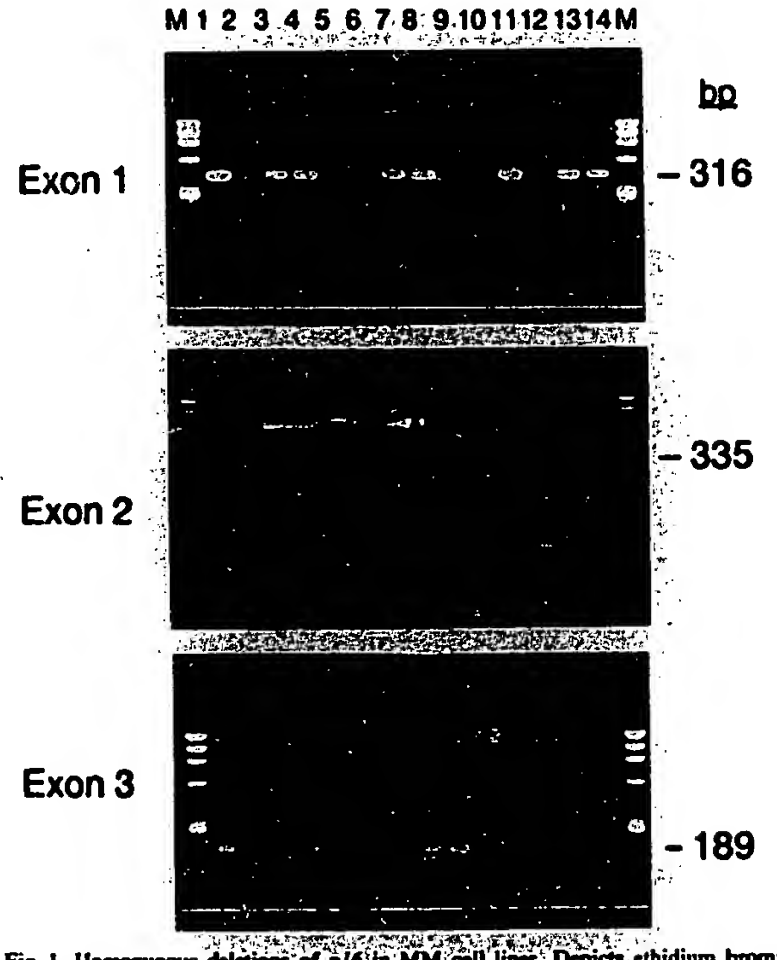

Fig. 1. Homozygous deletions of *p16* in MM cell lines. Depicts ethidium bromide-stained gels of representative PCR products amplified using primer sets for each of the three *p16* exons (identical lines are shown in each gel). Note deletions of only exon 1 in DNA shown in *Lanes 9* and *10* (HMESO-1, M126), whereas deletions were confined to exons 2 and 3 in DNA shown in *Lanes 13* and *14* (M155, M363). *bp*, base pairs.

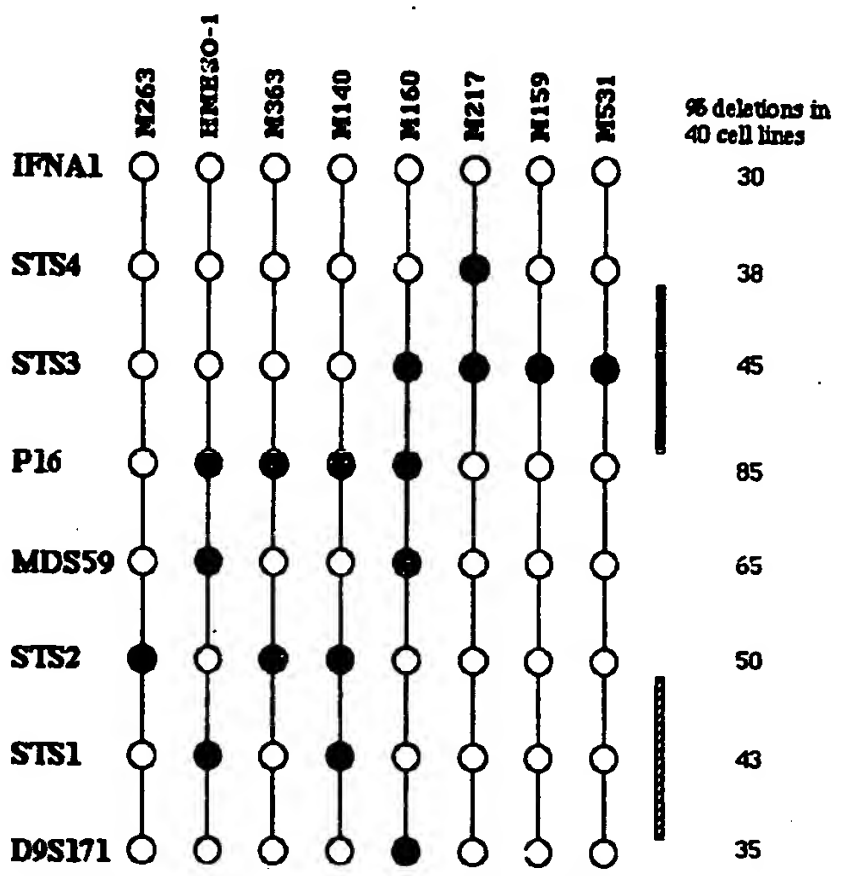

Fig. 2. Homozygous deletions observed in 8 MM cell lines depicting 2 separate regions of homozygous loss, one proximal to and the other distal to *p16*. Five cell lines shown on the left exhibit homozygous losses within a 200–400-kilobase region between *STS2* and *STS1* or *D9S171*; this region is ~1 megabase proximal to *p16*. The 3 cell lines shown on the right display deletions of *STS3* or of *STS3* and *STS4*, ~400 kilobases distal to *p16*.

Furthermore, 2 cell lines (M159 and M531) showed a homozygous loss of only *STS3*, whereas the remaining 9p21–p22 loci tested were retained. Another cell line (M217) had homozygous deletions of both *STS4* and *STS3*, but all other markers were retained (Fig. 2). Thus, the deletions observed in these 3 cell lines could overlap within a small region between *STS3* and *STS4*, approximately 400 kilobases distal to *p16*. Two other cell lines (M250, M144) retained *STS3*, whereas loci distal to and proximal to this locus were deleted (data not shown).

Down-regulation and Rearrangement of *p16*. RNA was available from 4 of the 6 cell lines that did not exhibit homozygous deletions of part or all of *p16*. The mRNA expression was examined by Northern blot and reverse transcriptase-PCR analyses using cDNA primers for both *GAPDH* and the open-reading frame of *p16*. *GAPDH* was uniformly expressed in all lanes, whereas *p16* was detected only in normal mesothelial cells (Fig. 3*A*). Transfer of the gel to a filter and hybridization with the *p16* cDNA probe revealed marked down-regulation of *p16* (Fig. 3*B*) in the 4 MM cell lines as compared to normal mesothelial cells. The same result was obtained by Northern blot analysis (data not shown). Southern blot analysis revealed a *p16* rearrangement in 1 (M222) of these 4 MM cell lines which did not display deletions of any 9p21–p22 marker (data not shown). Two (M222, M224) of these 4 lines retained every 9p locus tested, whereas the remaining 2 lines (M263, M217) had a homozygous loss of only *STS2* or *STS4* and *STS3*, respectively.

Mutation of *p16*. Of the remaining 2 cell lines without a *p16* deletion, one (M159) showed a mutation in the second nucleotide of the intron adjacent to the donor splicing site of exon 2. The mutation involved an A→G transition (Fig. 4). Among the 18 primary tumor specimens without homozygous deletions of *p16*, no mutations or rearrangements were found by SSCP and Southern blotting analyses, respectively.

In addition, 5 of the 6 MM cell lines without a *p16* deletion had a C-G, rather than the G-C sequence reported previously (10) at nucleotide positions 177–178, causing a change in 2 amino acids, namely glutamine to asparagine and leucine to valine, respectively. Matched DNA from normal WBC was available in one case and displayed the same sequence found in the corresponding tumor cell line. Thus, this sequencing difference is likely to represent a polymorphism; it was not scored as a mutation (24).

Discussion

MM is characterized by a long latency period following the onset of exposure to asbestos and by a short survival period after diagnosis (25). The length of the latent period suggests that multiple genetic alterations may be required for tumorigenic conversion of a mesothelial cell (26). *TP53* and *KRAS* mutations have been reported in a low percentage of MM cell lines (27, 28). Our previous studies demonstrated that losses of 1p, 3p, 9p, and 22 are very common in MM (5, 17, 29). In this report, we describe *p16* alterations in human MMs, including homozygous deletions, point mutation, structural rearrangement, and down-regulation. Collectively, 39 of 40 (98%) cell lines displayed alterations of *p16*. Homozygous deletions represent the predominant genetic alteration of *p16* (85% of cell lines and 22% of primary tumor specimens). These findings suggest that *p16* abnormalities could be important in the development of some MMs. In addition, alterations of *p16* have been found in cell lines from a variety of other tumor types (11, 12); in a recent report, *p16* mutations were observed in ~50% of primary esophageal squamous cell carcinomas (13).

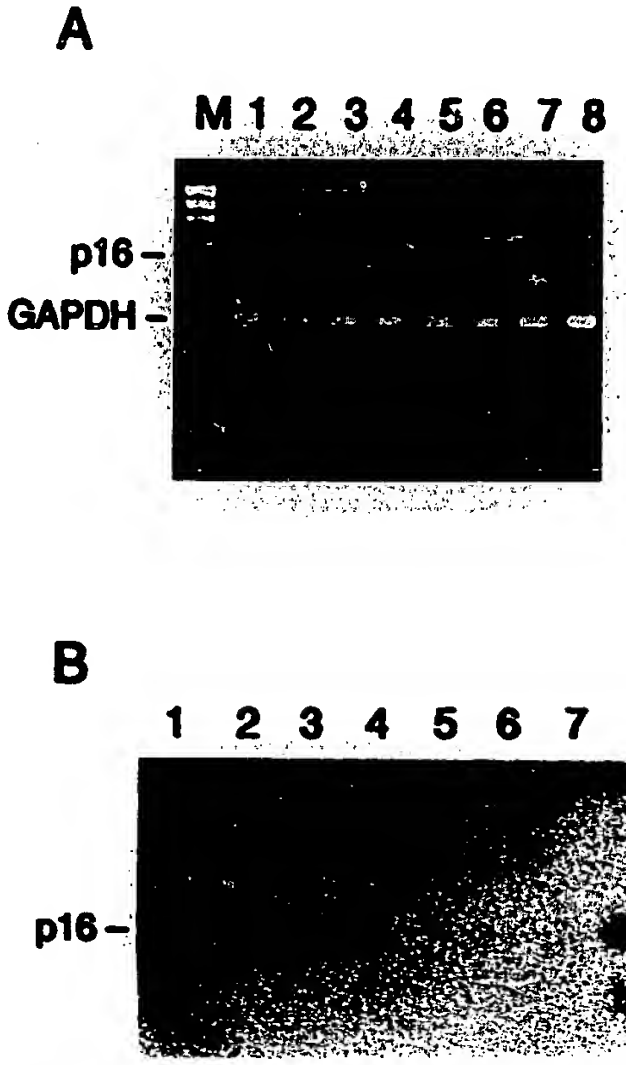

Fig. 3. (*A*) Reverse transcriptase-PCR analysis of *p16* in 7 MM cell lines (*Lanes 2-8*), including 4 cell lines (*Lanes 2-4, 8*) that did not exhibit homozygous deletions of *p16*. *Lane 1*, normal mesothelial cell line; *Lane 2*, M222; *Lane 3*, M224; *Lane 4*, M217; *Lane 5*, HMESO-1; *Lane 6*, M140; *Lane 7*, M237; *Lane 8*, M263. Ethidium bromide-stained gel shows uniform levels of expression of *GAPDH*, used as a control, whereas *p16* was detected only in normal mesothelial cells. In *B*, after the gel was blotted, the PCR products were hybridized with a radiolabeled *p16* cDNA probe. Note complete absence of *p16* expression in 3 MM cell lines having homozygous deletions of *p16* and down-regulation in 4 MM lines without deletions of the *p16* locus.

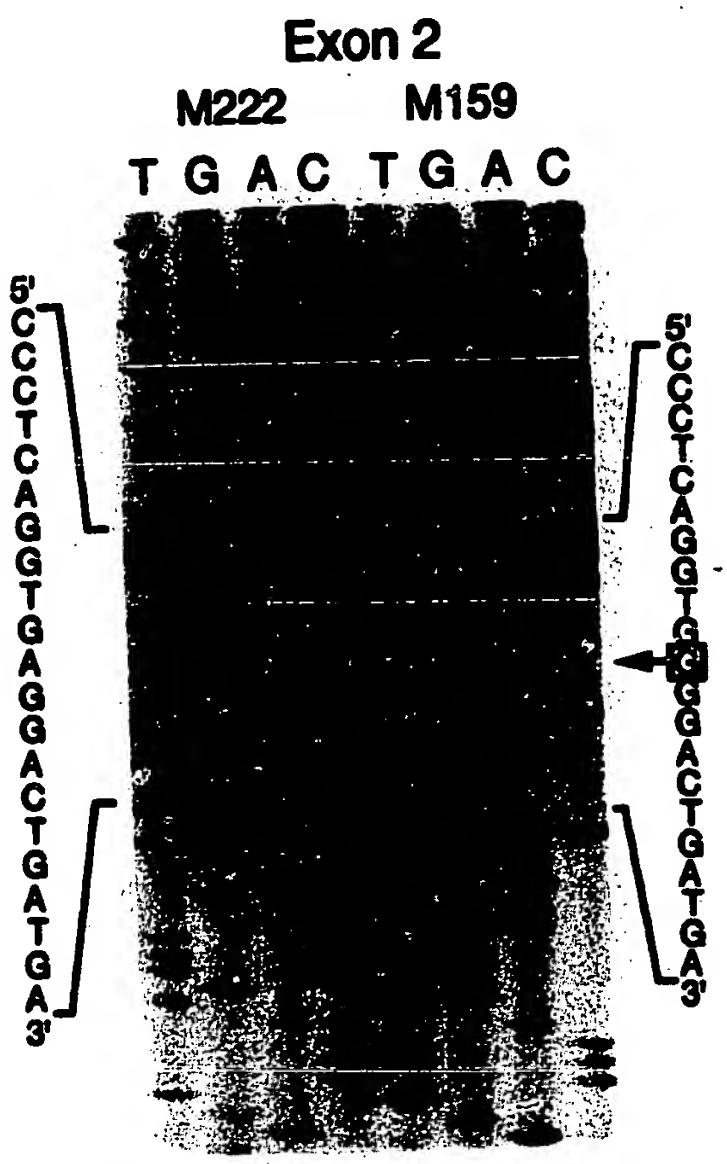

Fig. 4. Identification of a point mutation of *p16* in MM cell line M159. As shown within the *box*, MM cell line M159, compared to M222, displays an A→G transition in the second nucleotide of the intron adjacent to the donor-slicing site of the second exon.

A comparison of data from our MM cell lines with that of corresponding fresh tumors indicates that the frequency of *p16* alterations in cell lines is much higher than in primary tumor specimens. Among 21 cell lines/tumor pairs, homozygous deletions of *p16* were found in all 21 cell lines, but in only 5 tumors, suggesting that the high incidence of *p16* alterations in MM cell lines may reflect an *in vitro* phenomenon (24, 30, 31). That is, deletions of *p16* may provide a selective advantage for *in vitro* growth. On the other hand, primary MMs often contain a significant proportion of normal cells which could present difficulties in detecting homozygous deletions of *p16* in this tumor type. However, to exclude normal tissue contamination, other 9p probes such as *D9S3* and *D9S126* were used to rehybridize the Southern blots of DNAs from the 23 primary tumors originally probed with *p16*.

Presently, the role of *p16* in human cancer is controversial. For example, a recent study showed mutations of *p16* in only 2 of 75 primary tumors from a variety of organ types, each of which was previously shown to have loss of heterozygosity involving 9p21–p22 (31). However, as our data demonstrate, mutation within the noncoding region, rearrangement, and down-regulation of *p16* could play a role in the inactivation of this gene in some cases. In addition, mutations within the promoter region of *p16* may occur, although this type of mutation has not been described as a predominant mechanism of gene inactivation in human cancer (31).

Inactivation of TSGs in cancers can result from alterations in the properties of the protein product (*i.e.*, qualitative changes) or in a decrease or complete loss of gene products (quantitative changes). Qualitative changes are due to mutations or structural rearrangements within the coding region, whereas quantitative alterations can result from down-regulation or homozygous deletion. Most TSGs involved in human cancer are inactivated by mutation (1, 32). Alteration of *p16*, on the other hand, frequently involves the complete loss of the gene or a marked decrease of the protein product (11, 12).

Homozygous deletion of chromosome 9p21–p22 is a common event in a number of different types of cancer (3–9). Deletion mapping of melanoma and other tumors has indicated that there may be 2 or more TSGs residing within this region (33, 34). One report provided evidence suggesting that the minimally deleted region in melanoma resides between the markers *MTAP* and *D9S3*, whereas the critically deleted region in other malignancies such as leukemia, glioma, and lung cancer is located at a more distal site between *IFNA* and *MTAP* (34).

p16 was mapped between *IFNA* and *MTAP* (12). Physical mapping data suggest that the distance between *IFNA* and *D9S171* is at least 2 megabases with *p16* being located ~600 kilobases proximal to *IFNA1*. Among our 40 MM cell lines, 4 showed both a deletion of *p16* and a second, nonoverlapping, homozygous deletion within the region encompassed by *STS2* and *D9S171* (Fig. 2), ~1 megabase proximal to *p16*. Another cell line had a homozygous deletion of *STS2* and no other locus. Three other MM cell lines (M217, M159, and M531) without *p16* deletions displayed homozygous losses of *STS3* or of *STS4* and *STS3*, which are located ~400 kilobases distal to *p16* (Fig. 2). We have also characterized homozygous deletions of 9p in another 60 tumor cell lines from various organs. Three of these cell lines (one lung carcinoma, one leukemia, and one renal carcinoma) showed nonoverlapping deletions. In each case, *STS1* and *p16* were deleted, but the intervening markers *MDS59* and *STS2* were retained, consistent with the results observed in 5 of our MM cell lines (Fig. 2). These deletions outside the *p16* locus are enigmatic, and their interpretation awaits further investigation. One possibility is that in some cases the 9p21–p22 region may undergo extensive rearrangement (*e.g.*, an inversion followed by a deletion). Alternatively, these additional deleted regions could reflect the involvement of other putative TSGs within 9p21–p22 which could contribute to the pathogenesis of some MMs. We are currently generating a cosmid contig and attempting to isolate candidate genes from these regions.

Acknowledgments

We thank Dr. Alfred G. Knudson for valuable comments, Dr. Stefan K. Bohlander for *MDS59* primers, and Dr. Q. Chen for technical assistance.

References

1. Knudson, A. G. Antioncogenes and human cancer. Proc. Natl. Acad. Sci. USA, *90:* 10914–10921, 1993.
2. Cannon-Albright, L. A., Goldgar, D. E., Meyer, L. J., Lewis, C. M., Anderson, D. E., Fountain, J. W., Hegi, M. E., Wisman, R. W., Petty, E. M., Bale, A. E., Olopade, O. I., Diaz, M. O., Kwiatkowski, D. J., Piepkorn, M. W., Zone, J. J., and Skolnick, M. H. Assignment of a locus for familial melanoma, MLM, to chromosome 9p13–p22. Science (Washington DC), *258:* 1148–1152, 1992.
3. Diaz, M. O., Rubin, C. M., Harden, A., Ziemen, S., Larson, R., Le Beau, M. M., and Rowley, J. D. Deletions of interferon genes in acute lymphoblastic leukemia. N. Engl. J. Med., *322:* 77–82, 1990.
4. James, C. D., He, J., Carlbom, E., Nordenskjold, M., Cavenee, W., and Collins, V. P. Chromosome 9 deletion mapping reveals interferon α and interferon β-1 gene deletions in human glial tumors. Cancer Res., *51:* 1684–1688, 1991.
5. Cheng, J. Q., Jhanwar, S. C., Lu, Y. Y., and Testa, J. R. Homozygous deletions within chromosome region 9p21–p22 in human malignant mesotheliomas. Cancer Res., *53:* 4761–4764.1993.
6. Fountain, J. W., Karayiorgou, M., Ernstoff, M. S., Kirkwood, J. M., Vlock, D. R., Titus-Ernstoff, L., Bouchard, B., Vijayasaradhi, S., Houghton, A. N., Lahti, J., Kidd, V. J., Housman, D. E., and Dracopoli, N. C. Homozygous deletions within human chromosome band 9p21 in melanoma. Proc. Natl. Acad. Sci. USA, *89:* 10557–10561, 1992.
7. Olopade, O. I., Buchhagen, D. L., Malik, K., Sherman, J., Nobori, T., Bader, S., Nau, M. M., Gazdar, A. F., Minna, J. D., and Diaz, M. O. Homozygous loss of the interferon genes defines the critical region on 9p that is deleted in lung cancers. Cancer Res., *53:* 2410–2415, 1993.

8. van der Riet, P., Nawroz, H., Hruban, R. H., Corio, R., Tokino, K., Koch, W., and Sidransky, D. Frequent loss of chromosome 9p21–22 early in head and neck cancer progression. Cancer Res., *54:* 1156–1158, 1994.
9. Cairns, P., Shaw, M. E., and Knowles, M. A. Initiation of bladder cancer may involve deletion of a tumor suppressor gene on chromosome 9. Oncogene, *8:* 1083–1085, 1993.
10. Serrano, M., Hannon, G. J., and Beach, D. A new regulatory motif in cell-cycle control causing specific inhibition of cyclin D/CDK4. Nature (London), *366:* 704–707, 1993.
11. Kamb, A., Gruis, N. A., Weaver-Feldhaus, J., Liu, Q., Harshman, K., Tavtigian, S. V., Stockert, E., Day, R. S., III, Johnson, B. E., and Skolnick, M. H. A cell cycle regulator potentially involved in genesis of many tumor types. Science (Washington DC), *264:* 436–440, 1994.
12. Nobori, T., Miura, K., Wu, D. J., Lois, A., Takabayashi, K., and Carson, D. A. Deletions of the cyclin-dependent kinase-4 inhibitor gene in mutiple human cancers. Nature (Lond.), *238:* 753–756, 1994.
13. Mori, T., Miura, K., Aoki, T., Nishihira, T., Mori, S., and Nakamura, Y. Frequent somatic mutation of the *MTS1/CDK4I* (multiple tumor suppressor/cyclin-dependent kinase 4 inhibitor) gene in esophageal squamous cell carcinoma. Cancer Res., *54:* 3396–3397, 1994.
14. Jiang, W., Kahn, S. M., Zhou, P., Zhang, Y-J., Cacace, A. M., Infante, A. S., Doi, S., Santella, R. M., and Weinstein, I. B. Overexpression of cyclin D1 in rat fibroblasts causes abnormalities in growth control, cell cycle progression and gene expression. Oncogene, *8:* 3447–3457, 1993.
15. Tiainen, M., Tammilehto, L., Mattson, K., and Knuutila, S. Non-random chromosomal abnormalities in malignant pleural mesothelioma. Cancer Genet. Cytogenet., *33:* 251–274. 1988.
16. Hagemeijer, A., Versnel, M. A., Van Drunen, E., Moret, M., Bouts, M. J., van der Kwast, T. H., and Hoogsteden, H. C. Cytogenetic analysis of malignant mesothelioma. Cancer Genet. Cytogenet., *47:* 1–28, 1990.
17. Taguchi, T., Jhanwar, S. C., Siegfried, J. M., Keller, S. M., and Testa, J. R. Recurrent deletions of specific chromosomal sites in 1p, 3p, 6q, and 9p in human malignant mesothelioma. Cancer Res., *53:* 4349–4355. 1993.
18. Antman, K. H., Li, F. P., Osteen, R., and Sugarbaker, D. J. Mesothelioma. *In:* V. T. DeVita, S. Hellman, and S. Rosenberg (eds.), Update. Cancer Principles and Practice, Vol. 3, pp. 1–16. Philadelphia: J. P. Lippincott Co., 1989.
19. Rodriguez, E., Rao, P. H., Ladanyi, M., Altorki, N., Albino, A. P., Kelsen, D. P., Jhanwar, S. C., and Chaganti, R. S. K. 11p13–15 is a site of specific chromosome rearrangement in gastric and esophageal adenocarcinomas. Cancer Res., *50:* 6410–6416, 1990.
20. Reale, F. R., Griffin, T. W., Compton, J. M., Graham, S., Townes, P. L., and Bogden, A. Characterization of a human malignant mesothelioma cell line (H-MESO-1): A biphasic solid and ascitic tumor model. Cancer Res., *47:* 3199–3205, 1987.
21. Chomczynski, P., and Sacchi, N. Single-step method of RNA isolation by acid guanidinium thiocyanate-phenol-chloroform extraction. Anal. Biochem., *162:* 156–159, 1987.
22. Bianchi, A. B., Hara, T., Ramesh, V., Gao, J., Klein-Szanto, A. J. P., Morin, F., Menon A. G., Trofatter, J. A., Gusella, J. F., Seizinger, B. R., and Kley, N. Mutations in transcript isoforms of the neurofibromatosis 2 gene in multiple human tumour types. Nat. Genet., *6:* 185–192, 1994.
23. Stadler, W. M., Sherman, J., Bohlander, S. K., Roulston, D., Dreyling, M., Rukstalis, D., and Olopade, O. I. Homozygous deletions within chromosome bands 9p21–22 in bladder cancer. Cancer Res., *54:* 2060–2063, 1994.
24. Spruck, C. H., III, Gonzalez-Zulueta, M., Shibata, A., Simoneau, A. R., Lin, M-F., Gonzales, F., Tsai, Y. C., and Jones, P. A. *p16* gene in uncultured tumours. Nature (Lond.), *370:* 183–184, 1994.
25. Gross, P., and Braun, D. C. Asbestos, talc, inorganic fibers, man-made vitreous fibers, and organic fibers. *In:* Toxic and Biomedical Effects of Fibers, pp. 94–96. Park Ridge, NJ: Noyes, 1984.
26. Fearon, E. R., and Vogelstein, B. A genetic model for colorectal tumorigenesis. Cell, *61:* 758–767, 1990.
27. Cote, R. J., Jhanwar, S. C., Novick, S., and Pellicer, A. Genetic alterations of the *p53* gene are a feature of malignant mesothelioma. Cancer Res., *51:* 5410–5416, 1991.
28. Metcalf, R. A., Welsh, J. A., Bennett, W. P., Seddon, M. B., Lehman, T. A., Pelin, K., Linnainmaa, K., Tammilep, L., Mattson, K., Gerwin, B. I., and Harris, C. C. *p53* and Kirsten-*ras* mutation in human mesothelioma cell lines. Cancer Res., *52:* 2610–2615, 1992.
29. Lu, Y. Y., Jhanwar, S. C., Cheng, J. Q., and Testa, J. R. Deletion mapping of the short arm of chromosome 3 in human malignant mesothelioma. Genes Chromosomes Cancer, *9:* 76–80, 1994.
30. Marx, J. A challenge to *p16* gene as a major tumor suppressor. Science (Washington DC), *264:* 1846, 1994.
31. Cairns, P., Mao, L., Merlo, A., Lee, D. J., Schwab, D., Eby, Y., Tokino, K., van der Riet, P., Blaugrund, J. E., and Sidransky, D. Rates of *p16* (*MTS1*) mutations in primary tumors with 9p loss. Science (Washington DC), *265:* 415–416, 1994.
32. de Fromentel, C. C., and Soussi, T. TP53 tumor suppressor gene: a model for investigating human mutagenesis. Genes Chromosomes Cancer, *4:* 1–15, 1992.
33. Holland, E. A., Beaton, S. C., Edwards, B. G., Kefford, R. F., and Mann, G. J. Loss of heterozygosity and homozygous deletions on 9p21–22 in melanoma. Oncogene, *9:* 1361–1365, 1994.
34. Coleman, A., Fountain, J. W., Nobori, T., Olopade, O. I., Robertson, G., Housman, D. E., and Lugo, T. G. Distinct deletion of chromosome 9p associated with melanoma versus glioma, lung cancer, and leukemia. Cancer Res., *54:* 344–348, 1994.

[CANCER RESEARCH 55, 984–988, March 1, 1995]

Advances in Brief

Detection of *CDKN2* Deletions in Tumor Cell Lines and Primary Glioma by Interphase Fluorescence *in Situ* Hybridization[1]

M. H. Dreyling, S. K. Bohlander, M. O. Adeyanju, and O. I. Olopade[2]

Section of Hematology/Oncology, Department of Medicine, The University of Chicago, Chicago, Illinois 60637

Abstract

Deletions of chromosomal band 9p21 have been detected in various tumor types including melanoma, glioma, lung cancer, mesothelioma, and bladder cancer. Recently, the *CDKN2* gene (*p16^{INK4A}*, *MTS 1*, *CDK4I*) has been proposed as a candidate tumor suppressor gene because it is frequently deleted in cell lines derived from multiple tumor types. We performed fluorescence *in situ* hybridization (FISH) with interphase cells using yeast artificial chromosome clones and a cosmid contig of the *CDKN2* region. In 10 cell lines (4 glioma, 2 melanoma, 2 non-small cell lung cancer, 2 bladder cancer) with 9p alterations detected by molecular or cytogenetic analysis, interphase FISH with the *CDKN2* cosmid contig detected all 9p deletions previously identified by molecular analysis. Using this probe, FISH analysis of primary glioblastoma tumors revealed homozygous deletions of the *CDKN2* region in 6 of 9 tumors (67%) whereas a yeast artificial chromosome probe containing the interferon type I (*IFN*) gene cluster was deleted in only 4 cases (44%). Thus, it is likely that the *CDKN2* region is the target of 9p deletions in gliomas. Interphase FISH will play an important role in defining the clinical significance of 9p deletions in primary tumors because it is especially applicable to clinical samples which may be contaminated by normal cells.

Introduction

The malignant transformation of tumor cells is known to be driven by the accumulation of different genetic events including numerical and structural alterations of distinct chromosomal regions. Among the specific alterations associated with neoplasia, the loss of tumor suppressor genes has been recognized as an important phenomenon. Hemizygous and homozygous deletions of chromosomal band 9p21 have been detected in various tumor types including melanoma, glioma, lung cancer, mesothelioma, and bladder cancer (1). In primary glioma the *IFN*[3] gene cluster which is located telomeric to the tumor suppressor region was found to be deleted in up to 50% of the primary tumors (2–4). Recently, the *CDKN2* gene (*$I6^{INK4}$*) which encodes an inhibitor of the cyclin-dependent kinase 4 (CDK4), was found to be frequently involved in 9p deletions in tumor cell lines and has been proposed as a candidate tumor suppressor gene (1, 5, 6). In Southern blot analysis, 78% of our glioma cell lines and 45% of primary tumors showed homozygous deletions of *CDKN2*.[4] However, the frequency of point mutations of *CDKN2* in glioblastoma and other primary tumors is rather low (7–9). Therefore, it appears that the preferred mechanism of inactivation of *CDKN2* is by homozygous deletions. Interphase FISH is a well established technique for identifying genetic alterations in neoplasias on a single-cell level. This technique is especially suited to analyze clinical tumor samples which are "contaminated" with normal cells. In addition, loss of one allele can be readily determined. We performed interphase FISH analysis on 10 tumor-derived cell lines (4 glioma, 2 melanoma, 2 non-small cell lung cancer, 2 bladder cancer) with rearrangement of the short arm of chromosome 9 detected by molecular or cytogenetic analysis and 9 primary glioblastoma, to determine the accuracy of different probes in detecting 9p deletions in tumor cell lines and primary tumor tissue. To our knowledge, this is the first report showing the utility of interphase FISH to detect deletions of the *CDKN2* region in primary tumors.

Materials and Methods

Cell Lines. We used 10 cell lines (4 glioma, 2 melanoma, 2 non-small cell lung carcinoma, and 2 bladder cancer) that had been well characterized by conventional cytogenetic analysis. The cell lines were obtained from the American Type Culture Collection or from the investigators who had established them. Cytogenetic deletions of the short arm of chromosome 9 were detected in 4 of 10 cell lines. The cell lines as well as phytohemagglutinin-stimulated normal peripheral blood cells were harvested using standard cell culture techniques. Metaphase chromosomes were prepared as described previously (11).

Patient Materials. Tumor specimens obtained from 9 patients undergoing biopsy or resection of brain tumors were frozen in liquid nitrogen and stored at −70°C. The tumors were graded as glioblastoma multiforme according to the WHO classification system. Touch preparations were made by touching a freshly cut and thawed tumor surface on a slide. The slides were fixed in methanol:glacial acetic acid (3:1), treated with 5 μg/ml proteinase K (Boehringer Mannheim, Mannheim, Germany), and postfixed in 0.5% paraformaldehyde (Sigma Chemical Co., St. Louis, MO).

FISH Probes. YAC A88E10 (330 kilobases), later referred to as YAC 11, and YAC 802B11 (1450 kilobases), later referred to as YAC 23, were obtained by screening the St. Louis and the CEPH YAC libraries with *IFN A1* primers (12). YAC 883G5 (1100 kilobases), later referred to as YAC 17, were obtained from the CEPH MegaYAC library by screening with *D9S966* primers (13). YAC 284D6 (320 kilobases), later referred to as YAC 10/2, from chromosomal band 8q22 was used as a control probe (14).

Eight cosmids encompassing a 250-kilobase region around *CDKN2* were used. The cosmid contig was assembled by screening a flow-sorted human chromosome 9 library (Lawrence Livermore Laboratories) with probes from a YAC contig of the region. The exact localization of the FISH probes is shown in Fig. 1. FISH probes were prepared as described previously (10). YACs were purified on a pulsed-field gel. The DNA of the excised YAC bands as well as the cosmid DNA (20–100 pg) was amplified using a SIA (15). The amplification products were PCR labeled with biotin-11-dUTP (Enzo Diagnostics) and finally treated with DNase (DNase I, 200 pg/ml for 10–20 min; Boehringer Mannheim) to reduce the average fragment size to 150–450 base pairs. pHuR98, a variant satellite 3 sequence, which hybridizes specifically to the heterochromatic region of chromosome 9 (9qh), was used to determine the copy number of chromosome 9 (16). The plasmid with a 158-base pair insert was amplified by SIA, PCR labeled with Spectrum Orange-11-dUTP (Imagenetics, Framingham, MA), and treated with DNase as described. The copy

Received 1/3/95; accepted 1/24/95.

The costs of publication of this article were defrayed in part by the payment of page charges. This article must therefore be hereby marked *advertisement* in accordance with 18 U.S.C. Section 1734 solely to indicate this fact.

[1] The work was supported in part by J. S. McDonnell Foundation Grant 92-51 (O. I. O.), DOE Grant DE-FG02-86ER60408 (J. D. Rowley), and a training grant from the Deutsche Forschungsgemeinschaft (M. H. D.).

[2] To whom requests for reprints should be addressed, at the Department of Medicine, Section of Hematology/Oncology, University of Chicago, 5841 S. Maryland, Box 2115, Chicago, IL 60637.

[3] The abbreviations used are: IFN, interferon type I; FISH, fluorescence *in situ* hybridization; YAC, yeast artificial chromosome; CDK4, cyclin-dependent kinase; SIA, sequence independent amplification.

[4] O. I. Olopade *et al.*, unpublished data.

Table 1 *Interphase analysis of normal peripheral blood*

Dual color FISH was performed with normal peripheral blood cells of 10 probands.

FISH probe	Region/ marker	No. of hybridization signals/cell (%)					
		0	1	2	3	4	>4
pHuR	9qh	0.02 ± 0.06[a]	3.22 ± 0.54	95.70 ± 0.50	0.78 ± 0.37	0.32 ± 0.32	0
YAC 17	*D9S966*	0.30 ± 0.27	3.90 ± 1.33	94.66 ± 1.63	0.74 ± 0.39	0.40 ± 0.27	0
COS p16	*CDKN2*	0.10 ± 0.19	2.68 ± 1.00	96.02 ± 1.46	0.82 ± 0.62	0.32 ± 0.23	0.04 ± 0.13
YAC 11	*IFN A*	0.06 ± 0.10	2.12 ± 0.8	96.60 ± 1.10	0.80 ± 0.49	0.42 ± 0.32	0
YAC 23	*IFN A*	0.04 ± 0.08	1.92 ± 0.33	97.08 ± 0.65	0.78 ± 0.69	0.12 ± 0.10	0
YAC 10/2	8q22	0.16 ± 0.18	1.94 ± 0.65	97.04 ± 0.65	0.62 ± 0.30	0.24 ± 0.16	0

[a] Mean ± SD of hybridization signals/cell.

Table 2 *Molecular and cytogenetic features of human tumor cell lines*

The number of chromosome 9 copies were determined by FISH analysis of the centromere 9 probe (pHuR 98). The presence of the interferon A cluster (*IFN A*) and of the molecular markers *REY24*, *CDKN2*, *D9S966*, and *D9S171* were determined by Southern blots.

Cell line	Tumor type	Cytogenetic alterations of chromosome 9	Ploidy	No. of chromosomes 9 (FISH)	*IFNA*	*REY24*	*CDKN2*	*D9S966*	*D9S171*
A172	Glioma	9p on marker, 16 marker chromosomes	Near triploid	4	−p[a]	−	−	−	+
H4	Glioma	del(9p) 3X	Hypertriploid	3	−p[a]	−	−	−	+
T98	Glioma	14–16 marker chromosomes	Hyperpentaploid	>4	+	+	−	+	+
U410	Glioma	ND	Near diploid	2	−	−	−	−	+
HS294T	Melanoma	Normal	Near triploid	3	+	−	−	+	+
RPMI7951	Melanoma	ND	Heteroploid (>2X <6X)	>4	+	+	+	+	+
H290	NSCLC	der(9)t(6;9)(p11;p11), del(9)(p11), del(9)(p22)	Near tetraploid	4	−p[a]	−	−	−	−
H322	NSCLC	del(9)(p13), 25 marker chromosomes	Near tetraploid	4	−	−	−	−	+
RT4	Bladder carcinoma	−9, del(9)(p21p22) 3X	Hypotetraploid	3	−p[a]	−	−	−	+
UM-UC3	Bladder carcinoma	+9, del(9)(q12 or q34), add(9)(q12)	Hypertriploid	4	+	−	−	−	+

[a] +, autoradiographic signal comparable to the control; −, no signal; p, partial deletion of the *IFNA* gene cluster (only some of the multiple bands are present); ND, not done; NSCLC, non-small cell lung carcinoma.

number of chromosome 8 was determined by a centromeric FISH probe CEP 8 Spectrum Orange (Imagenetics).

FISH Procedure. Two color FISH with YAC or cosmid probes and a centromeric probe was performed as described previously (17). The hybridization solution contained approximately 0.1 μg of each probe, 1 μg of human Cot1-DNA (BRL), 0.6 μg of human placental DNA, and 3 μg of salmon sperm DNA/slide in a 10-μl volume. The biotinylated probes were detected with FITC-conjugated avidin. The slides were counterstained with 4′,6′-diamidino-2-phenylindole dihydrochloride and were analyzed using epifluorescence and a single-pass filter (Chroma Technology) to avoid superimposition of the centromeric and the YAC signals. For interphase analysis of the cell lines, the FISH signals of a total of 500 single, intact cells were counted by 2 independent observers. In addition, 25 metaphase cells of each cell line were analyzed. In the tumor samples 100 single intact cells were analyzed. For Fig. 2, separate gray scale images of 4′,6′-diamidino-2-phenylindole-stained cells and fluorescence signals were captured using a cooled charge-coupled device camera (Photometrics, Tucson, AZ) and were pseudocolored and merged using NIH Image or Adobe Photoshop.

Molecular Analysis. Cell line DNA was extracted and treated with restriction enzyme (*Hind*III), electrophoresed on a 1% agarose gel, and transferred to a nylon-based nitrocellulose membrane (Gene Screen Plus; NEN, Boston). DNA filters were hybridized with ^{32}P-labeled probes from 9p21 and exposed to X-ray film. The probes used were *REY24*, *CDKN2* cDNA, *D9S966*, and *D9S171* (13).[5] The exact order of the molecular markers is shown in Fig. 1.

Results

Interphase Analysis in Normal Peripheral Blood. To determine the reliability of the FISH probes in nonmalignant cells, ten test hybridizations of peripheral blood cells from normal individuals were performed with each probe (Table 1). Both centromeric and YAC probes showed an almost identical distribution of signals/cell comparable to previously published results for centromeric probes. In 500 nuclei scored, 2 signals were detected in 94–97% of the cells.

Interphase Analysis in Tumor Cell Lines. 9p deletions were determined by molecular analysis in 9 of 10 cell lines (Table 2). All deletions were detected as well by Interphase FISH with the COSp16 probe. The results of the FISH analysis are summarized as a deletion map (Fig. 1). YAC 23 was homozygously deleted in one cell line (H322). YAC 11 which covers the proximal *IFN* gene cluster was absent in 2 cell lines (U410, H322); only one copy was retained in one cell line (H4). Moreover, the intensity of the hybridization signals for YAC 11 was significantly reduced in 3 cell lines (H290, H4, A172). Previous detailed molecular analysis revealed that the distal deletion breakpoints of these cell lines lie within the YAC 11 region (3, 18). Therefore the intensity of the signal is reduced. However, we were still able to detect signals for YAC 11 in one cell line [H4 (Fig. 2*a*)] even though 90% of the YAC region was deleted. YAC 17 was homozygously deleted in 2 cell lines (H290, RT4), the number of copies was reduced in 2 other cell lines (A172, H4), and 1 cell line showed a partial deletion of one allele (U410). The cosmid probe which covers the region of *CDKN2* was homozygously deleted in 8 of 10 cell lines. In one cell line (T98) the signal was significantly reduced indicating a partial deletion of the region. Southern blot analysis showed a homozygous deletion of *CDKN2* in this cell line, whereas another molecular marker of the region was retained (data not shown). In 5 cell lines (H4, U410, HS294T, RT4, UM-UC3), both control probes, the chromosome 8 centromere probe and the YAC 10/2 probe, showed a similar distribution of signals/cell indicating the comparable hybridization efficiency of centromeric and YAC probes. However, in the 5 remaining cell lines (all with 4 or more copies of

[5] O. I. Olopade *et al.*, manuscript in preparation.

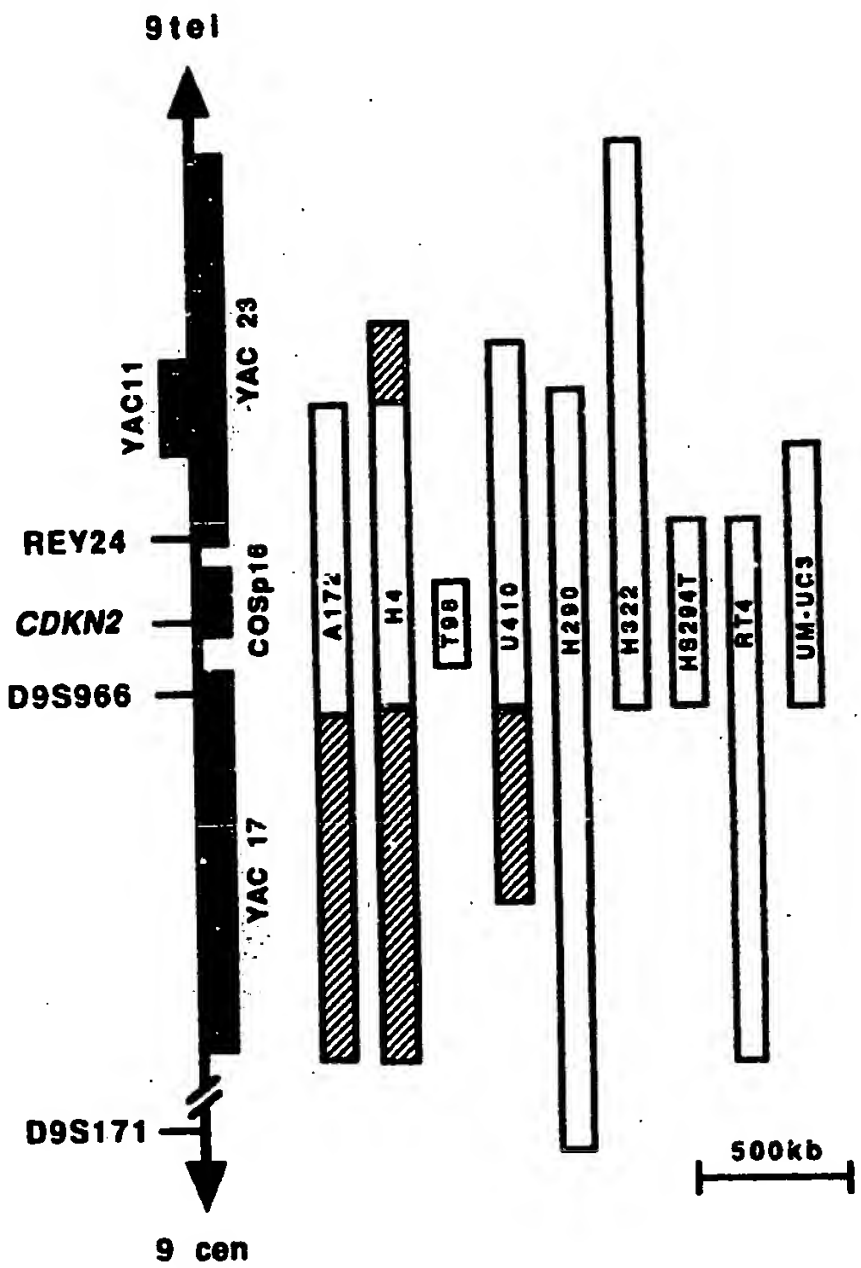

Fig. 1. 9p deletion map of the cell lines. The position of different FISH probes (YAC 11, YAC 23, YAC 17, COSp16) and molecular markers (*REY24*, *CDKN2*, *D9S966*, *D9S171*) are shown. □, homozygous deletions; ▨, nonhomozygous deletions. *kb*, kilobases.

chromosome 8) the number of chromosome 8 centromere signals/cell differed from the number of YAC 10/2 signals/cell suggesting the presence of rearrangements affecting chromosome 8.

Subpopulations of cells showed an aberrant number of centromere 8 and 9 signals reflecting the heterogeneity of the cell lines. Metaphase analysis confirmed these subpopulations of cells with a loss or gain of a chromosome homologue in 5 of 10 cell lines. However, the heterogeneity of the cell lines did not affect the analysis of 9p deletions, because all subpopulations of a cell line uniformly had either deleted or retained the tumor suppressor region on 9p. In the latter group the number of signals/cell was highly comparable to the centromere 9 data. In contrast, in the cell lines with homozygous deletions 99.5 ± 0.4% (SD) of the cells showed no hybridization signal (Fig. 3*A*). Nonhomozygous deletions could be detected with a similar accuracy. Thus, there was good concordance between the molecular results and the FISH data. All the homozygous deletions determined by molecular analysis were detected by Interphase FISH (Table 2). In addition, cell lines with a partial loss of the *IFN* gene cluster had a reduced intensity of the hybridization signal of YAC 11.

Interphase Analysis in Tumor Specimens. To determine 9p deletions in primary tumors, we analyzed 9 brain tumors, pathologically classified as glioblastoma multiforme, using the FISH probes YAC 11, COSp16, and YAC 10/2 for detection of the deletion of the proximal *IFN* gene cluster (YAC 11), the *CDKN2* region (COSp16), and a control probe (YAC 10/2). Of 9 tumors, 4 tumors (44%) had a deletion of the proximal *IFN* gene cluster [YAC 11 (Fig. 3*B*)]. No cosmid signal for *CDKN2* was detectable in 5 tumors. In one additional tumor sample [sample 1 (Fig. 3*B*)] the intensity of the hybridization signals of the cosmid contig was significantly reduced in comparison to the control YACs, indicating a partial deletion of the cosmid contig.

In one tumor sample [sample 7 (Fig. 3*B*)] 7% of the cells did not show any YAC 11 signal. This tumor had only one copy of chromosome 9. Therefore, the number of cells without hybridization signal probably results from an incomplete hybridization efficiency. In aneuploid tumors (6 cases, determined by interphase FISH) a subpopulation of cells (13.4 ± 4.8%) had 2 copies of chromosome 9. This cell population was not identified in cell lines and probably represents the contamination with normal cells (stromal cells, lymphocytes, etc.).

Discussion

Interphase FISH analysis is a well established method to determine chromosomal aberrations in hematological malignancies and solid tumors. Using the appropriate probes, interphase analysis is able to detect chromosomal aberrations in clinical tumor specimens contaminated with normal cells and is also able to detect these changes in small subpopulations of cells. In this study, we describe the analysis of 10 cell lines derived from gliomas, melanomas, non-small lung cancer, and bladder cancer and 9 primary gliomas using interphase FISH analysis. For our experiments, we generated FISH probes from YACs and a cosmid contig by a SIA technique developed in our laboratory (10). This procedure yields consistent and strong FISH signals for interphase analysis. In contrast, single cosmids of the 9p region had a hybridization signal of only moderate intensity due to the small insert size. At present, FISH probes of YACs or similar vectors have been generated previously by Alu-PCR (19). This amplification technique is limited by the number of Alu sequences per clone which varies considerably. Hybridization of YAC probes generated by Alu-PCR to extended chromatin preparations showed incomplete repre-

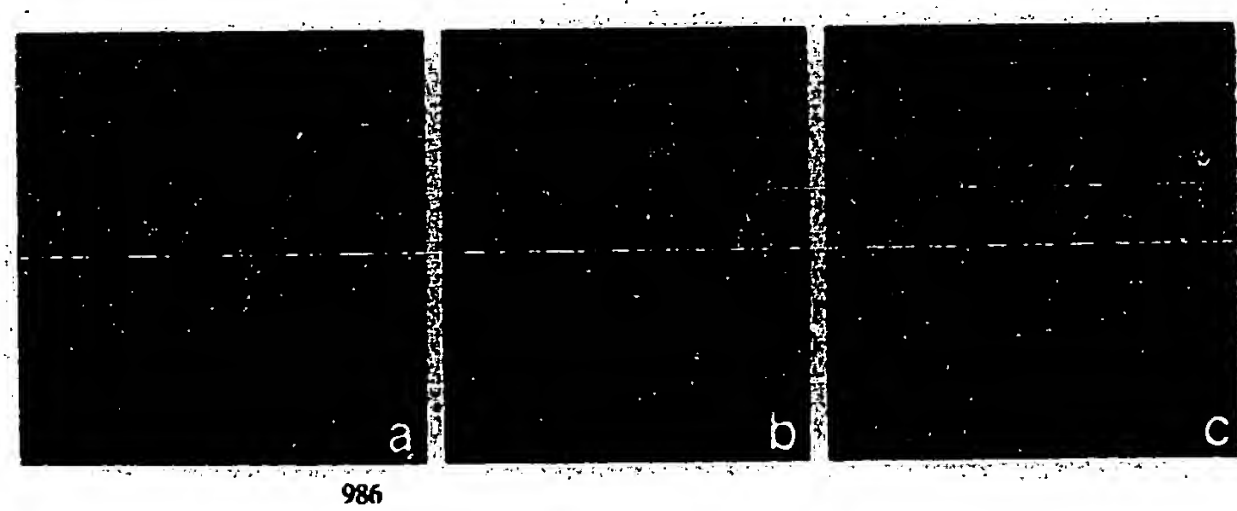

Fig. 2. *a*, FISH with YAC 11 (FITC)/pHUR98 (Spectrum Orange). H4 is a hypertriploid cell line. About 10% of one copy of the YAC 11 region is retained. An interphase cell with 3 signals for the centromere 9 and 1 faint YAC signal (*arrow*) is shown. *b*, FISH with YAC 11 (FITC)/pHUR98 (Spectrum Orange). *c*, FISH with COSp16 (FITC)/pHUR98 (Spectrum Orange). Tumor 3 is a glioblastoma with deletion of the p16 region. An interphase cell with 5 centromere 9 and 5 YAC11 signals is shown (*b*) whereas no COSp16 signal is detectable (*c*).

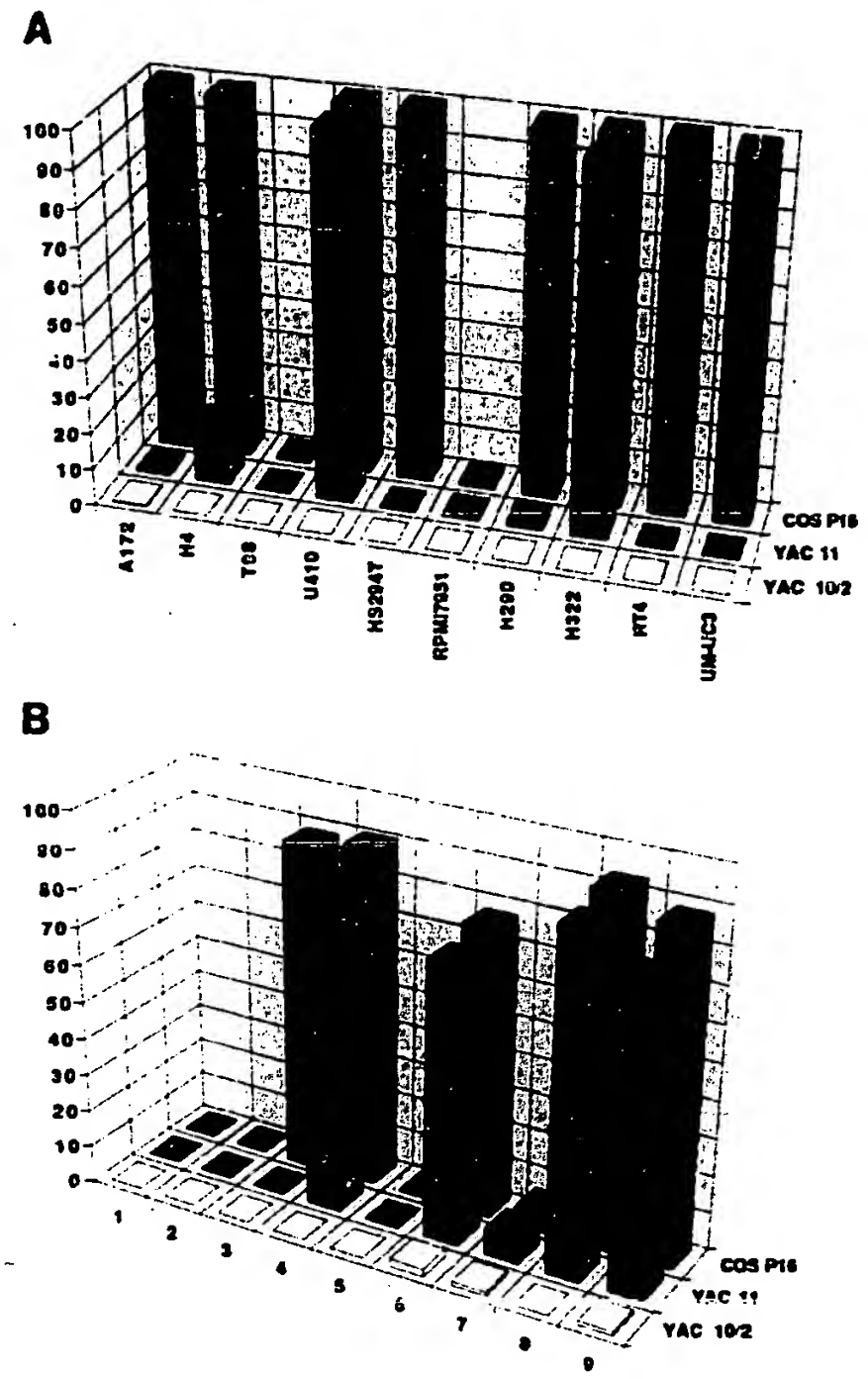

Fig. 3. *A*, FISH analysis in 10 tumor cell lines. The percentage of cells without hybridization signal (YAC 10/2, YAC 11, COSp16) is shown. *B*, FISH analysis in 9 glioblastomas. The percentage of cells without hybridization signal (YAC 10/2, YAC 11, COSp16) is shown.

sentation of the YAC insert (20). Therefore, Alu-PCR generated probes may not accurately detect partial deletions of the hybridization region.

In our experiments, the cosmid contig probe identified all homozygous deletions of the *CDKN2* region in 9 of 10 cell lines. Only 3 of these cell lines had cytogenetically visible deletions of the short arm of chromosome 9. The deletions were confirmed by molecular analysis of the cell lines. The remaining melanoma cell line (RPMI7951) had a rather complex cytogenetic rearrangement of the short arm of chromosome 9 but did not show any deletion of the *CDKN2* region. Sequencing data of this cell line did not detect any mutation within the second exon of *CDKN2*. The majority of previously described point mutations of *CDKN2* were located in this region (7–9).

The proximal *IFN* gene cluster was deleted in 4 of the 9 primary tumors. Although the small number of tumors does not allow an estimation of the overall frequency of 9p deletions in glioblastoma, our present results are consistent with our previous studies (3). Another study detected *IFN* gene deletions in 50% of the high grade glioma (2). The authors proposed a tumor suppressor activity of the proximal *IFN* gene cluster in glioblastoma (21). However, our data exclude the *IFN* genes from the critical region of deletion, inasmuch as they were deleted in only 4 of 6 tumors with 9p deletions. The *CDKN2* region was deleted in 6 of 9 tumors (67%). Other studies showed *CDKN2* deletions in 17–69% of the tumors (9, 22, 23). In our own series of primary gliomas, Southern blot analysis showed homozygous deletions of *CDKN2* in 45% of the tumors.[5] However, Southern blot analysis may miss some of the 9p deletions because of contamination with normal cells. In addition, it is well known that some tumors are heterogeneous, and 9p deletions may be present in only a subpopulations of cells.

Our data suggest that the 250-kilobase region covered by the cosmid contig includes the target gene of the 9p deletions in primary glioma. *CDKN2* is located in the smallest region of deletion on 9p. However, the frequency of point mutations detected in primary tumors is rather low (8, 9). Therefore, the simultaneous deletion of the neighboring genes may be responsible for the selective growth advantage for the malignant cells. Hannon and Beach (24) proposed that *p15* (*MTS2*, *CDKN2*^{b}), a transforming growth factor β-regulated member of the *p16* family, also plays an important role in carcinogenesis. *p15* maps approximately 20 kilobases centromeric to *CDKN2* and is included in our cosmid contig (1). It may well be that the predominant mechanism of 9p rearrangements in primary tumors is the deletion of a large genomic region which would inactivate both genes in one step. In fact, in cell lines as well as in primary glioblastoma, the vast majority of deletions includes both genes (1, 5, 9). Therefore, we believe that homozygous deletions are the predominant mechanism for inactivating this region. Because further mapping data are crucial to determine the clinical significance of these rather large deletions in primary tumors, FISH will play an important role in characterizing the deletions.

Recently, the overexpression of *CDK4*, the target molecule of p16, was proposed as an additional mechanism of functional p16 inactivation (22, 23). Both events would result in a disinhibition of the cell cycle. However, in a number of cell lines and primary gliomas the homozygous deletion of *CDKN2* was the much more frequent event (22, 23).

Acknowledgements

We thank Janet D. Rowley for critically reading the manuscript, Fitsum Hagos for his technical assistance, Walter Stadler for part of the molecular analysis (RI4, UM-UC3), David Beach for providing the *CDKN2* cDNA probe, and Sandra Bigner and John Minna for providing cell lines.

References

1. Kamb, A., Gruis, N. A., Weaver, F. J., Liu, Q., Harshman, K., Tavtigian, S. V., Stockert, E., Day, R., III, Johnson, B. E., and Skolnick, M. H. A cell cycle regulator potentially involved in genesis of many tumor types. Science (Washington DC), *264*: 436–440, 1994.
2. James, C. D., He, J., Carlbom, E., Nordenskjold, M., Cavenee, W. K., and Collins, V. P. Chromosome 9 deletion mapping reveals interferon α and interferon β-1 gene deletions in human glial tumors. Cancer Res., *51*: 1684–1688, 1991.
3. Olopade, O. I., Jenkins, R. B., Ransom, D. T., Malik, K., Pomykala, H., Nobori, T., Cowan, J. M., Rowley, J. D., and Diaz, M. O. Molecular analysis of deletions of the short arm of chromosome 9 in human gliomas. Cancer Res., *52*: 2523–2529, 1992.
4. Bello, M. J., de Campos, J. M., Vaquero, J., Kusak, M. E., Sarasa, J. L., Pestana, A., and Rey, J. A. Molecular and cytogenetic analysis of chromosome 9 deletions in 75 malignant gliomas. Genes Chromosomes Cancer, *9*: 33–41, 1994.
5. Nobori, T., Miura, K., Wu, D. J., Lois, A., Takabayashi, K., and Carson, D. A. Deletions of the cyclin-dependent kinase-4 inhibitor gene in multiple human cancers. Nature (Lond.), *368*: 753–756, 1994.
6. Serrano, M., Hannon, G. J., and Beach, D. A new regulatory motif in cell-cycle control causing specific inhibition of cyclin D/CDK4. Nature (Lond.), *366*: 704–707, 1993.
7. Cairns, P., Mao, L., Merlo, A., Lee, D. J., Schwab, D., Eby, Y., Tokino, K., van der Riet, P., Blaugrund, J. E., and Sidransky, D. Rates of p16 (*MTS1*) mutations in primary tumors with 9p loss. Science (Washington DC), *265*: 415–416, 1994.
8. Giani, C., and Finocchiaro, G. Mutation rate of the *CDKN2* gene in malignant gliomas. Cancer Res., *54*: 6338–6339, 1994.

9. Jen, J., Harper, J. W., Bigner, S. H., Bigner, D. D., Papadopoulos, N., Markowitz, S., Willson, J. K. V., Kinzler, K. W., and Vogelstein, B. Deletion of p16 and p15 genes in brain tumors. Cancer Res., *54:* 6353–6358, 1994.
10. Bohlander, S. K., Espinosa, R., III, Fernald, A. A., Rowley, J. D., Le Beau, M. M., and Diaz, M. Sequence-independent amplification and labeling of yeast artificial chromosomes for fluorescence *in situ* hybridization. Cytogenet. Cell Genet., *65:* 108–110, 1994.
11. Le Beau, M. M. Cytogenetic analysis of hematological malignant diseases. *In:* M. J. Barch (eds.), The ACT Cytogenetics Laboratory Manual, pp. 395–445. New York: Raven Press, 1994.
12. Henco, K., Brosius, J., Fujisawa, A., Fujisawa, J. I., Haynes, J. R., Hochstadt, J., Kovacic, T., Pasek, M., Schambock, A., Schmid, S., Todokoro, K., Walchli, M., Nagata, S., and Weissman, C. Structural relationship of human interferon α genes and pseudogenes. J. Mol. Biol., *185:* 227–260, 1988.
13. Bohlander, S. K., Dreyling, M. H., Hagos, F., Sveen, L., Olopade, O. I., and Diaz, M. O. Mapping of a putative tumor suppressor gene on chromosome 9 band p21–22 with microdissection probes. Genomics, in press, 1995.
14. Erickson, P., Gao, J., Chang, K. S., Look, T., Whisenant, E., Raimondi, S., Lasher, R., Trujillo, J., Rowley, J. D., and Drabkin, H. Identification of breakpoints in t(8;21) acute myelogenous leukemia and isolation of a fusion transcript AML1/ETO, with similarity to *Drosophila* segmentation gene, *runt*. Blood, *80:* 1825–1831, 1992.
15. Bohlander, S. K., Espinosa, R., III, Le Beau, M. M., Rowley, J. D., and Diaz, M. O. A method for the rapid sequence-independent amplification of microdissected chromosomal material. Genomics, *13:* 1322–1324, 1992.
16. Moyzis, R. K., Albright, K. L., Bartholdi, M. F., Cram, L. S., Deaven, L. L., Hildebrand, C. E., Joste, N. E., Longmire, J. L., Meyne, J., and Schwarzacher-Robinson, T. Human chromosome-specific repetitive DNA sequences: novel marker for genetic analysis. Chromosoma (Berl.), *95:* 375–386, 1987.
17. Rowley, J. D., Diaz, M. O., Espinosa, R., III, Patel, Y. D., van Melle, E., Ziemin, S., Taillon-Miller, P., Lichter, P., Evans, G. A., Kersey, J. H., Ward, D. C., Domer, P. H., and Le Beau, M. M. Mapping chromosome band 11q23 in human acute leukemia with biotinylated probes: identification of 11q23 translocation breakpoints with a yeast artificial chromosome. Proc. Natl. Acad. Sci. USA, *87:* 9358–9362, 1990.
18. Olopade, O. I., Buchhagen, D. L., Malik, K., Sherman, J., Nobori, T., Bader, S., Nau, M. M., Gazdar, A. F., Minna, J. D., and Diaz, M. O. Homozygous loss of the interferon genes defines the critical region on 9p that is deleted in lung cancers. Cancer Res., *53:* 2410–2415, 1993.
19. Nelson, D. L., Ledbetter, S. A., Corbo, L., Victoria, M. F., Ramirez-Solis, R., Webster, T. D., Ledbetter, D. H., and Caskey, C. T. Alu polymerase chain reaction: a method for rapid isolation of human-specific sequences from complex DNA sources. Proc. Natl. Acad. Sci. USA, *86:* 6686–6690, 1989.
20. Tocharoentanaphol, C., Cremer, M., Schroeck, E., Blonden, M., Kilian, K., Cremer, T., and Ried, T. Multicolor fluorescence *in situ* hybridization on metaphase chromosomes and interphase Halo-preparations using cosmid and YAC clones for the simultaneous high resolution mapping of deletions in the dystrophin gene. Hum. Genet., *93:* 229–235, 1994.
21. James, C. D., He, J., Collins, V. P., Allalunis, T. M., and Day, R., III. Localization of chromosome 9p homozygous deletions in glioma cell lines with markers constituting a continuous linkage group. Cancer Res., *53:* 3674–3676, 1993.
22. He, J., Allen, J. R., Collins, V. P., Allalunis-Turner, M. J., Godbout, R., Day, R. S., III, and James, C. D. CDK4 amplification is an alternative mechanism to p16 homozygous deletion in glioma cell lines. Cancer Res., *54:* 5804–5807, 1994.
23. Schmidt, E. E., Ichimura, K., Reifenberger, G., and Collins, V. P. *CDKN2* (p16/MTS1) gene deletion or CDK4 amplification occurs in the majority of glioblastomas. Cancer Res., *54:* 6321–6324, 1994.
24. Hannon, G. J., and Beach, D. $p15^{INK4B}$ is a potential effector of TGF-β-induced cell cycle arrest. Nature (Lond.), *371:* 257–261, 1994.

C18

[CANCER RESEARCH 53, 1098–1101, March 1, 1993]

Methylthioadenosine Phosphorylase Deficiency in Human Non-Small Cell Lung Cancers[1]

Tsutomu Nobori,[2] Istvan Szinai, Diane Amox, Barbara Parker, Olufunmilayo I. Olopade, Dorothy L. Buchhagen, and Dennis A. Carson

Department of Medicine and the Sam and Rose Stein Institute for Research on Aging, University of California, San Diego, La Jolla, California 92093-0663 [T. N., I. S., D. A., D. A. C.]; Cancer Center, University of California, San Diego, La Jolla, California 92093-0658 [B. P.]; Section of Hematology/Oncology, Department of Medicine, University of Chicago, Chicago, Illinois 60637 [O. I. O]; National Cancer Institute-Navy Oncology Branch, National Cancer Institute, Bethesda, Maryland 20814 [D. L. B.]

ABSTRACT

Methylthioadenosine (MeSAdo) phosphorylase, a purine metabolic enzyme, is present in all normal mammalian tissues. A deficiency of this enzyme has been reported in some human leukemias and lymphomas and in a few solid tumors. In the present study, a specific immunoassay was used to assess the enzyme levels in human non-small cell lung cancer cell lines and primary tumors. We also tested the effects of MeSAdo phosphorylase-selective chemotherapy on the *in vitro* growth of enzyme-positive and enzyme-negative lung cancer cell lines. Of 29 non-small cell lung cancers, 9 (6 cell lines and 3 primary tumors, 31%) lacked detectable immunoreactive enzyme protein. Both 5,10-dideazatetrahydrofolate, an inhibitor of *de novo* purine synthesis, and methionine depletion, combined with MeSAdo, prevented the growth of the enzyme-negative non-small cell lung cancer cells under conditions in which enzyme-positive cells utilized MeSAdo to endogenously synthesize purine nucleotides and methionine. Our data suggest that MeSAdo phosphorylase deficiency is frequently found in non-small cell lung cancers and can be exploited in designing enzyme-selective chemotherapy.

INTRODUCTION

MeSAdo[3] phosphorylase (methylthioadenosine: orthophosphate methylthioribosyltransferase) is involved in the metabolism of polyamines and purines. This enzyme is abundant in all normal tissues and in cell lines derived from normal cells (1) but is deficient in some cell lines established from leukemias, lymphomas, and solid tumors such as melanoma, breast cancer, lung squamous carcinoma, and rectal adenocarcinoma (1, 2). However, because the assay for MeSAdo phosphorylase catalytic activity requires commercially unavailable radiochemical substrates, because the enzyme is catalytically labile, and because contaminating normal cells (especially in the case of solid tumors) may give erroneous results with the enzyme assay, it has been difficult to determine the true incidence of the deficiency in human primary tumors. In an earlier report, we established the validity of an immunoassay in which antibodies against MeSAdo phosphorylase were used, and we quantitated the immunoreactive MeSAdo phosphorylase protein in primary human gliomas (3).

In mammalian cells, MeSAdo, the substrate for MeSAdo phosphorylase, is produced during synthesis of polyamines from decarboxylased *S*-adenosylmethionine (Fig. 1). MeSAdo does not accumulate in normal tissues but is cleaved rapidly to adenine and MTR-1-P by MeSAdo phosphorylase (4). The adenine presumably is recycled to purine nucleotides via adenine phosphoribosyltransferase (5). The loss of MeSAdo phosphorylase, by decreasing adenine formation, would be expected to interfere with this salvage pathway. On the other hand, MTR-1-P is converted to methionine (6–9), which may also be synthesized from homocysteine by methionine synthase (10) and betaine-homocysteine methyltransferase (11). In the enzyme-negative malignant cells, however, methionine is synthesized solely from homocysteine. Accordingly, MeSAdo phosphorylase-deficient malignant cells might become more dependent than normal cells on an exogenous supply of methionine.

Thus, MeSAdo phosphorylase deficiency in human malignancy may permit the development of enzyme-selective chemotherapy, in which enzyme-negative cancer cells will be killed with drugs causing the depletion of purine nucleotides or methionine, under conditions in which enzyme-positive normal cells can be rescued by giving MeSAdo as a source of purines or methionine.

In this study, we used an immunoblotting method to screen human NSCLC cell lines and primary tumors for MeSAdo phosphorylase deficiency. The ability of a selective inhibitor of *de novo* purine synthesis, DDATHF (12, 13), in combination with MeSAdo to selectively prevent the growth of MeSAdo phosphorylase-negative NSCLC cells was also tested. Finally, we determined whether enzyme-negative NSCLC cells could proliferate in methionine-depleted medium supplemented with MeSAdo. The results indicate that 31% (9 of 29) of NSCLC cell lines and primary tumors lacked detectable enzyme protein. Moreover, only enzyme-negative NSCLC cells were prevented from growing by DDATHF, or by methionine depletion, in the presence of MeSAdo. Thus, MeSAdo phosphorylase deficiency distinguishes many NSCLCs from normal cells, and this tumor-specific metabolic abnormality may be exploited to selectively treat NSCLCs.

MATERIALS AND METHODS

DDATHF was kindly provided by Lilly Research Laboratories (Indianapolis, IN). Solutions of DDATHF were made in 0.1 N NaOH and were adjusted to pH 7.4 with phosphate-buffered saline (14). Dialyzed horse serum and D-MEM containing or lacking methionine were obtained from GIBCO BRL (Life Technologies, Inc., Gaithersburg, MD). All other chemicals were from Sigma Chemical Co. (St. Louis, MO).

Cell Lines and Tumor Tissue Specimens. The NSCLC cell lines listed in Table 1 either came from the American Type Culture Collection (Rockville, MD) or were established at the National Cancer Institute. Primary tumor specimens were obtained from the Frozen Tissue Bank at the Cancer Center of University of California, San Diego, and from the San Diego Veterans Administration Medical Center. All tested tumor specimens were estimated to contain <10% normal cells.

MeSAdo Phosphorylase Assay. Enzyme activity was measured by the radiochemical method of Pegg and Williams-Ashman (4), using [*methyl*-^{3}H]-MeSAdo as the substrate, exactly as described earlier (5). The protein concentrations were determined by the method of Bradford (15) with bovine serum albumin as the standard.

Immunoblot Analysis. Enzyme protein was detected by a semiquantitative immunoblotting procedure, as described earlier (3). Briefly, crude extracts

Received 9/16/92; accepted 12/22/92.

The costs of publication of this article were defrayed in part by the payment of page charges. This article must therefore be hereby marked *advertisement* in accordance with 18 U.S.C. Section 1734 solely to indicate this fact.

[1] This work was supported in part by grants 1KT112 and 3RT0075 from the University of California Tobacco Related Disease Research Program, by grants GM23200 and AI24466 from the National Institutes of Health, and by a grant to the UCSD Cancer Center (P30 CA23100). I.S. was supported by the Fogarty International Center, National Institutes of Health, Special Postdoctoral Research Program in AIDS, T22 TW00011.

[2] To whom requests for reprints should be addressed, at Department of Medicine, University of California, San Diego, La Jolla, CA 92093-0663.

[3] The abbreviations used are: MeSAdo, methylthioadenosine; MTR-1-P, 5'-methyl thioribose 1-phosphate; NSCLC, non-small cell lung cancer; DDATHF, 5,10-dideazatetrahydrofolate; Dulbecco's modified Eagle's medium (D-MEM); BBS, buffered borate saline; MTT, 3-(4,5-dimethylthiazol-2-yl)-2,5-diphenyltetrazolium bromide; kDa, kilodalton.

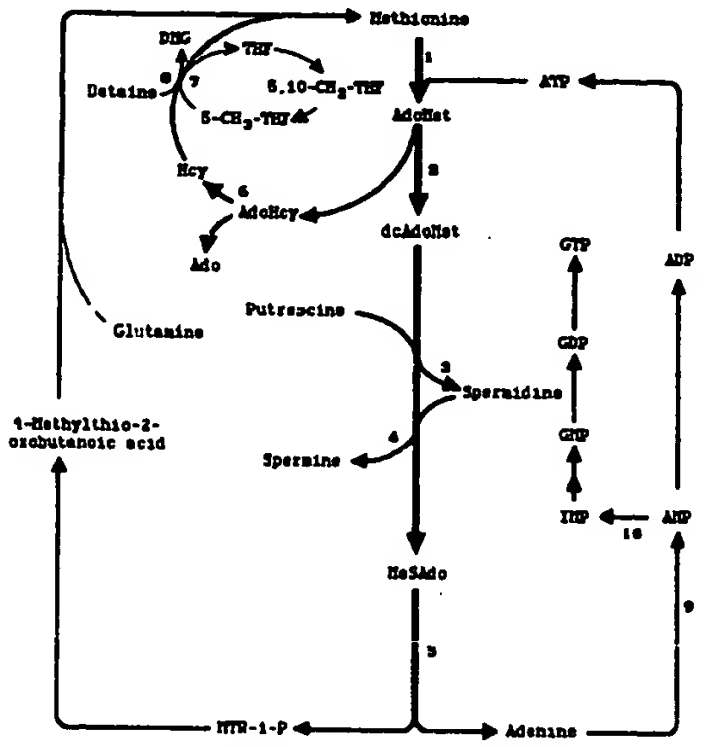

Fig. 1. Metabolic map of polyamine synthesis and MeSAdo reutilization. AdoMet, *S*-adenosylmethionine; dcAdoMet, decarboxylated AdoMet; MeSAdo, methylthioadenosine; AdoHcy, *S*-adenosylhomocysteine; Hcy, homocysteine; THF, tetrahydrofolate; Ado, adenosine; DMG, dimethylglycine. The enzymes involved are: *1*, methionine adenosyltransferase; *2*, AdoMet decarboxylase; *3*, spermidine synthase; *4*, spermine synthase; *5*, MeSAdo phosphorylase; *6*, AdoHcy hydrolase; *7*, methionine synthase; *8*, betaine-homocysteine methyltransferase; *9*, adenine phosphoribosyltransferase; *10*, AMP deaminase.

were separated by electrophoresis in 12.5% polyacrylamide gels containing 0.1% sodium dodecyl sulfate (16). After electrotransfer to polyvinylidene difluoride membranes (Immobilon-P; Millipore Corp., Bedford, MA), nonspecific binding sites were blocked with 1% powdered milk in BBS (0.2 M sodium borate-0.15 M NaCl, pH 8.5) containing 0.1% gelatin. The proteins were then probed for 1 h at room temperature with rabbit antiserum to MeSAdo phosphorylase, diluted 1:200 in BBS containing 1% powdered milk. After the proteins were washed with BBS containing 0.05% Tween 20, reactive bands were detected by the binding of ^{125}I-protein-A (1 mCi/ml; ICN Radiochemicals, Irvine, CA) for 1 h. After washing, the membranes were exposed to Koduk XAR-5 film at −80°C.

Growth Inhibition of MeSAdo Phosphorylase-negative Cells. Enzyme-positive (SK-MES-1) and -negative (A-549) cells were cultured in 96-well plates (0.2 ml/well; 5×10^4 cells/ml) with various concentrations of DDATHF in D-MEM medium containing 10% dialyzed horse serum with or without MeSAdo. Alternatively, the cells were cultured in methionine-depleted medium supplemented with 10% dialyzed horse serum in the presence or absence of 16 μM MeSAdo. The growth of the cultures was measured spectrophotometrically with MTT after 4 days of incubation as described previously (17).

RESULTS

Incidence of MeSAdo Phosphorylase Deficiency in NSCLC. Having verified the validity of the immunoassay to quantitate MeSAdo phosphorylase in human gliomas (3), we used the antibodies to analyze 19 human NSCLC cell lines (10 adenocarcinomas, 4 squamous cell carcinomas, 3 large cell carcinomas, and 2 bronchoalveolar carcinomas). Immunoblot analysis demonstrated that the 32-kDa band corresponding to the homotrimeric subunit of MeSAdo phosphorylase was present in 13 cell lines, whereas 6 cell lines (3 adenocarcinomas, 2 large cell carcinomas, one bronchoalveolar carcinoma) were entirely deficient in immunoreactive enzyme protein (Table 1). Fig. 2 illustrates the appearance of representative immunoblots. In previous studies, the results with the immunoassay were found to correlate perfectly with measurements of MeSAdo phosphorylase catalytic activities (3). The lack of MeSAdo phosphorylase activity in some of the NSCLC cell lines that were deficient in immunoreactive enzyme protein was also confirmed by direct enzyme assay (Table 1). We then analyzed 10 specimens from primary NSCLCs with different histological subtypes (Table 2). In immunoblots, the 32-kDa band was not detected in cases 1, 6, and 9 (Fig. 2*B*, *lanes* 2, 7, and 10). These three enzyme-negative tumors had the histological characteristics of adenocarcinoma.

Selective Chemotherapy of Enzyme-deficient NSCLC. We tested two chemotherapeutic regimens for the exploitation of MeSAdo phosphorylase deficiency in the NSCLC cells. When either enzyme-positive (SK-MES-1) or -negative (A-549) cells were cultured in a medium containing DDATHF, the growth of both cell lines was markedly inhibited. The concentration of DDATHF for 50% growth inhibition was 240 or 300 nM for SK-MES-1 or A-549, respectively. Why the MeSAdo phosphorylase-positive cell line was more sensitive to DDATHF is not clear. However, if MeSAdo was added to the same medium, only the SK-MES-1 cells containing MeSAdo phosphorylase were able to proliferate (Fig. 3). These data indicate that the combination of DDATHF and MeSAdo can selectively inhibit the growth of the enzyme-negative NSCLC cells.

In normal mammalian cells, methionine is synthesized from homocysteine and from MTR-1-P (6–11). MeSAdo phosphorylase-neg-

Table 1 *MeSAdo phosphorylase deficiency in non-small cell lung cancer cell lines*

Enzyme activities were measured radiochemically. Each value is the mean of at least two determinations and is expressed as nmol of product formed/min/mg of protein. The immunoreactive enzyme protein was determined by Western immunoblotting.

Cell line	Histology	MeSAdo phosphorylase	
		Activity	Protein[a]
A-427	Adenocarcinoma	0.283	+
A-549	Adenocarcinoma	<0.01	−
CALU-1	Squamous cell carcinoma	0.223	+
CALU-3	Adenocarcinoma	0.454	+
CALU-6	Adenocarcinoma	0.219	+
SK-LU-1	Adenocarcinoma	<0.01	−
SK-MES-1	Squamous cell carcinoma	0.261	+
Hs 242T	Adenocarcinoma	0.373	+
H322	Bronchoalveolar	<0.01	−
H441	Bronchoalveolar	0.119	+
H460	Large cell carcinoma	0.194	+
H520	Squamous cell carcinoma	N.D.[b]	+
H552	Adenocarcinoma	0.194	+
H676	Adenocarcinoma	N.D.	+
H1264	Squamous cell carcinoma	N.D.	+
H1334	Large cell carcinoma	N.D.	−
H1437	Adenocarcinoma	N.D.	−
H1581	Large cell carcinoma	N.D.	−
H1819	Adenocarcinoma	N.D.	+

[a] +, present; −, absent.
[b] N.D., not determined.

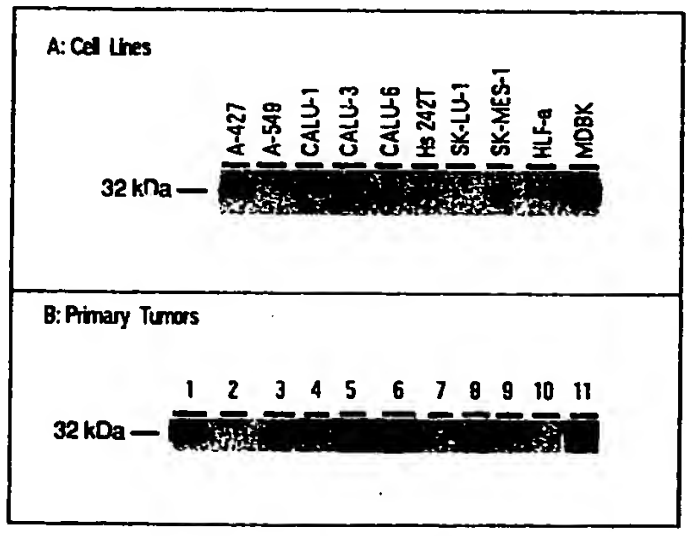

Fig. 2. Immunoblot analysis of representative cell lines (*A*) and primary tumors (*B*) from human non-small cell lung cancers. Crude extracts (150 and 200 μg per lane in *A* and *B*, respectively) were separated electrophoretically, transferred to polyvinylidene difluoride membranes, and probed with an antibody against MeSAdo phosphorylase. The bovine kidney MDBK cell line (20 μg) and the human lung fibroblast line HLF-a (150 μg) were used as positive controls. *B*, *lane 1*, MDBK cells; *lanes 2–11*, cases 1–10 in Table 2.

Table 2 *Clinical characteristics of primary lung cancers*

Case	Age (yr)/Sex	Tumor type[a]	Stage[b]	MeSAdo phosphorylase[c]
1	45/F	ADC	IIIA	–
2	[d]/F	ADC	I	+
3	79/F	LCC	IV	+
4	[d]/M	LCC	I	+
5	32/F	ADC	IV	+
6	[d]	ADC	[d]	–
7	71/M	ADC	I	+
8	52/M	ADC	I	+
9	59/M	ADC	I	–
10	65/M	SQC	IIIA	+

[a] ADC, adenocarcinoma; LCC, large cell carcinoma; SQC, squamous cell carcinoma.
[b] According to the classification of Mountain (31).
[c] +, present; –, absent.
[d] No further information available.

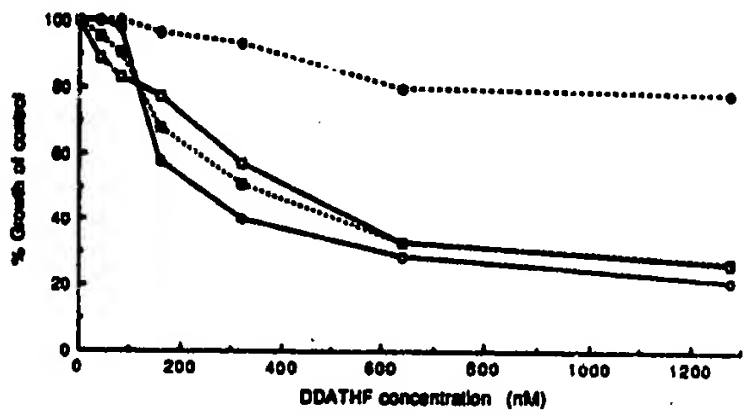

Fig. 3. Reversal of DDATHF growth inhibition of non-small cell lung cancer cells by MeSAdo. Enzyme-positive (SK-MES-1) and enzyme-negative (A-549) cell lines were incubated for 4 days with the indicated concentrations of DDATHF in D-MEM medium supplemented with 10% dialyzed horse serum in the presence or absence of 16 μM MeSAdo. Viable cell numbers were compared with controls by the MTT colorimetric assay. The results are the average of triplicate experiments. ○, SK-MES-1 incubated with DDATHF alone; ●, SK-MES-1 incubated with DDATHF and MeSAdo; □, A-549 incubated with DDATHF alone; ■, A-549 incubated with DDATHF and MeSAdo.

ative malignant cells might become more dependent on an exogenous supply of methionine because of no methionine synthesis from MTR-1-P. We carried out experiments to determine whether the proliferation of the enzyme-negative cells could be selectively prevented in methionine-depleted medium supplemented with MeSAdo. The enzyme-positive (SK-MES-1) and -negative (A-549) cell lines were cultured for 4 days in (*a*) methionine-containing medium supplemented with 10% dialyzed horse serum, (*b*) methionine-depleted medium supplemented with 10% dialyzed horse serum, and (*c*) methionine-depleted medium supplemented with 10% dialyzed horse serum and 16 μM MeSAdo. The proliferation of both cell lines, especially of the enzyme-negative A-549 cells, was markedly retarded in medium lacking methionine (27 and 3.3% growth of control for SK-MES-1 and A-549 cells, respectively). When MeSAdo was added to the same medium, it augmented the growth of enzyme-positive SK-MES-1 cells (77% growth of control). However, the proliferation of enzyme-negative A-549 cells was not enhanced in the presence of MeSAdo (4.3% growth of control) (Table 3). These data indicate that the growth of the MeSAdo phosphorylase-negative cells may be blocked selectively in methionine-depleted, MeSAdo-supplemented medium.

DISCUSSION

The absence of MeSAdo phosphorylase was first found in four murine leukemic cell lines (18). Among established human malignant tumor cell lines, 7 (23%) of 31 cell lines analyzed lacked detectable MeSAdo phosphorylase (1). In contrast, all 16 cell lines of nonmalignant origin, derived from lymphoblasts, fibroblasts, and epithelial cells, contained substantial enzyme activity (1). The enzyme deficiency is not confined to tissue culture cells. Several human leukemias, as well as a few melanomas, one lung squamous carcinoma, and a rectal adenocarcinoma, have been reported to lack MeSAdo phosphorylase catalytic activity (2, 19). To facilitate screening for MeSAdo phosphorylase deficiency, we have generated antibodies to the enzyme and have developed a simple, semiquantitative immunoblot assay (3). Recently, this assay was successfully used to demonstrate that 75% of human glioma cell lines and primary malignant gliomas lack MeSAdo phosphorylase (3).

We have now used the immunoassay to quantitate MeSAdo phosphorylase in NSCLC cell lines and primary tumors. Nine (31%) of 29 NSCLC cell lines and primary tumors were completely MeSAdo phosphorylase deficient. The enzyme deficiency was most frequent in adenocarcinoma (6 of 10 enzyme-negative NSCLCs). All normal human tissues, including lung, are known to contain MeSAdo phosphorylase (1). Moreover, other studies have shown that RBCs from patients with MeSAdo phosphorylase-deficient neoplasms, including lung squamous cell carcinoma, have normal enzyme activity (2). Thus, MeSAdo phosphorylase deficiency in human NSCLCs is related to their malignant phenotype.

Lung cancer is the leading cause of death from cancer in men and the second leading cause in women. There are about 150,000 cases diagnosed each year in the United States, with almost 90% of the patients dying from the disease within 2 years of diagnosis (20). Therefore, it is of critical importance to develop procedures for its early detection that are coupled to effective therapeutic strategies. As depicted in Fig. 1, MeSAdo phosphorylase is related to the polyamine biosynthetic pathway and also to a pathway for the recycling of the stoichiometric products, adenine and MTR-1-P, to adenine nucleotides and methionine, respectively. Based on this metabolic difference between some malignant cells and normal cells, drugs such as azaserine and methotrexate have been used previously for the selective growth inhibition of MeSAdo phosphorylase-deficient leukemia cells (1). Neither enzyme-positive nor -negative cells proliferated in a medium containing azaserine alone or containing methotrexate supplemented with uridine and thymidine. But if MeSAdo was added to the same media, only cells containing MeSAdo phosphorylase divided, whereas enzyme-negative cells did not. However, because thymidylate synthesis is also inhibited by methotrexate and because azaserine is too toxic for clinical use, these strategies have not been tested *in vivo*. Recently, a new folate analogue, DDATHF, was found to inhibit glycinamide ribonucleotide transformylase, one of the key folate-dependent enzymes in *de novo* purine synthesis (13). The cytotoxic effects of DDATHF are reversed by purines (12). Our data indicate that DDATHF combined with MeSAdo can selectively prevent the proliferation of MeSAdo phosphorylase-negative cells in medium depleted of exogenous purines by dialysis. *In vivo*, purines can be obtained from dietary sources. However, in phase I studies, DDATHF has been found to have significant antitumor activity against various murine

Table 3 *Selective killing of MeSAdo phosphorylase-negative cells*

Cells were seeded at a density of 5×10^4 cells/ml in methionine-depleted medium supplemented with 10% dialyzed horse serum in the presence or absence of 16 μM MeSAdo. Control cell cultures contained methionine-containing medium supplemented with 10% dialyzed horse serum. After 4 days, viable cell numbers were determined by MTT assay. The results are the means ± SEM ($n = 10$).

Cell line	Enzyme status[a]	Growth (% of control)[b]	
		Methionine free	
		Without MeSAdo	With MeSAdo
SK-MES-1	+	27 ± 2.6	77 ± 4.7
A-549	–	3.3 ± 0.6	4.3 ± 1.1

[a] +, present; –, absent.
[b] Percentage of control growth = 100 × (cell growth in methionine-depleted medium with or without MeSAdo)/(cell growth in methionine-containing medium).

and human solid tumors (21, 22). This suggests that diet alone cannot supply sufficient purines to support the proliferation of the malignant cells. Furthermore, folinic acid and folic acid decreased the toxicity, but not the antitumor activity, of DDATHF (21, 22). The increased tumor specificity of DDATHF coadministered with folinic acid or folic acid is likely due to the competitive interaction of these compounds with membrane-associated folate-binding proteins (23). The specificity of DDATHF plus MeSAdo for MeSAdo phosphorylase is based on an alternative biochemical rationale. Therefore, it is conceivable that one can use DDATHF combined with folinic acid/folic acid and MeSAdo to prevent the growth of enzyme-negative malignant cells more specifically than with DDATHF combined with either folinic acid/folic acid or MeSAdo.

Methionine dependency is a well-known characteristic of some malignant cells (24, 25), although its metabolic basis is unclear. Since MTR-1-P, one of the products of the MeSAdo phosphorylase reaction, is recycled to methionine, the loss of the enzyme will interfere with methionine salvage from MTR-1-P. Our data indicate that only enzyme-negative NSCLC cells fail to grow *in vitro* in methionine-depleted, MeSAdo-supplemented medium. However, we did not achieve two full logs of cell kill during the period of exposure. Although this might theoretically limit the clinical effectiveness of the chemotherapeutic protocol, Kreis et al. (26–29) have shown that purified L-methioninase (L-methionine-α-deamino-γ-mercaptomethane-lyase), an L-methionine-degrading enzyme, effectively lowered plasma methionine levels and significantly inhibited the growth of Walker 256 carcinoma in rats, with negligible toxicity (25). Taken together with our data, these results suggest that chemotherapy with L-methioninase and MeSAdo may be selective for MeSAdo phosphorylase-negative NSCLC cells *in vivo*, under conditions in which normal cells can utilize MeSAdo to supplement methionine through the recycling pathway of MTR-1-P, the product of MeSAdo cleavage. Since L-methioninase, in the presence of pyridoxal 5′-phosphate, also catalyzes the α,γ elimination of L-homocysteine (30), the antitumor activity of L-methioninase and MeSAdo against enzyme-negative NSCLCs should not be prevented by the reconversion of homocysteine to methionine.

Thus, the common presence of MeSAdo phosphorylase deficiency in human NSCLC may facilitate the selective chemotherapy of this common malignancy.

ACKNOWLEDGMENTS

We thank Eddie Nguyen for technical assistance. We are also grateful to Nancy Noon for secretarial help.

REFERENCES

1. Kamatani, N., Nelson-Rees, W. A., and Carson, D. A. Selective killing of human malignant cell lines deficient in methylthioadenosine phosphorylase, a purine metabolic enzyme. Proc. Natl. Acad. Sci. USA, *78:* 1219–1223, 1981.
2. Fitchen, J. H., Riscoe, M. K., Dana, B. W., Lawrence, H. J., and Ferro, A. J. Methylthioadenosine phosphorylase deficiency in human leukemias and solid tumors. Cancer Res., *46:* 5409–5412, 1986.
3. Nobori, T., Karras, J. G., Della Ragione, F., Waltz, T. A., Chen, P. P., and Carson, D. A. Absence of methylthioadenosine phosphorylase in human gliomas. Cancer Res., *51:* 3193–3197, 1991.
4. Pegg, A. E., and Williams-Ashman, H. G. Phosphate-stimulated breakdown of 5′-methylthioadenosine by rat ventral prostrate. Biochem. J., *115:* 241–247, 1969.
5. Kamatani, N., and Carson, D. A. Dependence of adenine production upon polyamine synthesis in cultured human lymphoblasts. Biochem. Biophys. Acta, *675:* 344–350, 1981.
6. Backlund, P. S., Jr., and Smith, R. A. Methionine synthesis from 5′-methylthioadenosine in rat liver. J. Biol. Chem., *244:* 1533–1535, 1981.
7. Backlund, P. S., Jr., and Smith, R. A. 5′-Methylthioadenosine metabolism and methionine synthesis in mammalian cells grown in culture. Biochem. Biophys. Res. Commun., *108:* 687–695, 1982.
8. Backlund, P. S., Jr., Chang, C. P., and Smith, R. A. Identification of 2-keto-4-methylthiobutyrate as an intermediate compound in methionine synthesis from 5′-methylthioadenosine. J. Biol. Chem., *257:* 4196–4202, 1982.
9. Carson, D. A., Willis, E. H., and Kamatani, N. Metabolism to methionine and growth stimulation by 5′-methylthioadenosine and 5′-methylthioinosine in mammalian cells. Biochem. Biophys. Res. Commun., *112:* 391–397, 1983.
10. Kamely, D., Littlefield, J. W., and Erbe, R. W. Regulation of 5-methyltetrahydrofolate: homocysteine methyltransferase activity by methionine, vitamin B_{12}, and folate in cultured baby hamster kidney cells. Proc. Natl. Acad. Sci. USA, *70:* 2585–2589, 1973.
11. Griffith, O. W. Mammalian sulfur amino acid metabolism: an overview. Methods Enzymol., *143:* 366–376, 1987.
12. Beardsley, G. P., Moroson, B. A., Taylor, E. C., and Moran, R. G. A new folate antimetabolite, 5,10-dideaza-5,6,7,8-tetrahydrofolate is a potent inhibitor of *de novo* purine synthesis. J. Biol. Chem., *264:* 328–333, 1989.
13. Baldwin, S. W., Tse, A., Gossett, L. S., Taylor, E. C., Rosowsky, A., Shih, C., and Moran, R. G. Structural features of 5,10-dideaza-5,6,7,8-tetrahydrofolate that determine inhibition of mammalian glycinamide ribonucleotide formyltransferase. Biochemistry, *30:* 1997–2006, 1991.
14. Pizzorno, G., Sokoloski, J. A., Cashmore, A. R., Moroson, B. A., Cross, A. D., and Beardsley, G. P. Intracellular metabolism of 5,10-dideazatetrahydrofolic acid in human leukemia cell lines. Mol. Pharmacol., *39:* 85–89, 1991.
15. Bradford, M. M. A rapid and sensitive method for the quantitation of microgram quantities of protein utilizing the principle of protein-dye binding. Anal. Biochem., *72:* 248–254, 1976.
16. Laemmli, U. K. Cleavage of structural proteins during the assembly of the head of bacteriophage T4. Nature (Lond.), *227:* 680–685, 1970.
17. Scudiero, D., Shoemaker, R. H., Paul, K. D., Monks, A., Tierney, S., Nofziger, T. H., Currens, M. J., Seniff, D., and Boyd, M. R. Evaluation of a soluble tetrazolium/formazan assay for cell growth and drug sensitivity in culture using human and other tumor cell lines. Cancer Res., *48:* 4827–4833, 1988.
18. Toohey, J. I. Methylthio group cleavage from methylthioadenosine. Description of an enzyme and its relationship to the methylthio-requirement of certain cells in culture. Biochem. Biophys. Res. Commun., *78:* 1273–1280, 1977.
19. Kamatani, N., Yu, A. L., and Carson, D. A. Deficiency of methylthioadenosine phosphorylase in human leukemic cells *in vivo*. Blood, *60:* 1387–1391, 1982.
20. Minna, J. D., Pass, H., Glatstein, E., and Ihde, D. C. Lung cancer. *In:* V. T. DeVita, Jr., S. Hellman, and S. A. Rosenberg (eds.), Cancer: Principles and Practice of Oncology, pp. 591–705. Philadelphia, PA: J. B. Lippincott, 1989.
21. Pagani, O., Sessa, C., deJong, J., Kern, H., Hatty, S., Schmitt, H., and Cavalli, F. Phase I studies of lometrexol (DDATHF) given in combination with leucovorin. Proc. Am. Soc. Clin. Oncol., *11:* 109, 1992.
22. Young, C. W., Currie, V. E., Muindi, J. F., Saltz, L. B., Pisters, K. M. W., Esposito, A. J., and Dyke, R. W. Improved clinical tolerance of lometrexol with oral folic acid. Proc. Am. Assoc. Cancer Res., *33:* 406, 1992.
23. Jansen, G., Westernhof, G. R., Kathmann, I., Rijksen, G., and Schornagel, J. H. Growth-inhibitory effects of 5,10-dideazatetrahydrofolic acid on variant murine L1210 and human CCRF-CEM leukemia cells with different membrane-transport characteristics for (anti)folate compounds. Cancer Chemother. Pharmacol., *28:* 115–117, 1991.
24. Hoffman, R. M. Methionine dependence in cancer cells: a review. In Vitro, *18:* 421–428, 1982.
25. Kreis, W. Methionine dependency of malignant tumors. J. Natl. Cancer Inst., *83:* 725, 1991.
26. Kreis, W., and Hession, C. Isolation and purification of L-methionine-α-deamino-γ-mercaptomethane-lyase (L-methioninase) from *Clostridium sporogense*. Cancer Res., *33:* 1862–1865, 1973.
27. Kreis, W. Tumor therapy by deprivation of L-methionine: rationale and results. Cancer Treat. Rep., *63:* 1069–1072, 1979.
28. Kreis, W., Baker, A., Ryan, V., Effect of nutritional and enzymatic methionine deprivation upon human normal and malignant cells in tissue culture. Cancer Res., *40:* 634–641, 1980.
29. Kreis, W., and Hession, C. Biological effects of enzymatic deprivation of L-methionine in cell culture and an experimental tumor. Cancer Res., *33:* 1866–1869, 1973.
30. Esaki, N., and Soda, K. L-Methionine γ-lyase from *Pseudomonas putida* and *Aeromonas*. Methods Enzymol., *143:* 459–465, 1987.
31. Mountain, C. F. A new international staging system for lung cancer. Chest, *89*(Suppl.): 225s–235s, 1986.

quently removed, then progressive renal failure, characterized by glomerular sclerosis, interstitial fibrosis and uraemia, can follow[11]. We suggest that the fibrosis in treated kidneys results from damage sustained before taxol was administered. Histological examination of the brain, heart, lung, liver and spleen of taxol-treated polycystic mice did not reveal any gross abnormalities. Normal control mice ($n=6$) treated for 200 days with weekly doses of taxol have normal kidney histology. In addition to the survival data and renal histology, the retardation of disease progression in taxol-treated *cpk* mice was confirmed by measurements of the kidney weight, body weight and serum creatinine levels (Table 1).

Because taxol interferes specifically with microtubule functions[12], it has antimitotic properties. Inhibitors of DNA synthesis were therefore evaluated for their ability to inhibit *cpk* cyst formation *in vivo*. Weekly interperitoneal injection of 15 µl of 1.1 mg ml^{-1} methotrexate produced a reduction in growth comparable to that in mice treated with 15 µl of 10 mg ml^{-1} taxol. This sublethal weekly methotrexate treatment had no effect on the survival of polycystic *cpk* mice (Fig. 2). Sublethal doses of cytosine arabinoside (ara-C) were also ineffective (data not shown). Moreover, as doses of methotrexate and ara-C sufficient to inhibit DNA synthesis did not block lumen formation *in vitro*, the increased proliferative potential of PKD epithelia[13,16] probably does not play an important part in cyst formation but may generate cells to line expanding cysts.

Apart from their role in mitosis, microtubules contribute to and maintain cellular architecture. They also participate in membrane vesicle trafficking[17], exocytosis and endocytosis[18], and the movement of intermediate vesicles between the endoplasmic reticulum and Golgi[19,20]. During the formation of trophectoderm, microtubules play important parts in the biogenesis of epithelial polarity[21,22]. After polarity is established, specific pathways deliver secreted and membrane proteins to their target membrane domains and, although these sorting processes are not well characterized, microtubules are clearly involved[23,24]. Our data implicate the microtubule network in the genesis of PKD cysts both *in vitro* and *in vivo*. It remains to be determined whether altered tubulins or altered microtubule-associated proteins are primary lesions in *cpk* mice or other forms of PKD. It is feasible that aberrations of cellular functions mediated by microtubules may lead to the apical mislocation of Na^+, K^+-ATPase and epidermal growth factor receptors in both human[25] and murine PKD[26]. Finally, the ability of taxol to prevent the uraemic death in a mouse model for PKD suggests that taxol or its analogues may be useful in the treatment of human polycystic kidney diseases. □

Received 7 October 1993; accepted 4 February 1994.

1. Russell, E. S. & McFarland, E. *Mouse Newsletter* **56**, 40 (1977).
2. Preminger, G. M., Koch, W. E., Fried, F. A., McFarland, E. & Murphy, E. M. *J. Urol.* **127**, 556–560 (1982).
3. Avner, E. D. *et al. Pediat. Nephrol.* **1**, 587–596 (1987).
4. Wilson, P. D., Schrier, R. W., Breckon, R. D. & Gabow, P. A. *Kidney Int.* **30**, 371–378 (1986).
5. Yang, A. H., Gould, K. J. & Oberley, T. D. *In Vitro Cell Dev. Biol.* **23**, 34–46 (1987).
6. Carone, F. A., Nakamura, S., Schumacher, B. S., Punyarit, P. & Bauer, K. D. *Kidney Int.* **35**, 1351–1357 (1989).
7. Valentich, J. D., Tchao, R. & Leighton, J. *J. Cell Physiol.* **100**, 291–304 (1979).
8. Mangoo, K. R. *et al. FASEB J.* **3**, 2629–2632 (1989).
9. Neufeld, T. K. *et al.* **43**, 1222–1236 (1992).
10. Fleming, T. P. & Johnson, M. H. *A. Rev. cell. Biol.* **4**, 459–485 (1988).
11. Brenner, B. M. *Kidney Int.* **23**, 647–655 (1983).
12. Schiff, P. & Horwitz, S. *Proc. natn. Acad. Sci. U.S.A.* **77**, 1561–1565 (1980).
13. Gattone, V. H. *et al. Lab. Invest.* **58**, 231–238 (1988).
14. Cowley, B. D. J., Smardo, F. L. J., Grantham, J. J. & Calvert, J. P. *Proc. natn. Acad. Sci. U.S.A.* **84**, 8394–8398 (1987).
15. Avner, E. D., Sweeney, W. E. J., YOung, M. C. & Ellis, D. *Pediat. Nephrol.* **2**, 210–218 (1988).
16. Cowley, B., Chadwick, L., Grantham, J. & Calvert, J. *J. Am. Soc. Neph.* **1**, 1048–1053 (1991).
17. Kelly, R. *Cell* **60**, 5–7 (1990).
18. Rogalski, A. A., Bergmann, J. E. & Singer, S. J. *J. Cell Biol.* **99**, 1101–1109 (1984).
19. Thyberg, J. & Moskalewski, S. *Expl Cell Res.* **159**, 1–16 (1985).
20. Lippincott-Schwartz, J. *et al. Cell* **60**, 821–836 (1990).
21. Bloom, T. *Development* **108**, 159–171 (1989).
22. Maro, R., Gueth-Hallonet, C. J. A. & Antony, C. *Development* Vol. 1. suppl. 1, 17–25 (1991).
23. Parczyk, K., Haase, W. & Kondor-Koch, C. *J. biol. Chem.* **264**, 16837–16846 (1989).
24. De Almeida, J. B. & Stow, J. L. *Am. J. Physiol.* **259**, C691–C700 (1991).
25. Wilson, P. D. *et al. Am. J. Physiol.* **260**, F420–F430 (1991).
26. Avner, E., Sweeney, W. & Nelson, W. *Proc. natn. Acad. Sci. U.S.A.* **89**, 7447–7451 (1992).
27. Slot, C. *Scand. J. Clin. Lab. Invest.* **17**, 381–387 (1965).

ACKNOWLEDGEMENTS. This work is supported by NIH grants and A.S.W. is a National Kidney Research Fund Senior Fellow. Normal and polycystic human kidneys are obtained from the International Institute for the Advance of Medicine (Exton, Pennsylvania), the National Disease Research Interchange (Philadelphia) and the Polycystic Kidney Research Foundation (Kansas City).

Deletions of the cyclin-dependent kinase-4 inhibitor gene in multiple human cancers

Tsutomu Nobori*, Kaoru Miura*, David J. Wu*, Augusto Lois*, Kenji Takabayashi† & Dennis A. Carson*

* Department of Medicine, University of California, San Diego, 9500 Gilman Drive, La Jolla, California 92093-0663, USA
† CIBA-GEIGY Pharmaceuticals Division, CH-4002 Basel, Switzerland

CYTOGENETIC abnormalities of chromosome 9p21 are characteristic of malignant melanomas[1,2], gliomas[3], lung cancers[4] and leukaemias[5]. From a panel of 46 human malignant cell lines, we localized by positional cloning the most frequently deleted region on 9p21. Sequence analysis of the isolated fragment reveals two open reading frames identical to the recently described complementary DNA for the inhibitor of cyclin-dependent kinase 4 (CDK4)[6]. Polymerase chain reaction and Southern blot analysis confirmed the frequent deletion or rearrangement of the CDK4-inhibitor gene in melanomas, gliomas, lung cancers and leukaemias, and the absence of detectable gene transcripts. One carcinoma had a deletion entirely within the CDK4-inhibitor gene. The CDK4-inhibitor gene from a patient with dysplastic nevus syndrome had a germline nonsense mutation. The CDK4 inhibitor is thought to be a physiological suppressor of proliferation. Cells unable to produce the inhibitor may be prone to neoplastic transformation.

Many malignant cell lines with chromosome 9p21 deletions either lack the enzyme methylthioadenosine phosphorylase (MTAP), or have hemizygous or homozygous deletions of the interferon-α (*IFN-α*) gene cluster[5,7,8]. The T98G glioma cell line has a small 9p deletion centromeric to the *IFN-α* locus, but has normal methylthioadenosine phosphorylase activity[3]. These results suggested that the putative tumour-suppressor gene on chromosome 9p resided between the *MTAP* and *IFN-α* loci.

MTAP cDNA was isolated and used to probe a human placenta λ-phage library. A 2-kilobase (kb) *Hin*dIII fragment (clone 7-2) contained the 3′ end of the *MTAP* gene by sequence analysis. Chromosome walking was performed, starting with the 3′ end of *MTAP*. Several screening cycles of P1 phage[9], and subsequent λ-phage libraries led to the isolation of clones encompassing the deleted region in T98G. Restriction fragments of these phage were subcloned, partially sequenced, and mapped by Southern blotting and pulsed-field gel electrophoresis. Figure 1 shows the map of human chromosome 9p21 between the *MTAP* and interferon-β (*IFN-β*) gene loci, focusing on the deleted segment in T98G.

The polymerase chain reaction (PCR) was used to determine the frequency of deletion of several-tagged sites (STS) from chromosome 9p in 46 different human malignant cell lines (Table 1). Depending on the cell type, either STS *54F* or STS *5BS* was deleted most frequently. These results focused our attention on the 50-kb region between STS *54F* and STS *5BS*.

Eight malignant cell lines with breakpoints between *54F* and *5BS* were then analysed by STS-PCR, with new probes from the intervening region. The deletion maps are shown at the

TABLE 1 Homozygous loss of chromosome 9p loci in human cancer cells

Cell line (number)		Frequency of negative STS-PCR (%)								
		MTAP	3.21	*2F*	*54F*	*CDK4I*	*5BS*	*71F*	*3.3B*	*IFN-α8*	*IFN-β*
Melanoma	(13)	30.8	38.5	53.8	53.8	61.5	61.5	61.5	15.4	7.7	0
Glioma	(8)	62.5	75.0	87.5	87.5	87.5	75.0	75.0	62.5	62.5	25.0
Lung cancer	(11)	27.3	27.3	27.3	27.3	36.4	36.4	36.4	9.1	9.1	0
Leukaemia	(14)	50.0	50.0	64.3	64.3	64.3	57.1	57.1	28.6	28.6	21.4

Homozygous deletion of these loci was detected by STS-PCR. PCR, except for *CDK4I* and *CDK4I3'*, was carried out in a total volume of 20 μl, containing 0.1 μg of genomic DNA, 1 × PCR buffer (10 mM Tris-HCl, pH 8.3, 50 mM KCl, 1.5 mM $MgCl_2$, 0.01% gelatin), 200 μM of each dNTP, 20 ng each of sense and antisense primers, and 0.5 units of *Taq* DNA polymerase. Thirty cycles were performed, each cycle consisting of denaturation (94 °C, 1 min), annealing (50 °C or 55 °C, 1 min), and extension (72 °C, 1 min). 10-μl aliquots were resolved on 2% agarose gels. The locations of the STS-PCR sites are shown in Fig. 1*a*. CDK4I-PCR was performed as described for Fig. 2.

bottom of Fig. 1. A 19-kb λ-phage clone (10B1) identified the most frequently deleted site. We concluded that the 10B1 phage should contain part of the putative tumour-suppressor gene.

The sequence of a plasmid subclone (10B1-10) from 10B1 contained a 306-base-pair (bp) open reading frame with sequence identity to the 3' region of the recently described cDNA for the human cyclin-dependent kinase-4 (CDK4) inhibitor, apart from the last 15 bp[8] (Fig. 2*a*). The 3' end of the coding region, and the 3' non-coding region, was located 2.6 kb towards *MTAP*. The 5' end of the gene was telomeric to the deleted region in T98G (Fig. 1). We rescreened the 46 malignant cell lines with STS-PCR primers, corresponding to the isolated fragment of the CDK4-inhibitor gene, designated *CDK4I* in Table 1. Sixty-one per cent of melanomas, 87% of gliomas, 36% of non-small-cell lung cancers, and 64% of leukaemias have homozygous deletions of the *CDK4I* gene fragment. Melanoma cell line WM266-4 has only the 5' end of the CDK4-inhibitor gene deleted. It was positive for STS *CDK4I*, negative for STS *5BS*, and produced an abnormal 7.0-kb band after *Eco*RI digestion, electrophoresis and hybridization to a probe from the 5' region of the CDK4-inhibitor gene (Fig. 2*c*). On the other hand, melanoma cell line SK-MEL-31 has only the 3' end of the CDK4-inhibitor gene deleted. It was negative for STS *CD4KI* (Fig. 2*b*), but produced a normal 4.0-kb band, indistinguishable from

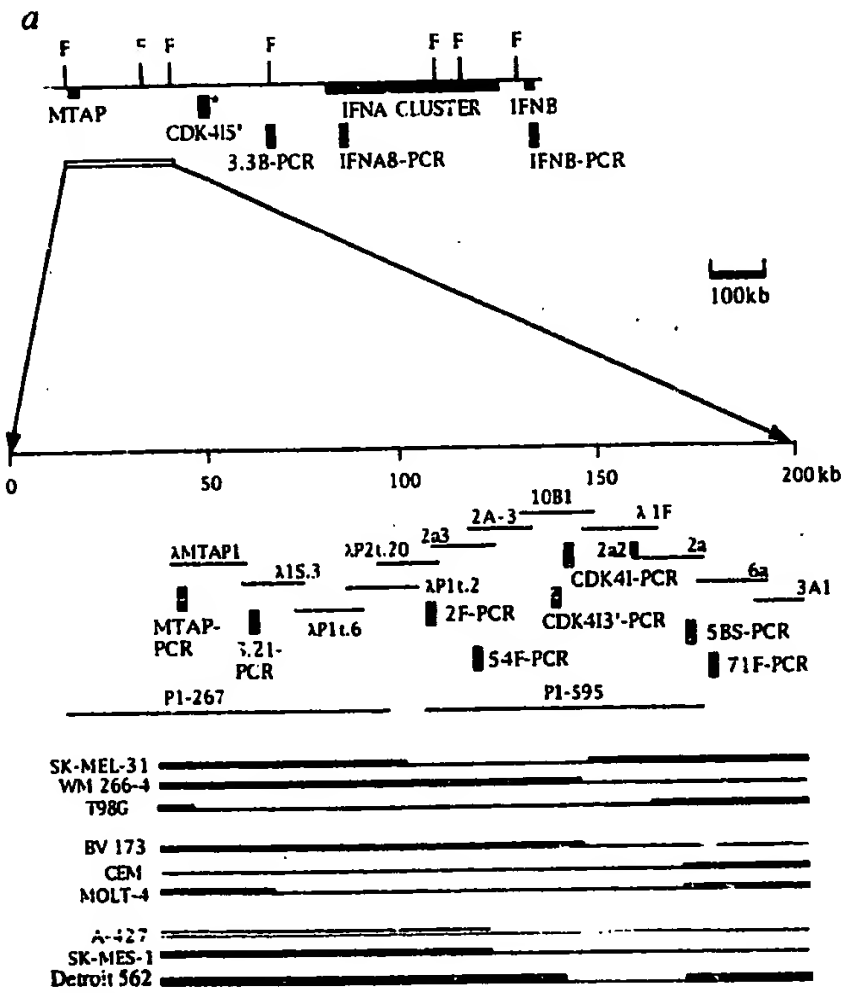

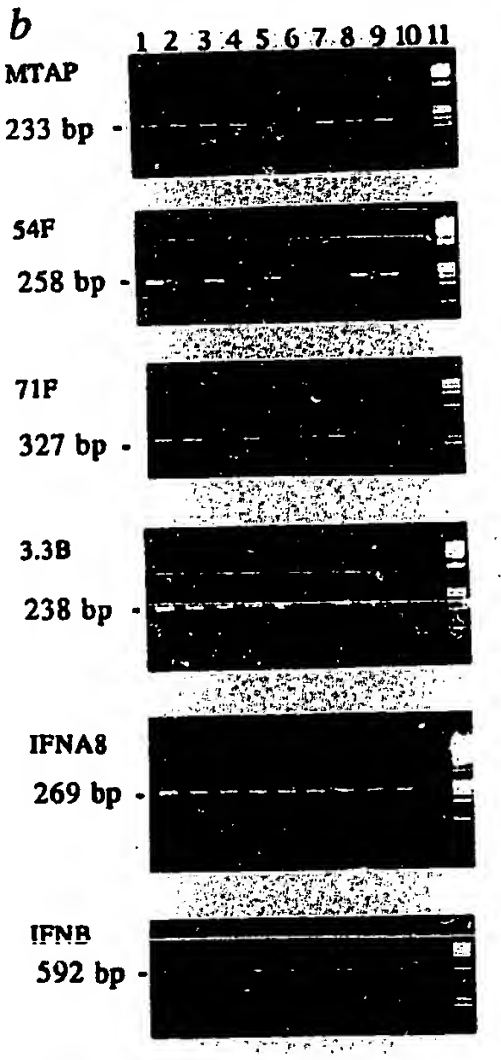

FIG. 1 Physical map of chromosome 9p21 between the *MTAP* and *IFN-β* gene loci. *a*, The P1 phage clones and λ-phage clones are indicated by thin lines. The sequence-tagged sites (STSs) used for PCR are shown as cross-hatched bars. The *CDK4I* and *CDK4I3'* sequences come from phage 10B1 and are separated by a 2.6-kb intron. These 11 STS-PCR assays localized the approximate breakpoints in the nine malignant cell lines with the most informative deletions. SK-MEL-31 and WM 266-4 are melanomas; T98G is a glioma; BV173, CEM, and MOLT-4 are leukaemias; A-427 and SK-MES-1 are non-small-cell lung cancers; Detroit 562 is a pharyngeal carcinoma. Homozygous deletions are indicated by thin horizontal lines. Asterisk indicates that the location of *CDK4I5'* in the 190-kb *Sfi*I fragment is not precise. F, *Sfi*I. *b*, STS-PCR analysis. All STS-PCR amplified fragments of the expected size in J640-51 cells containing a single human chromosome 9 on a Chinese hamster background (data not shown). Lanes: 1, human placenta; 2, SK-MEL-31; 3, WM 266-4; 4, T98G; 5, BV173; 6, CEM; 7, MOLT-4; 8, A-427; 9, SK-MES-1; 10, no template DNA; 11, DNA markers.

METHODS. *a*, The λMTAP1 clone was obtained by screening a human placenta λFIX II genomic library (Stratagene) with MTAP cDNA. A 2-kb *Hin*dIII fragment containing the 3' end of the *MTAP* gene was used for chromosome walking in human P1 phage (Genome Systems), λ-phage (Stratagene), and chromosome-9-specific charon-40 phage (LL09NL01, ATCC) libraries. Clones encompassing the 190-kb region were isolated, subcloned, partially sequenced, and mapped by southern and pulsed-field-gel blotting. *b*, STS-PCR was developed on the basis of the partial sequences of the subclones. PCR amplification was done under conditions described in Table 1. PCR products were resolved on a 2% agarose gel.

a

CDK4I

```
GAATTCATTG TGTACTGAAG AATGGATAGA GAACTCAAGA Aggaaattgg aaactggaag     60
cAAATGTAGG GGTAATTAGA CACCTGGGGC TTGTGTGGGG GTCTGCTTGG CGGTGAGGGG    120
GCTCTACACA AGCTTCCTTT CCGTCATGCC GGCCCCCACC CTGGCTCTGA CCATTCTGTT    180
CTCTCTGGca ggtcatgatg atgggcagCG CCCGAGTGGC GGAGCTGCTG CTGCTCCACG    240
GCGCGGAGCC CAACTGCGCC GACCCCGCCA CTCTCACCCG ACCCGTGCAC GACGCTGCCC    300
GGGAGGGCTT CCTGGACACG CTGGTGGTGC TGCACCGGGC CGGGGGCGCG CTGGACGTGC    360
GCGATGCCTG GGGCGGTCTG CCCGTGGACC TGGCTGAGGA GCTGGGCCAT CGCGATGTCG    420
CACGGTACCT GCGCGCGGCT GCGGGGGGCA CCAGAGGCAG TAACCATGCC CGCATAGATG    480
CCGCGGAAGG TCCCTCAGGT GAGGACTGAT GATCTNAGAA TTTGNCCCCT GAGAGCTTCC    540
```

CDK4I3'

```
TTTTCTTTCT GCCCTCTGCA GACATCCCCG ATTGAAAGAA CCAGAGAGGC TCTGAGAAAC     60
CTCCGGAAAC TTAGATCATC AGTCACCGAA GGTCCTACAG GGCCACAACT GCCCCCGCCA    120
CAACCCACcc cgctttcgta gttttcatTT AGAAAATAGA GCTTTTAAAA ATGTCCTGCC    180
TTTTAACGTA GATATATGCC TTCCCCCACT ACCGTAAATG TCCATTTATA TCATTTTTTA    240
TATATTCTTA TAAAAATGTA AAAAAGAAAA ACACCGCTTC TGCCTTTTCA CTGTGTTGGA    300
GTTTTCTGGA GTGAGCACTC ACGCCCTAAG CGCACATTCA TGTGGGCATT TCTTGCGAGC    360
CTCGCAGCCT CCGGAAGCTG TCGACTTCAT GACAAGCATT TTGTGAACTA GGGAAGCTCA     42
GGGGGGTTAC TGGCTTCTCT TGAGTCACAC TGCTAGCAAA TGGcAgaccc aaagctcaaa    480
taaAAATAAA ATAATTTTCA TTCATTCACT CATTTATTGT                          520
```

b

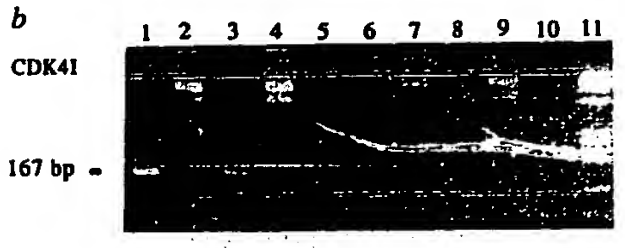

FIG. 2 Absence or rearrangement of the CDK4-inhibitor gene in malignant cell lines. *a*, Partial sequence of the genomic CDK4-inhibitor gene. The genomic sequence designated *CDK4I* has a 306-bp open reading frame with complete sequence identity to CDK4-inhibitor cDNA, from nucleotides 192 to 497 (underlined). The CDK4I3' sequence has a short open reading frame (underlined) corresponding to the last 15 bp of the coding region, with a stop codon and the 3' non-coding sequence, except for two nucleotides (T at 197 and A at 493). *b*, PCR analysis of malignant cell lines. Primers for *CDK4I*, shown as lower-case letters in *a*, were used to amplify an expected 167-bp product in human placenta (lane 1) SK-MEL-31 (lane 2), WM 266-4 (lane 3), T98G (lane 4), BV173 (lane 5), CEM (lane 6), MOLT-4 (lane 7), A-427 (lane 8), and SK-MES-1 (lane 9). Lane 10 has no template DNA. Lane 11 shows DNA markers. *c*, Southern blot analysis of melanoma cell lines hybridized to probes 2a2 and CDK4I5'. In *Sfi*I-digested pulsed-field blots, 2a2 hybridized to a 54-kb fragment. CDK4I5' hybridized to a 190-kb fragment which was

c

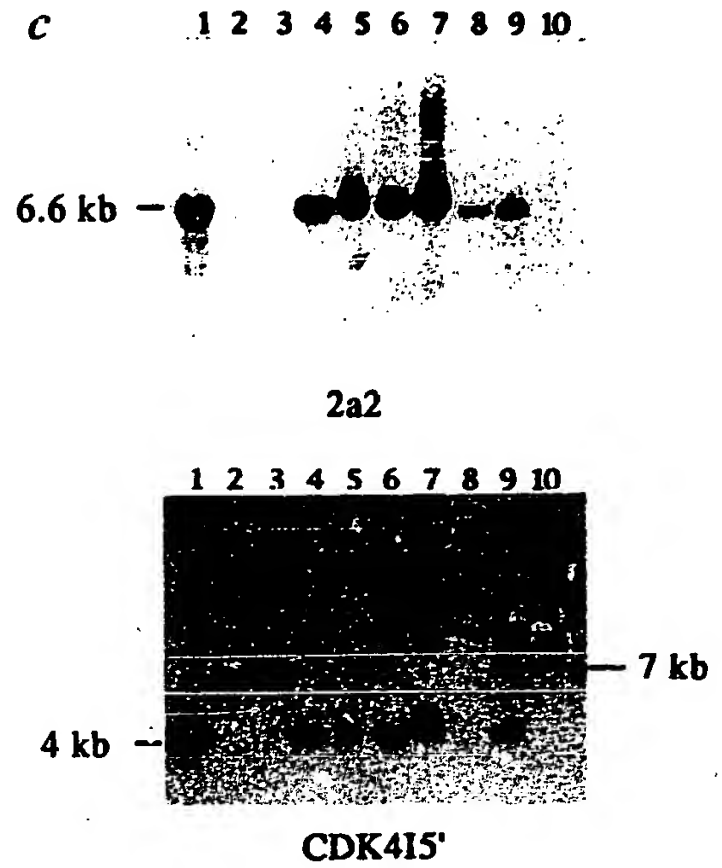

also detected with the 3.3B probe in the same blot (data not shown). Lanes: 1, human placenta; 2, Hs294T; 3, HT144; 4, RPMI7951; 5, SK-MEL-1; 6, SK-MEL-2; 7, SK-MEL-3; 8, SK-MEL-28; 9, SK-MEL-31; 10, WM 266-4.

METHODS. *a*, Phage DNA of clone 1081 was digested with *Eco*RI and subcloned into *Eco*RI-cut pBluescriptII SK(+) (Stratagene). Subclones were subjected to automated DNA sequencing. The 4.2-kb subclone 1081-10 contained both the *CDK4I* and the *CDK4I3'* sequences. *b*, PCR amplification was carried out as described in Table 1 legend except that 35 cycles were performed and annealing was at 64 °C and extension at 72° C. PCR was followed by gel electrophoresis. *c*, DNAs from human placenta and melanoma cell lines were digested with *Eco*RI, resolved on a 0.8% agarose gel, and transferred to nylon membranes. 2a2 is a 1.3-kb *Eco*RI–*Xho*I fragment of phage clone 2a. CDK4I5' is a 139-bp product generated by RT-PCR. cDNA from cell line H661 was amplified by PCR using a sense primer (5'-AATTCGGCACGAGGCAGCAT-3') and an antisense primer (5'-TTATTTGAGCTTTGGTTCTG-3'). PCR products were subcloned and sequenced. Clone p7-4 contained the 5' sequence of CDK4-inhibitor cDNA. A 139-bp product was amplified from clone p7-4 with a sense primer and a new antisense primer (5'-TCGGCCTCCGACCGTAACTA-3') and used for Southern blotting. Blots were hybridized at 65 °C overnight, washed at 65 °C in 0.1 × SSC containing 0.1% SDS, and exposed to X-ray film. After stripping off radioactivity, the same membrane was rehybridized with probe 2a2.

FIG. 3 Reverse transcriptase-PCR amplification of CDK4-inhibitor mRNA from human malignant cells lines. The glyceraldehyde 3-phosphate dehydrogenase gene (G3PDH) mRNA served as a control. WI-L2 in lane 1 is a normal lymphoblastoid cell line. U937 in lane 2 is a leukaemia cell line. T98G in lane 3 is a glioma cell line. H661 in lane 4, A-549 in lane 5, and SK-MES-1 in lane 6 are non-small-cell lung cancer cell lines. Lane M shows DNA markers. STS-PCR analysis confirmed the presence of STS CDK4I in WI-L2, U937, and H661 (data not shown). T98G and SK-MES-1 have the 9p21 deletions shown in Fig. 1*a*. The deletion in cell line A-549 spans STS *MTAP* to *71F* (data not shown). CDK4-inhibitor mRNA was not detected in cell lines with 9p21 deletions that included the CDK4-inhibitor gene.

METHODS. mRNA was purified with a FastTrack kit (Invitrogen) and was treated with RNase-free DNase I (Pharmacia) using human placenta DNA as a control to ensure complete digestion by DNase I. After first-strand cDNA synthesis with a Stratascript RT-PCR kit (Stratagene), cDNA was amplified with the CDK4I3' primers shown in lower-case in Fig. 2*a* (58 °C annealing and 70 °C extension). Primers for the G3PDH gene (5'-TGGTATCGTGGAAGGACTCATGAC-3' and 5'-ATGCCAGTGAGCTTCCCGTTCAGC-3') amplified a 190-bp product (55 °C annealing and 72 °C

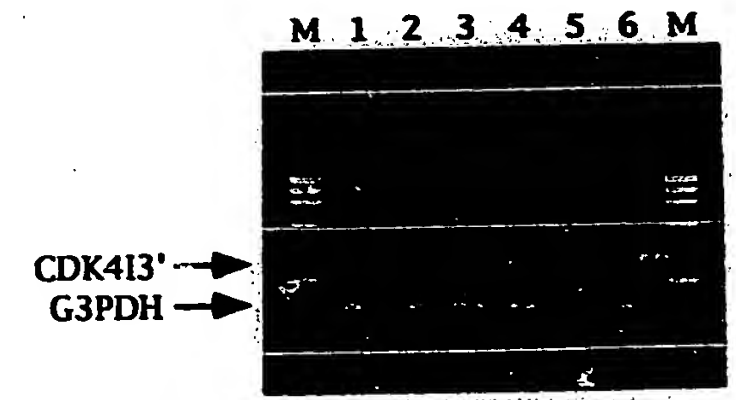

extension). RT-PCRs for CDK4I3' and G3PDH were done separately and resolved on a 2% agarose gel by loading onto the same lanes. As no product was amplified in DNase I-treated human placenta DNA with the CDK4I3' primers, the 355-bp RT-PCR product seen in lanes 1, 2 and 4 was derived from cDNA. Sequence analysis of the RT-PCR products confirmed the CDK4I cDNA sequence.

placental DNA, after *Eco*RI digestion, and hybridization to the 5'-region probe from the CDK4-inhibitor gene. The most informative cell line was Detroit 562 (a pharyngeal carcinoma) which has a 29-kb deletion within the CDK4-inhibitor gene (Fig. 1). It was positive for STS *CDK4I3'*, negative for STS *CDK4I*, but positive for STS *5BS* and STS *7IF*. The last two STSs are centromeric to the 5' end of the CDK4-inhibitor gene.

Reverse transcriptase-polymerase chain reaction (RT-PCR) assays revealed CDK4-inhibitor gene transcripts in normal cells, but not in cancers with established deletions of the CDK4-inhibitor gene (Fig. 3). Collectively, these results indicate that human cells contain a single CDK4-inhibitor gene, which is homozygously deleted or rearranged in the majority of melanomas, gliomas and leukaemias, and in almost one-third of non-small-cell lung cancers.

The complexes formed by CDK4 and the D-type cyclins control passage through the G1 phase of the cell cycle[6]. The inhibitor of CDK4 is a protein of relative molecular mass 16K which binds to and inhibits the catalytic activity of the CDK4/cyclin D enzymes. Because it is a negative regulator of cell-cycle progression, the inhibitor of CDK4 may be inactivated during cancer development[10]. The product of the p53 gene also inhibits growth by stimulating the production of a CDK-inhibitory protein[11,12].

About 10% of melanomas are familial[2]. Linkage analyses have pinpointed the locus for familial melanoma to the region on 9p21 that is deleted in sporadic melanomas[13]. Sequence analysis of the CDK4I coding region of a lymphoblastoid cell line (GM06921) derived from a patient with dysplastic nevus syndrome (familial melanoma) showed a C to T transition at position 166 of the mRNA[6] resulting in a nonsense mutation. Thus the CDK4 inhibitor is a strong candidate for the melanoma susceptibility gene. □

Received 25 February; accepted 28 March 1994.

1. Fountain, J. E. *et al. Proc. natn. Acad. Sci. U.S.A.* **89**, 10557–10561 (1992).
2. Petty, E. M. *et al. Am. J. hum. Genet.* **53**, 98–104 (1993).
3. Olopade, O. I. *et al. Cancer Res.* **52**, 2523–2529 (1992).
4. Olopade, O. I. *et al. Cancer Res.* **53**, 2410–2415 (1993).
5. Olopade, O. I. *et al. Genomics* **14**, 437–443 (1992).
6. Serrano, M., Hannon, G. J. & Beach, D. *Nature* **366**, 704–707 (1993).
7. Nobori, T. *et al. Cancer Res.* **51**, 3193–3197 (1991).
8. Nobori, T. *et al. Cancer Res.* **53**, 1098–10101 (1993).
9. Pierce, J. C. & Sternberg, N. L. *Meth. Enzym.* **210**, 549–574 (1992).
10. Marx, J. *Science* **263**, 319–321 (1994).
11. Harper, J. W., Adami, G. R., Wei, N., Keyomarsi, K. & Elledge, S. J. *Cell* **75**, 805–816 (1993).
12. Xiong, Y. *et al. Nature* **366**, 701–704 (1993).
13. Cannon-Albright, L. A. *et al. Science* **258**, 1148–1152 (1992)

ACKNOWLEDGEMENTS. We thank L. Orvis, A. Larson, P. Tran and B. Morinoue for technical assistance; C. Jones for J640-51 hybrid cells, and L. Bibbs for automated DNA sequencing. Supported by grants from the NIH, the American Cancer Society, the University of California Tobacco Related Diseases Research Program, and the CIBA-GEIGY Corporation.

Pancreatic islet cell toxicity of amylin associated with type-2 diabetes mellitus

Alfredo Lorenzo*, Bronwyn Razzaboni*, Gordon C. Weir† & Bruce A. Yankner*‡

* Department of Neurology, Harvard Medical School and The Children's Hospital, Enders 260, 300 Longwood Avenue, Boston, Massachusetts 02115, USA
† Joslin Diabetes Center and Harvard Medical School, Boston, Massachusetts 02215, USA

THE 37-amino-acid polypeptide amylin is the principal constituent of the amyloid deposits that form in the islets of Langerhans in patients with type-2 diabetes mellitus[1–5], but its role in the pathogenesis of this disease is unresolved[6–8]. In view of the fact that the β-amyloid protein that forms fibrils in Alzheimer's disease is toxic to neurons[9,10], we have investigated whether amylin fibrils could be toxic to pancreatic islet cells. We show here that human amylin is toxic to insulin-producing β-cells of the adult pancreas of rats and humans. This toxicity is mediated by the fibrillar form of the amylin peptide and requires direct contact of the fibrils with the cell surface. The mechanism of cell death involves RNA and protein synthesis and is characterized by plasma membrane blebbing, chromatin condensation and DNA fragmentation, indicating that amylin induces islet cell apoptosis. These findings indicate that amylin fibril formation in the pancreas may cause islet cell dysfunction and death in type-2 diabetes mellitus.

Islet cell cultures were established from adult rat pancreas and cell viability was assessed by a double-fluorescence assay. Exposure to human amylin resulted in substantial rat islet cell death after 24 h (Fig. 1*a*, *b*). Immunocytochemical analysis showed that human amylin caused the degeneration of 97 ± 1% (mean ± s.e.m., $n = 15$; $P < 0.001$ by ANOVA) of insulin-producing islet cells (Fig. 1*c*, *d*). Amylin was also toxic to human islet cells isolated from the pancreas of a 39-year-old woman. Incubation of dissociated human islets with human amylin resulted in the degeneration of 91 ± 2% ($n = 15$; $P < 0.001$) of insulin-producing islet cells (Fig. 1*e*, *f*). Incubation of non-disso-

FIG. 1 Toxicity of human amylin for rat and human pancreatic islet cells. *a*, Control rat islet cells treated with vehicle and then incubated with calcein–AM and propidium iodide. Epifluorescence microscopy shows viable cells which convert the calcein–AM substrate to a green fluorescent product. *b*, Rat islet cells after treatment with 20 μM human amylin for 24 h. There are many dead cells which show red fluorescence due to nuclear uptake of propidium iodide and few viable cells which show green calcein fluorescence. Insulin immunocytochemistry of control (*c*) and human amylin-treated rat islet (*d*) cells; *e*, control, and *f*, human amylin-treated human islet cells; *g*, control, and *h*, human amylin-treated, non-dissociated human islets. Note the degeneration of insulin-positive islet cells after exposure to human amylin (arrows). Scale bars: a, 40 μm; c, e and g, 20 μm.
METHODS. Islet cell cultures were maintained for 3–4 days (>90% viability) and then treated with vehicle or 20 μM human amylin for 24 h. Pancreatic islets were isolated by perfusion of the rat pancreas (from adult male Sprague-Dawley rats weighing 180–200 g) with collagenase[27]. Human islets were isolated from the pancreas of a 39-year-old woman as described[28]. Isolated islets were dissociated by incubation in trypsin–EDTA for 10 min at 37 °C and repetitive trituration with a Pasteur pipette. Dissociated islet cells or non-dissociated islets were cultured in 16-mm tissue-culture wells on glass coverslips coated with Matrigel (Collaborative Biomedical Products) in 300 μl per well of RPMI 1640 medium supplemented with 10% fetal bovine serum, 100 U ml^{-1} penicillin and 100 μg ml^{-1} streptomycin. Lyophilized peptides were dissolved in water to 346 μM and immediately added to the culture medium at the indicated concentration. An equal volume of sterile water was added to control cultures. Cell viability was determined by the calcein–AM/propidium iodide double-staining method (Molecular Probes)[29]. Culture medium was removed after treatment and cells were incubated with 1 μM calcein–AM and 10 μg ml^{-1} propidium iodide in phosphate-buffered saline (PBS) for 10 min at 37 °C. Viable cells cleave calcein–AM to calcein, producing uniform green fluroescence; dead cells take up propidium iodide into the nucleus, resulting in intense red fluorescence. Green and red fluorescence were simultaneously visualized using a Nikon transmission microscope equipped with a double-pass filter. For immunocytochemistry, cultures were fixed in 4% paraformaldehyde, 0.12 M sucrose in PBS, pre-incubated with swine serum and stained with a polyclonal primary antibody against insulin using the DAKO PAP kit. Fixed sections of pancreatic tissue were used as a positive control. The viability of insulin-positive cells was determined by propidium iodide staining and scored as described in Table 1 legend. HPLC-purified human, rat and cat amylin (full-length 37-amino-acid peptides) were obtained from Bachem California and Peninsula Laboratories. Human amylin from both sources gave the same results. Peptides were analysed by laser desorption mass spectroscopy (amylin *M*, values: human 3,903 ± 2 (mean ± s.e.m., $n = 8$; predicted *M*, 3,904); cat 3,910 ± 1 ($n = 3$; predicted *M*, 3,909); rat 3,919 ± 2 ($n = 4$, predicted *M*, 3,921)).

‡ To whom correspondence should be addressed.

[CANCER RESEARCH 51, 3193–3197, June 15, 1991]

C19

Absence of Methylthioadenosine Phosphorylase in Human Gliomas[1]

Tsutomu Nobori,[2] James G. Karras, Fulvio Della Ragione, Thomas A. Waltz, Pojen P. Chen, and Dennis A. Carson

Department of Medicine and the Sam and Rose Stein Institute for Research on Aging, University of California, San Diego, La Jolla, California 92093-0945 [T. N., J. G. K., P. P. C., D. A. C.]; Department of Macromolecular Biochemistry, First Medical School, University of Naples, Via Costantinopoli 16, Naples, Italy [F. D. R.]; and Division of Neurosurgery, Scripps Clinic and Research Foundation, La Jolla, California 92037 [T. A. W.]

ABSTRACT

All normal mammalian tissues contain methylthioadenosine phosphorylase, which plays a role in the recycling of purines and methionine consumed during polyamine synthesis. A complete deficiency of methylthioadenosine phosphorylase has been reported in some human leukemias and lymphomas and in a few solid tumors. The exact incidence of the enzyme deficiency among fresh human tumor specimens has been difficult to establish because the measurement of enzyme catalytic activity is laborious and requires carefully preserved specimens. We have generated two antibodies against methylthioadenosine phosphorylase and have used them to develop a simple immunoblot assay for the enzyme. Specifically, studies showed that all cells with catalytically active methylthioadenosine phosphorylase had a 32-kDa band that reacted with the anti-enzyme antibodies. In a reciprocal manner, all malignant cell lines that were naturally deficient in methylthioadenosine phosphorylase activity lacked detectable immunoreactive enzyme protein. The immunoassay was used to analyze human gliomas. Seventy-five % (9 of 12) of the gliomas were completely methylthioadenosine phosphorylase deficient. This common metabolic difference between most gliomas and all normal cells is a potential target for tumor-specific chemotherapy.

INTRODUCTION

MeSAdo[3] phosphorylase (methylthioadenosine:orthophosphate methylthioribosyltransferase) was first described in rat prostate tissue (1). The substrate for this enzyme, MeSAdo, is produced during the synthesis of the polyamines spermidine and spermine and is cleaved into adenine and 5-methylthioribose 1-phosphate, which are recycled to AMP and methionine, respectively. MeSAdo phosphorylase activity has been reported to change during the cell cycle (2). Recently, MeSAdo phosphorylase has been homogeneously purified from human placenta (3). The enzyme has a molecular mass of 98 kDa and is composed of three identical subunits of 32 kDa.

MeSAdo phosphorylase is abundant in all normal tissues and in cell lines derived from normal cells (4). In contrast, many murine and human malignant cell lines are deficient in MeSAdo phosphorylase activity (4, 5). The deficiency is not confined to tissue culture cells. From 10–20% of human leukemias, as well as a few melanomas, lung carcinomas, and rectal adenocarcinomas have been reported to lack MeSAdo phosphorylase (6, 7). However, because the assay for MeSAdo phosphorylase catalytic activity requires commercially unavailable radiochemical substrates, and because the enzyme activity is unstable, the true incidence of the deficiency in naturally occurring human tumors has not been clearly established.

To overcome this problem, we have generated antibodies against MeSAdo phosphorylase. In immunoblots, the antibodies bound to the 32-kDa MeSAdo phosphorylase subunit in all enzyme-positive cell lines. In contradistinction, no naturally occurring enzyme-deficient malignant cell line had immunoreactive MeSAdo phosphorylase protein. Having established the validity of the immunoassay, we used it to assess MeSAdo phosphorylase in human gliomas. The results showed that 9 of 12 glioma cell lines and tumors had undetectable enzyme protein. MeSAdo phosphorylase deficiency thus represents a defined metabolic abnormality that distinguishes a common and usually incurable human solid tumor from normal cells.

MATERIALS AND METHODS

Cell Lines and Tumor Biopsies. The cell lines studied are listed in Table 1. Among human leukemic cell lines, BV173, K562, K-T1, and SUP-T8 were provided by Dr. M. O. Diaz (University of Chicago) and Molt-16 was provided by Dr. J. Minowada (Fujisaki Cell Center, Okayama, Japan). MeSAdo phosphorylase-deficient variants of murine T-lymphoma cell line R1.1 were isolated following mutagenesis, as described previously (8). Clone H is completely deficient in MeSAdo phosphorylase (<0.1% of wild-type activity), whereas clone F is nearly deficient (approximately 6.6% of wild-type enzyme activity).

Brain tumor biopsies were obtained during surgery and were immediately frozen at −70°C for immunoblot assay. The pathological diagnosis was determined by the surgical pathology division at Scripps Clinic and Research Foundation.

MeSAdo Phosphorylase Assay. Enzyme activity was measured by the radiochemical method of Pegg and Williams-Ashman (1), using [methyl-^{3}H]MeSAdo as the substrate, exactly as described earlier (9). The protein concentrations were determined by the method of Bradford (10).

Anti-Enzyme Antibodies. MeSAdo phosphorylase was purified from bovine liver as described by Della Ragione *et al.* (11). Several tryptic peptides from the isolated enzyme were sequenced. Based upon the sequences obtained, peptides 40 (18 amino acids long) and 51 (14 amino acids long) were synthesized by a modification of the Merrifield solid-phase method as described before (12). All peptides contained a cysteine residue at the carboxy terminus to facilitate chemical coupling to the carrier protein, KLH, with *m*-maleimidobenzoyl-*N*-hydroxysuccimide ester, as described by Liu *et al.* (13).

New Zealand white rabbits (two rabbits per peptide) were immunized on a bimonthly basis with the peptide-KLH conjugates. The initial injections contained 1 mg of synthetic peptide-KLH conjugate emulsified in Freund's complete adjuvant. Booster injections had 1 mg of antigen in incomplete Freund's adjuvant. After 3–4 injections, sera were partially purified with 50% saturated ammonium sulfate and were screened for anti-peptide and anti-MeSAdo phosphorylase reactivities by ELISA.

ELISA. Microtiter plates were precoated with peptides or MeSAdo phosphorylase at 10 μg/ml in BBS (0.2 M sodium borate-0.15 M NaCl, pH 8.5) overnight at 4°C. The plates were washed once in BBS containing 0.05% Tween 20 and then were incubated for 4 h with BBS containing 1% bovine serum albumin to block nonspecific binding sites. Several dilutions of a control serum or peptide-induced antisera were then applied in 0.1-ml aliquots and incubated overnight. The plates were washed twice with BBS containing 0.05% Tween 20, and then exposed for 1 h to alkaline phosphatase-labeled goat F(ab')$_2$ anti-rabbit immunoglobulin (Jackson Laboratories, Inc., West Grove, PA) at a dilution of 1:1000 in BBS. After the plates were washed, 0.2 ml of 0.1 M *p*-nitrophenyl phosphate disodium in 0.1 M $NaHCO_3$, pH 9.0, was added to each well. The absorption at 405 nm was measured 30 min later.

Received 12/10/90; accepted 4/1/91.

The costs of publication of this article were defrayed in part by the payment of page charges. This article must therefore be hereby marked *advertisement* in accordance with 18 U.S.C. Section 1734 solely to indicate this fact.

[1] This work was supported in part by a grant from the National Foundation for Cancer Research, by Grants GM23200, AR39039, and A124466 from the National Institutes of Health, and by Grant 1KT112 from the University of California Tobacco Related Disease Research Program.

[2] To whom requests for reprints should be addressed, at Department of Medicine, University of California, San Diego, La Jolla, CA 92093-0945.

[3] The abbreviations used are: MeSAdo, methylthioadenosine; KLH, keyhole limpet hemocyanin; ELISA, enzyme-linked immunosorbent assay; BBS, buffered borate saline.

Table 1 *MeSAdo phosphorylase activities in cell lines*

Enzyme activities were measured radiochemically. Each value is the mean of at least two determinations and is expressed as nmol of product formed/min/mg of protein.

Cell line	Cell type	Enzyme activities
Human		
BV173	CML[a]	0.42
CEM	ALL	<0.01
DHL-9	Malignant lymphoma	<0.01
HSB2	ALL	<0.01
K562	CML	<0.01
K-T1	ALL	<0.01
Molt-4	ALL	0.59
Molt-16	ALL	0.58
NALL-1	ALL	<0.01
SUP-T8	ALL	0.26
U937	Histiocytic lymphoma	0.29
U-87MG[b]	Glioblastoma	<0.01
U-138MG[b]	Glioblastoma	<0.01
U-373MG[b]	Glioblastoma	0.34
A172[b]	Glioblastoma	<0.01
T98G[b]	Glioblastoma	0.50
Hs683[b]	Glioma	<0.01
Bovine		
MDBK[b]	Normal kidney	0.44
Monkey		
COS[b]	Normal kidney	0.77
Vero[b]	Normal kidney	<0.01
Mouse		
R1.1 wild type	Lymphoma	1.36
R1.1 clone F		0.09
R1.1 clone H		<0.01
L1210	Lymphocytic lymphoma	<0.01

[a] CML, chronic myelogenous leukemia; ALL, acute lymphocytic leukemia.
[b] Cells were obtained from American Type Culture Collection (Rockville, MD).

Immunoblot Analysis. The reactivity of the anti-peptide antisera with MeSAdo phosphorylase was assessed by an immunoblot method as described previously (14). Briefly, either purified MeSAdo phosphorylase protein or crude cell extracts (10–150 μg/lane) were separated by electrophoresis in 12.5% polyacrylamide gels containing 0.1% sodium dodecyl sulfate (15). After electrotransfer to nitrocellulose membranes (0.45 mm; Bio-Rad, Richmond, CA), nonspecific binding sites were blocked with 3% powdered milk in BBS. The proteins were then probed for 16 h at room temperature with antisera diluted 1:500 in BBS containing 3% powdered milk. After the proteins were washed extensively with BBS, reactive bands were detected by the binding of ^{125}I-protein A (1 mCi/ml; ICN Radiochemicals, Irvine CA) for 1 h. The membranes were washed and blotted onto paper towels and exposed to Kodak XAR-5 film at −70°C.

Specificity studies were carried out by inhibition of serum-immunoblotting activity with the peptides used to immunize the rabbits or with partially purified MeSAdo phosphorylase. Antisera at a dilution of 1:500 were preincubated with either peptide or MeSAdo phosphorylase at 50 μg/ml for 1 h at room temperature and then added to the blots. Otherwise, immunoblot analyses were carried out as described above.

Quantitation of MeSAdo Phosphorylase Protein in Cells. To estimate the cellular content of MeSAdo phosphorylase, a semiquantitative immunoblotting procedure was used. Cell extracts prepared from enzyme-positive cells were electrophoresed on a 12.5% polyacrylamide gel containing 0.1% sodium dodecyl sulfate along with various amounts of MeSAdo phosphorylase which was purified from bovine liver. Immunoblot analyses were carried out as described above. The bands on the autoradiographs were scanned with a desitometer (Bio-Rad) and were quantitated using a calibration curve obtained from the immunoreactive bands of the purified enzyme.

RESULTS

The reactivities of the two antisera with MeSAdo phosphorylase peptides or with purified enzyme protein were determined by ELISA and immunoblotting. As measured by ELISA, both peptide-KLH conjugates induced high titer antibodies against MeSAdo phosphorylase. Antiserum 6117 raised against peptide 40 showed 50% maximal response against the immunizing peptide at a 1:5000 dilution and against purified MeSAdo phosphorylase at a 1:1500 dilution. Antiserum 6120 raised against peptide 51 showed 50% anti-peptide response at a 1:10,000 dilution and reacted with the enzyme at a 1:4000 dilution.

Fig. 1 illustrates immunoblots of purified bovine MeSAdo phosphorylase probed with the two antibodies. The specificities of the two antisera were established by blocking experiments, in which immunoblots were probed with antisera preincubated with either peptide or MeSAdo phosphorylase. The reactivity of each antisera with MeSAdo phosphorylase was completely inhibited by preincubation with the same peptide as that used for immunization. Furthermore, the reactivities of antisera decreased significantly (>50%), when the antisera were preincubated with intact MeSAdo phosphorylase. On the other hand, when antisera against peptides 40 and 51 were preincubated with another MeSAdo phosphorylase peptide (peptide 22), there was no significant inhibition of the reactivity with MeSAdo phosphorylase (Fig. 1). In addition to a single major band corresponding to the 32-kDa subunit of MeSAdo phosphorylase, several minor bands were observed on the autoradiographs. These were nonspecific, since the identical bands were detected using preimmune sera and were not inhibitable by preincubation with peptides (results not shown). Collectively, these results indicate that antisera 6117 and 6120 were both specific for MeSAdo phosphorylase.

To test whether or not the antisera had species specificity, cell extracts made from human, cow, mouse, and monkey cells were analyzed by immunoblotting. As illustrated in Fig. 2, antiserum 6117 recognized the enzyme protein in the cells of all species analyzed (similar results were obtained with antisera 6120). Compared to MDBK (cow) cells, mouse, human, and monkey cells displayed weaker immunoreactivity in this order, when the same amount of total cell protein was analyzed by gel electrophoresis. Based upon a standard curve obtained with purified MeSAdo phosphorylase (Fig. 3), we estimate that bovine MDBK cells contain 0.25 μg MeSAdo phosphorylase/mg protein.

Approximately 20% of human leukemic cell lines have no detectable MeSAdo phosphorylase catalytic activity (4). However, it is unknown whether these cell lines have immunoreactive enzyme protein. To address this issue, several cell lines with no detectable enzyme activity were analyzed by immunoblotting with the anti-enzyme antibodies. As illustrated in Fig. 2, all of eight enzyme-positive cell lines, but none of eight enzyme-deficient cell lines, had immunoreactive enzyme pro-

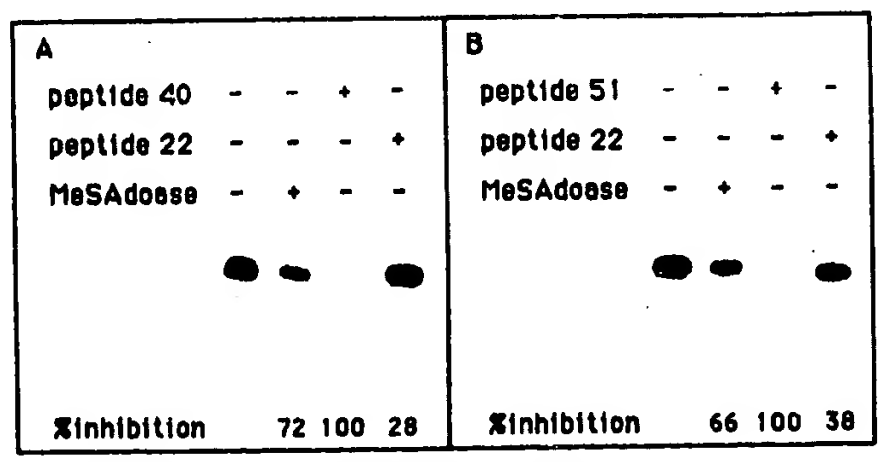

Fig. 1. The specificity of anti-peptide antibodies for purified MeSAdo phosphorylase (MeSAdoase). Specificity studies were carried out by inhibition of immunoblotting activity of antibodies (*A*, 6117; *B*, 6120) with the peptides used to immunize rabbits or purified enzyme as described in "Materials and Methods." An irrelevant peptide (peptide 22) was used as a control.

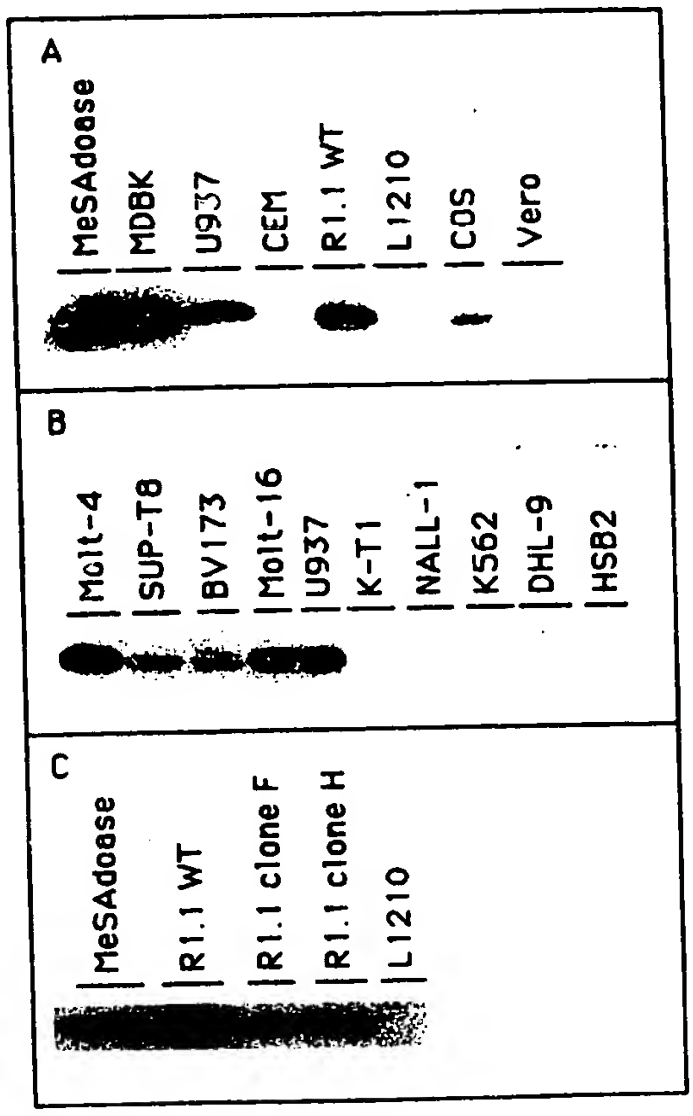

Fig. 2. Comparison of enzyme-positive and -negative cell lines by immunoblot analysis. *A*, enzyme-positive and -negative cell lines of different species along with purified bovine MeSAdo phosphorylase. *B*, human leukemia cell lines either having or lacking MeSAdo phosphorylase. *C*, mutant clones isolated from parental R1.1 cells along with L1210 cells lacking the enzyme activity naturally. WT, wild type.

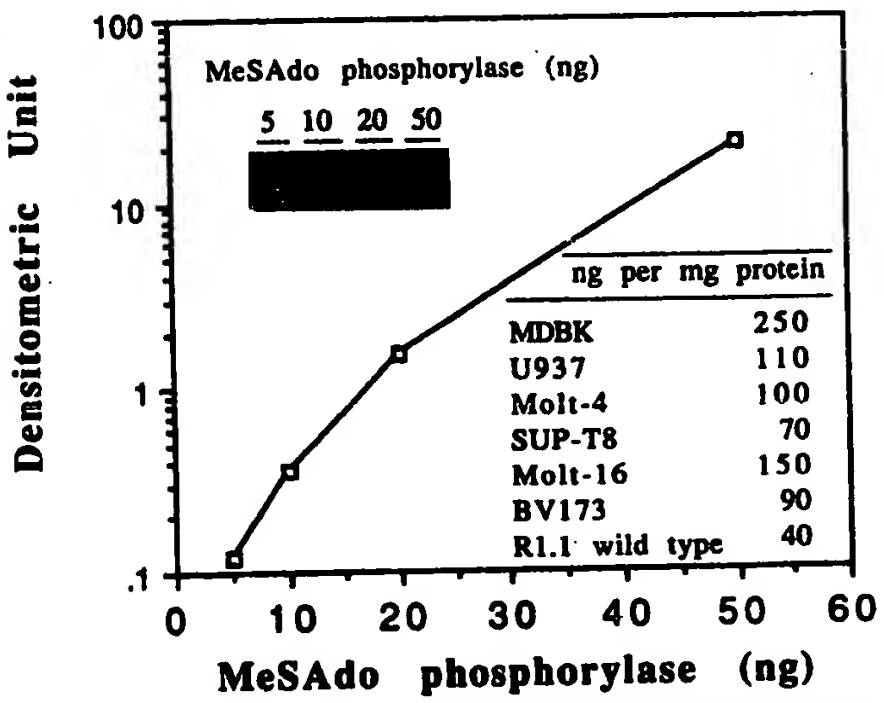

Fig. 3. Immunoblot analysis of purified bovine MeSAdo phosphorylase and seven different enzyme-positive cell lines. In this experiment, either purified enzyme at the indicated amounts or crude cell extracts (100 μg/lane) were separated electrophoretically, transferred to nitrocellulose membranes, and probed with antibody 6117.

tein. Similar results were obtained with both antibodies. One could attribute the absence of immunoreactive proteins in cell lines having no detectable enzyme activity to the monospecificity of a single antiserum for a certain region of the enzyme protein, which might be deleted or mutated in these cell lines.

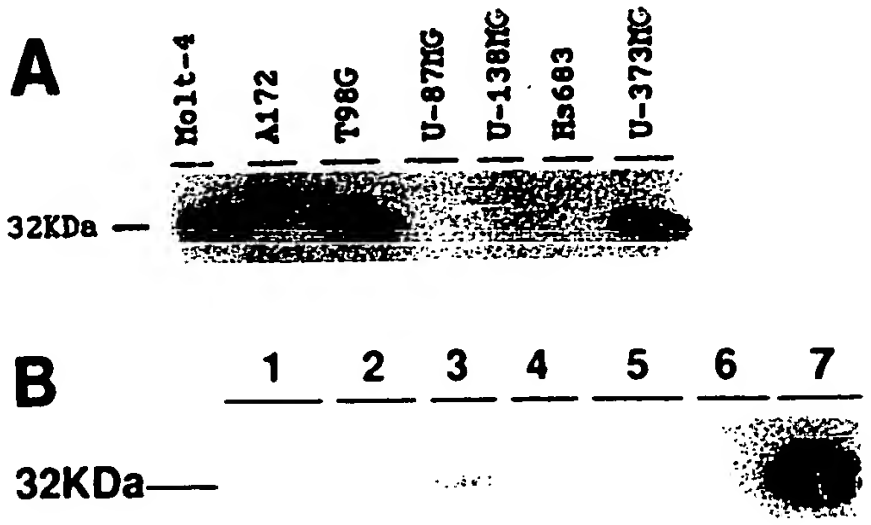

Fig. 4. Immunoblot analysis of the human brain tumor cell lines (*A*) and primary brain tumors (*B*). In this experiment, crude cell extracts (50 and 25 μg/lane for cell lines and primary tumors, respectively) were separated electrophoretically, transferred to nitrocellulose membranes, and probed with antibody 6117. Molt-4 cell line was used as a positive control. *B: lanes 1–6*, cases 1–6 shown in Table 2; *lane 7*, MDBK cells as a positive control.

Table 2 *Histological diagnosis of patients with brain tumors*

Biopsy specimens were removed during routine surgery, and tissue sections were examined by a single pathologist.

Case	Age (yr)	Sex	Histological diagnosis
1 PR	[a]	[a]	Astrocytoma (grade IV)
2 RS	60	F	Glioblastoma multiforme
3 LM	75	M	Glioblastoma multiforme
4 SM	39	F	Astrocytoma
5 GRA	45	M	Astrocytoma
6 GK	67	F	Oligoastrocytoma

[a] No further information was obtained.

Although we do not know how closely peptides 40 and 51 are located in the MeSAdo phosphorylase molecule, it seems unlikely that these two regions would be simultaneously deleted or mutated. Therefore, these data indicate that enzyme-deficient cell lines have no immunoreactive MeSAdo phosphorylase.

The possibility remained that various mutational alterations in MeSAdo phosphorylase reduced the rate of enzyme synthesis or accelerated enzyme degradation, such that little or no enzyme protein remained in the cell extracts. To address this possibility, two MeSAdo phosphorylase-deficient somatic mutant clones of the mouse R1.1 cell line were studied. These cells were selected by "tritium suicide" with MeSAdo labeled in the adenine moiety, as described previously (8). As shown in Table 1, clone F has 6.6% of wild-type MeSAdo phosphorylase activity, while clone H is completely enzyme deficient. Despite the partial or complete lack of MeSAdo phosphorylase, both clones have readily detectable immunoreactive enzyme protein (Fig. 2). In contrast, the mouse L1210 cell line, which naturally lacks enzyme activity, has no immunoreactive enzyme protein.

Having verified the specificity and sensitivity of the immunoassay for MeSAdo phosphorylase, we used the antibodies to analyze eight human glioma cell lines. Sixty-seven % (4 of 6) were entirely deficient in immunoreactive enzyme (Fig. 4). The lack of MeSAdo phosphorylase was confirmed by direct enzyme assay (Table 1). We then analyzed six successive biopsy specimens from human gliomas, with different histological characteristics (Table 2). Five were entirely deficient (Fig. 4). Control experiments showed that normal human brain has abundant MeSAdo phosphorylase activity.[4] Thus, complete MeSAdo phosphorylase deficiency is a common and specific metabolic abnormality in human gliomas.

[4] T. Nobori, F. Della Ragione, and D. A. Carson., manuscript in preparation.

DISCUSSION

In the present experiments, two high titer antibodies to MeSAdo phosphorylase peptides were used (*a*) to quantitate the enzyme protein in bovine cells, (*b*) to compare immunological cross-reactivities among the enzymes from different species, (*c*) to search for immunoreactive enzyme in both naturally occurring MeSAdo phosphorylase-deficient cell lines and enzyme-deficient cells selected following *in vitro* mutagenesis, and (*d*) to identify MeSAdo phosphorylase deficiency in human glioma biopsies and cell lines. In immunoblots, the antibodies identified the 32-kDa monomeric subunit of purified bovine MeSAdo phosphorylase and a band of the same molecular mass in extracts of enzyme-purified cow, human, monkey, and mouse cells. Antibody binding was inhibited specifically by preincubation with the respective immunizing peptides but not by irrelevant peptides. Both anti-peptide antibodies thus reacted specifically with the MeSAdo phosphorylase protein.

Della Ragione *et al.* (11) described attempts to produce antibodies against native bovine MeSAdo phosphorylase. Following a laborious purification procedure, they obtained 2.4 mg enzyme protein from 1 kg liver. Our estimate of 0.25 μg MeSAdo phosphorylase/mg protein in MDBK cells is in accord with these data and indicates that the enzyme is present in relatively low amounts in most cells. The purified enzyme was found by Della Ragione *et al.* to be nonimmunogenic in rabbits, guinea pigs, and goats, unless it was coupled to KLH or agarose prior to immunization. These results led the investigators to conclude that the structure of MeSAdo phosphorylase was conserved among different mammalian species. The interspecies cross-reactivity of two different anti-peptide antibodies prepared against sequences corresponding to the bovine enzyme, as reported here, support these earlier conclusions.

The broad cross-reactivity of the anti-enzyme antibodies enabled us to search for the presence of immunoreactive MeSAdo phosphorylase in naturally occurring enzyme-deficient cell lines of mouse (L1210), monkey (Vero), and human (CEM, K-T1, NALL-1, K562, DHL-9, HSB2) origin. None of these cell lines displayed immunoreactive 32-kDa MeSAdo phosphorylase polypeptide. In marked contrast to the results obtained with naturally enzyme-deficient malignant cells, neither of two the MeSAdo phosphorylase clones selected from the murine T-lymphoma cell line R1.1 by mutagenesis and tritium suicide with [^{3}H]MeSAdo was deficient in immunoreactive enzyme protein. Related tritium suicide methods have been used for the selection of mammalian cells with structural gene mutations (16–19). The fact that clone F had 6.6% of wild-type enzyme activity, and a normal amount of immunoreactive protein, is consistent with a structural gene mutation. Thus, our results suggest that mutations that destroy most MeSAdo phosphorylase catalytic activity do not necessarily deplete immunoreactive enzyme protein. In contradistinction, the naturally MeSAdo phosphorylase-deficient L1210 mouse leukemia cell line had no immunoreactive enzyme protein. Consistent with these conclusions, we have shown that the enzyme deficiency in L1210 behaves as a recessive characteristic in intraspecies somatic cell hybrids (20) and, hence, is not secondary to a transacting factor that inhibits enzyme expression.

The naturally enzyme-deficient cells analyzed, CEM, K-T1, NALL-1, and K562 are known to have cytogenetic abnormalities in the short arm of chromosome 9 (21). It is important to note that the locus of MeSAdo phosphorylase (designated MTAP) has been assigned to this same region (22). Furthermore, the above-mentioned cell lines are hemizygous or nullizygous for the interferon-α and interferon-β1 genes, which have been mapped to chromosome 9p13–22 and 9p22, respectively (23). Taken together, these results suggest that the enzyme deficiency in these four cell lines may be attributed to an alteration of the region on chromosome 9 encompassing the MTAP locus, although the precise mechanism producing the deficiency remains to be determined.

Approximately 50% of human gliomas have structural rearrangements affecting chromosome 9 (24). Therefore, we used the rapid immunoassay to quantitate MeSAdo phosphorylase activities in glioma cell lines and fresh tumor biopsies. Nine of 12 tumors (75%) were completely MeSAdo phosphorylase deficient. The six tumor biopsies studied included astrocytomas, an oligoastrocytoma, and two glioblastomas multiforme. All normal human tissues, including brain, contain MeSAdo phosphorylase.[5] Moreover, other studies have shown that RBCs from patients with MeSAdo phosphorylase-deficient neoplasms have normal enzyme activity (7). Thus, the high frequency of MeSAdo phosphorylase deficiency in human gliomas is related to their malignant phenotypes.

Several chemotherapeutic regimens have been described for the selective killing of MeSAdo phosphorylase-deficient leukemia cells (4). Because of the problems associated with potential metabolic cooperation between leukemic and normal leukocytes, these strategies have not been tested *in vivo*. However, no adequate chemotherapy exists for human gliomas, and the incidence of these is increasing, particularly in patients older than 65 years (25). The relatively confined growth pattern of gliomas, and the absence of any effective alternative, may make MeSAdo phosphorylase a reasonable target for tumor-specific chemotherapy. Animals undergoing a MeSAdo phosphorylase-deficient tumor transplantation displayed elevated plasma MeSAdo levels, in proportion to the tumor burden (26). Hence, it may be feasible to diagnose gliomas, and follow their response to therapy, by the measurement of MeSAdo concentrations in cerebrospinal fluids. With the simple enzyme immunoassay described here, and the available assays for MeSAdo phosphorylase, it should now be possible to determine with precision the prevalence and metabolic consequences of MeSAdo phosphorylase deficiency in a diverse series of human brain tumors.

ACKNOWLEDGMENTS

We thank Drs. M. O. Diaz and J. Minowada for providing the cell lines and Drs. C. J. Carrera and G. J. Silverman for their helpful discussions. We are also grateful to Nancy Noon for preparing the manuscript.

REFERENCES

1. Pegg, A. E., and Williams-Ashman, H. G. Phosphate-stimulated breakdown of 5′-methylthioadenosine by rat ventral prostate. Biochem. J., *115:* 241–247, 1969.
2. Sunkara, P. S., Chang, C. C., and Lachman, P. J. Cell proliferation and cell cycle dependent changes in the methylthioadenosine phosphorylase activity in mammalian cells. Biochem. Biophys. Res. Commun., *127:* 546–551, 1985.
3. Della Ragione, F., Carteni Farina, M., Gragnaniello, V., Schettino, M. I., and Zappia, V. Purification and characterization of 5′-deoxy-5′-methylthioadenosine phosphorylase from human placenta. J. Biol. Chem., *261:* 12324–12329, 1986.
4. Kamatani, N., Nelson-Rees, W. A., and Carson, D. A. Selective killing of human malignant cell lines deficient in methylthioadenosine phosphorylase, a purine metabolic enzyme. Proc. Natl. Acad. Sci. USA, *78:* 1219–1223, 1981.
5. Toohey, J. I. Methylthio group cleavage for methylthioadenosine. Description of an enzyme and its relationship to the methylthio- requirement of certain cells in culture. Biochem. Biophys. Res. Commun., *78:* 1273–1280, 1977.

[5] T. Nobori and D. A. Carson, unpublished data.

6. Kamatani, N., Yu, A. L., and Carson, D. A. Deficiency of methylthioadenosine phosphorylase in human leukemic cells *in vivo*. Blood, *60:* 1387–1391, 1982.
7. Fitchen, J. H., Riscoe, M. K., Dana, B. W., Lawrence, H. J., and Ferro, A. J. Methylthioadenosine phosphorylase deficiency in human leukemias and solid tumors. Cancer Res., *46:* 5409–5412, 1986.
8. Kubota, M., Kamatani, N., and Carson, D. A. Biochemical genetic analysis of the role of methylthioadenosine phosphorylase in a murine lymphoid cell line. J. Biol. Chem., *258:* 7288–7291, 1983.
9. Kamatani, N., and Carson, D. A. Dependence of adenine production upon polyamine synthesis in cultured human lymphoblasts. Biochim. Biophys. Acta, *675:* 344–350, 1981.
10. Bradford, M. M. A rapid and sensitive method for the quantitation of microgram quantities of protein utilizing the principle of protein-dye binding. Anal. Biochem., *72:* 248–254, 1976.
11. Della Ragione, F., Oliva, A., Gragnaniello, V., Russo, G. L., Palumbo, R., and Zappia, V. Physicochemical and immunological studies on mammalian 5′-deoxy-5′-methylthioadenosine phosphorylase. J. Biol. Chem., *265:* 6241–6246, 1990.
12. Chen, P. P., Houghten, R. A., Fong, S., Rhodes, G. H., Gilbertson, T. A., Vaughan, J. H., Lener, R. A., and Carson, D. A. Anti-hypervariable region antibody induced by a defined peptide: an approach for studying the structural correlates of idiotypes. Proc. Natl. Acad. Sci. USA, *81:* 1784–1788, 1984.
13. Liu, F-T., Zinnecker, M., Hamaoka, T., and Katz, D. H. New procedures for preparation and isolation of conjugates of proteins and a synthetic copolymer of D-amino acids and immunochemical characterization of such conjugates. Biochemistry, *18:* 690–697, 1979.
14. Towbin, H., Staehelin, T., and Gordon, J. Electrophoretic transfer of proteins from polyacrylamide gels to nitrocellulose sheets: procedure and some applications. Proc. Natl. Acad. Sci. USA, *76:* 4350–4354, 1979.
15. Laemmli, U. K. Cleavage of structural proteins during the assembly of the head of bacteriophage T4. Nature (Lond.), *227:* 680–685, 1979.
16. Bryant, R. E., Schauer, I. E., and Hatcher, D. G. Isolation of hypoxanthine phosphoribosyltransferase-defective mutants in Chinese hamster V79 cells by tritium suicide. Mutat. Res., *83:* 117–126, 1981.
17. Medrano, L., and Green, H. A uridine kinase-deficient mutant of 3T3 and a selective method for cells containing the enzyme. Cell, *1:* 23–26, 1974.
18. Steglich, C., and Scheffler, I. E. An ornithine decarboxylase-deficient mutant of Chinese hamster ovary cells. J. Biol. Chem., *257:* 4603–4609, 1982.
19. Dantzig, A. H., Slayman, C. W., and Adelberg, E. A. Isolation of a spontaneous CHO amino acid transport mutant by a combination of tritium suicide and replica plating. Somat. Cell Genet., *8:* 509–520, 1982.
20. Kamatani, N., Kubota, M., Willis, E. H., and Carson, D. A. 5′-Methylthioadenosine phosphorylase deficiency in malignant cells: recessive expression of the defective phenotype in intraspecies (mouse × mouse) hybrids. Adv. Exp. Med. Biol., *165:* 279–283, 1984.
21. Diaz, M. O., Ziemin, S., Le Beau, M. M., Pitha, P., Smith, S. D., Chilcote, R. R., and Rowley, J. D. Homozygous deletion of the α- and β1- interferon genes in human leukemia and derived cell lines. Proc. Natl. Acad. Sci. USA, *85:* 5259–5263, 1988.
22. Carrera, C. J., Eddy, R. L., Shows, T. B., and Carson, D. A. Assignment of the gene for methylthioadenosine phosphorylase to human chromosome 9 by mouse-human somatic cell hybridization. Proc. Natl. Acad. Sci. USA, *81:* 2665–2668, 1984.
23. Smith, M., and Simpson, N. E. Report of the committee on the genetic constitution of chromosome 9 and 10. Cytogenet. Cell. Genet., *51:* 202–225, 1989.
24. Bigner, S. H., Mark, J., Bullard, D. E., Mahaley, S. M., Jr., and Bigner, D. D. Chromosomal evolution in malignant human gliomas starts with specific and usually numerical deviations. Cancer Genet. Cytogenet., *22:* 121–135, 1986.
25. Greig, N. H., Ries, L. G., Yancik, R., and Rapoport, S. I. Increasing annual incidence of primary malignant brain tumors in the elderly. J. Natl. Cancer Inst., *82:* 1621–1624, 1990.
26. Carrera, C. J., Willis, E. H., Chilcote, R. R., Kubota, M., and Carson, D. A. 5′-Deoxy-5′-methyladenosine phosphorylase deficiency in leukemia: genetics and biochemical aspects. Adv. Exp. Med. Biol., *195B:* 643–650, 1986.

Proc. Natl. Acad. Sci. USA
Vol. 92, pp. 6489–6493, July 1995
Medical Sciences

Construction of a 2.8-megabase yeast artificial chromosome contig and cloning of the human methylthioadenosine phosphorylase gene from the tumor suppressor region on 9p21

(chromosomal loss/purine nucleoside phosphorylase/enzyme deficiency/*CDKN2* gene)

OLUFUNMILAYO I. OLOPADE*, HELEN M. POMYKALA, FITSUM HAGOS, LISE W. SVEEN, RAFAEL ESPINOSA III, MARTIN H. DREYLING, SUSAN GURSKY, WALTER M. STADLER, MICHELLE M. LE BEAU, AND STEFAN K. BOHLANDER

Section of Hematology/Oncology, Department of Medicine and The University of Chicago Cancer Research Center, The University of Chicago Pritzker School of Medicine, Chicago, IL 60637

Communicated by Janet D. Rowley, The University of Chicago Pritzker School of Medicine, Chicago, IL, March 10, 1995

ABSTRACT **Many human malignant cells lack methylthioadenosine phosphorylase (MTAP) enzyme activity. The gene (*MTAP*) encoding this enzyme was previously mapped to the short arm of chromosome 9, band p21–22, a region that is frequently deleted in multiple tumor types. To clone candidate tumor suppressor genes from the deleted region on 9p21–22, we have constructed a long-range physical map of 2.8 megabases for 9p21 by using overlapping yeast artificial chromosome and cosmid clones. This map includes the type I *IFN* gene cluster, the recently identified candidate tumor suppressor genes *CDKN2* ($p16^{INK4A}$) and *CDKN2B* ($p15^{INK4B}$), and several CpG islands. In addition, we have identified other transcription units within the yeast artificial chromosome contig. Sequence analysis of a 2.5-kb cDNA clone isolated from a CpG island that maps between the *IFN* genes and *CDKN2* reveals a predicted open reading frame of 283 amino acids followed by 1302 nucleotides of 3′ untranslated sequence. This gene is evolutionarily conserved and shows significant amino acid homologies to mouse and human purine nucleoside phosphorylases and to a hypothetical 25.8-kDa protein in the *pet* gene (coding for cytochrome bc_1 complex) region of *Rhodospirillum rubrum*. The location, expression pattern, and nucleotide sequence of this gene suggest that it codes for the MTAP enzyme.**

Unbalanced translocations or interstitial deletions of 9p are recurring abnormalities in a variety of tumor types including acute lymphoblastic leukemia, glioma, melanoma, non-small cell lung cancer, head and neck cancer, bladder cancer, and mesothelioma (1). Homozygous deletion of DNA sequences on 9p or loss of heterozygosity has now been described in multiple tumor types (2–7). A number of the cell lines and patient samples with 9p gene deletions also lack methylthioadenosine phosphorylase (MTAP) enzyme activity. To our knowledge, the gene encoding MTAP has not been cloned but has been mapped to 9p22–9q13 (8). In a few cases, the deletions that included both the *IFN* gene cluster and the *MTAP* gene were interstitial and submicroscopic, suggesting that these genes or a tumor suppressor gene (TSG) closely linked to them was the target of the 9p deletions. This hypothesis was further supported by the linkage of a gene that confers susceptibility to melanoma (*MLM*) to 9p21 in the region between *D9S126* and the *IFNA* gene cluster (9).

CDKN2 ($p16^{INK4A}$) was recently proposed as a candidate TSG in this locus because the gene has been shown to be rearranged, deleted, or mutated in a majority of tumor cell lines (6, 7). This gene codes for a 16-kDa protein (p16) that inhibits CDK4 and CDK6 by binding in competition with cyclin D (10). In humans, *CDKN2* is adjacent to a gene encoding a similar protein, now called *CDKN2B* ($p16^{INK4B}$), that shares 44% homology with *CDKN2* in the first 50 amino acids and up to 97% homology in the remainder of the protein (11). Whether *CDKN2* is *MLM* remains unclear, because two recent studies (12, 13) provide conflicting evidence. Hussussian *et al.* (12) described six disease-related germ-line mutations in *CDKN2* in 33 of 36 melanoma patients from nine families and suggested that *CDKN2* likely is *MLM*. This is in contrast to 2 of 13 mutations in 9p21-linked families and 0 of 38 familial melanoma patients described by Kamb *et al.* (13). These reports raise the possibility that *CDKN2* may not be the only clinically relevant TSG on 9p and that loss of tumor suppression may involve inactivation of other as yet unidentified genes in the region in certain tumor types. In support of this possibility Cheng *et al.* (14) published their findings of two additional regions of nonoverlapping homozygous deletions on 9p21 in malignant mesothelioma, one telomeric to *CDKN2* and the other centromeric to it.

The coincident loss of MTAP enzyme activity in many tumor cell lines with homozygous *IFN* gene deletions suggests that *MTAP* is closely linked to the *IFN* gene cluster. We have suggested (15) that a 9p TSG should be localized between the *IFN* gene cluster and the *MTAP* locus based on *IFN* gene rearrangements seen in two cell lines and leukemia cells from one patient with deletions on 9p. In the reports published to date, it has been difficult to determine the exact position of the *MTAP* gene in relation to the homozygous deletions on 9p.

In this manuscript, we describe the construction of a long-range physical map around the *IFN* gene cluster that covers a distance of 2.8 megabases (Mb), as determined by pulsed-field gel electrophoresis (PFGE) and also the isolation of the *MTAP* gene cDNA.† We have localized all of the known genes and several CpG islands on this map. Restriction sites and PFGE fragment sizes are clearly delineated on the resultant map, which extends further proximally than the one presented by Weaver-Feldhaus *et al.* (16). Also, several additional markers are described and localized on this map. The approximate location of the shortest region of overlap of 9p deletions in gliomas, melanomas, lung cancer, leukemia, mesothelioma, head and neck cancer, and bladder cancers in relation to this map is discussed.

Abbreviations: YAC, yeast artificial chromosome; TSG, tumor suppressor gene; Mb, megabase(s); STS, sequence tagged site; FISH, fluorescence *in situ* hybridization; SRO, shortest region of overlap; PNP, purine nucleoside phosphorylase; PFGE, pulsed-field gel electrophoresis.

*To whom reprint requests should be addressed at: The University of Chicago Medical Center, 5841 South Maryland Avenue, MC 2115, Chicago, IL 60637-1470.

†The sequence reported in this paper has been deposited in the GenBank data base (accession no. U22233).

The publication costs of this article were defrayed in part by page charge payment. This article must therefore be hereby marked "*advertisement*" in accordance with 18 U.S.C. §1734 solely to indicate this fact.

Table 1. Homozygous loss of 9p markers in tumor cell lines

Cell type (*n*)	% cell lines test showing homozygous deletions							
	IFNB1	*IFNA*	*D9S736*	M1.4	*CDKN2*	*CDKN2B*	*D9S966*	*D9S171*
Leukemia (18)	39	44	ND	65	89	78	44	6
Melanoma (18)	0	0	0	ND	45	45	15	0
Glioma (26)	27	42	42	63	69	65	42	12
Bladder (16)	0	31	ND	50	50	50	44	ND
Head and neck (8)	0	0	0	0	38	25	0	ND
Lung (58)	6	8	ND	34	34	29	5	2
Mesothelioma (5)	0	0	0	100	100	100	40	20

Homozygous deletion of these markers was detected by Southern blot analysis or STS–PCR. The location of the markers is shown in Fig. 1. ND, not done; M1.4, 1.4-kb fragment from the 3′ untranslated portion of the *MTAP* gene.

rare-cutting restriction endonucleases *Not* I, *Sac* II, *Sal* I, and *Sfi* I. After PFGE and Southern blot transfer, the blots were hybridized to a battery of probes including the *IFNA*, *IFNB1*, the left and right vector arm probes, *D9S966*, six end probes, and the *CDKN2* cDNA probe. The resulting map is shown in Fig. 1. The *IFN* genes contained within YACs 802B11 and 886F9 were identified and aligned with our previous map of the *IFN* gene cluster (17). Except for YAC 886F9, none of the YACs demonstrated any unusual deletions or rearrangements, as determined by STS content. YAC 886F9, described by Weaver-Feldhaus *et al.* (16), is larger and extends further centromeric than the clone isolated in our laboratory, suggesting that this YAC may have undergone an internal deletion. However, the STS content of the remaining human insert was consistent with the other *IFN*-derived YACs in our laboratory. To characterize the YAC clones further, single-copy DNA fragments obtained from the YAC-end clones were used as probes on Southern blot hybridization. The results are included in Fig. 1. Each end-clone probe mapped back to the respective YACs and to chromosome 9 by FISH analysis. This map does not show every restriction site for the enzymes *Sal* I, *Sac* II, and *Sfi* I because sites that are further away from the probes used were not detected. However, several CpG islands can readily be identified on this map.

Deletion Mapping Analysis. Each unique fragment from the end clones and additional STSs were tested on our panel of cell lines to refine the deletion map. The results are summarized in Table 1. Homozygous deletion of at least one marker derived from this YAC contig was detected in 69% of the glioma cell lines, 45% of the melanoma cell lines, 50% of the bladder cancer cell lines, 89% of the leukemias, 100% of the mesotheliomas, 38% of the head and neck cancer, and 34% of the lung cancer cell lines. The majority of the cell lines had large homozygous deletions that overlapped around *CDKN2/CDKN2B*. We have shown (27) that the deletion in Hs294T, a melanoma cell line, could not be complemented by introducing a chromosome 9 derived from the T98G cell line by microcell chromosome transfer. However, introducing a normal short arm of chromosome 9 derived from a human fibroblast cell line induced senescence in Hs294T (27). The region deleted in Hs294T is flanked by *D9S736* and *D9S966*. In T98G, the homozygous deletion is flanked by *MTAP* and *CDKN2B* (data not shown). Therefore, a region of ≈100 kb was defined by the overlapping homozygous deletions in these two cell lines. Thus, we were able to define a shortest region of overlap (SRO) of these 9p deletions between the 3′ end of *MTAP* and *CDKN2B*. From Table 1, it is apparent that the pattern and percentage of 9p homozygous deletions differ in different tumor types. For example, in melanomas, mesotheliomas, and head and neck cancers, the deletions rarely extend into the *IFN* gene cluster, whereas the *IFN* genes are included in 27–44% of the deletions in leukemias, bladder cancer, and gliomas. Moreover, *MTAP* is homozygously deleted with the same frequency as *CDKN2* in some tumor types.

The following markers were not present in our YAC contig: *D9S3*, *D9S126*, *D9S171*, *D9S162*, *D9S962* (MDS10), *D9S963* (MDS36), and an STS from the *D9S171* YAC that maps at least 500 kb telomeric of *D9S171* (refs. 19 and 28 and Joseph Testa, personal communication). We were able to localize *D9S736* within YACs 802B11 and 886F9 in a 170-kb *Sal* I–*Sfi* I fragment centromeric to the *IFN* gene cluster and close to the right end of YAC 886F9; 1063.7 was present in YAC 807E4 only and c1.b was in YACs 942A3 and 807E4 (Fig. 1) (7, 16). Because the distance from the *IFN* gene cluster to the centromeric end of this YAC contig is 1.8 Mb, we estimate that *D9S171* should be a minimum distance of 2.3 Mb from the centromeric end of the *IFN* gene cluster and *D9S736* would be at least 2.0 Mb from *D9S171*. This is consistent with previous estimates. *D9S736* has been estimated to be 2 centimorgans from *D9S171* (16), whereas *D9S126* was estimated to be at a minimum distance of 1.0 Mb from the *IFN* gene cluster (29).

Expressed Sequences Within and Around the SRO. An 85-bp exon-trapped product obtained from a cosmid that maps in the CpG island at the right end of YAC 886F9 was used to screen a cDNA library. One of the clones, a 2.5-kb cDNA, detects two major transcripts of ≈2.3 kb and 6.0 kb, as shown in Fig. 2. This gene is expressed to various degrees in all tissue types and is conserved in all mammalian species, as judged by zoo-blot hybridization (data not shown). The nucleotide sequence reveals an open reading frame coding for 283 amino acids that included the initiator methionine codon (Fig. 3*a*). The protein sequence shows homology to the human, mouse, and bacteria purine nucleoside phosphorylase (PNP) gene and to a hypothetical 25.8-kDa protein in the *pet* genes (coding for cytochrome bc_1 complex) region of *Rhodospirillum rubrum*, and also to a recently described open reading frame from *Saccharomyces cerevisiae* (Fig. 3*b*). MTAP is a PNP but has different substrate specificity than the PNPs that have been cloned to date. As shown in Fig. 3*b*, the region of homology to

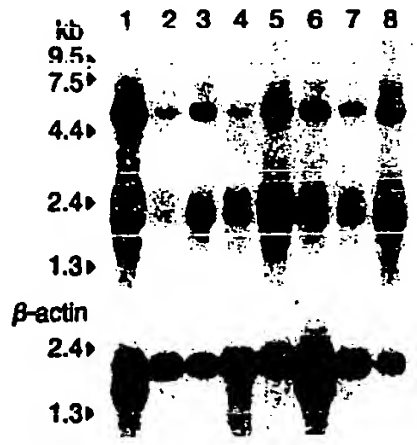

FIG. 2. (*Upper*) Northern blot of RNA from multiple human tissues hybridized with the 3′ 1.4-kb fragment of the *MTAP* cDNA clone. (*Lower*) The blot was reprobed with β-actin cDNA. Lanes: 1, heart; 2, brain; 3, placenta; 4, lung; 5, liver; 6, skeletal muscle; 7, kidney; 8, pancreas.

a

```
                                                        GAATTCCGCTCCGCACTGCTCAC
TCCCCGGCAGTGAGGTTGGCACAGCCACCGCTCTGTGGCTCGCTTGGTTCCCTTAGTCCCGAGCG
CTCGCCCACTGCAGATTCCTTTCCCGTGCAGAC ATG GCC TCT GGC ACC ACC ACC ACC
                                   M  A  S  G  T  T  T  T  8
GCC GTG AAG ATT GGA ATA ATT GGT GGA ACA GGC CTG GAT GAT CCA GAA
 9 A  V  K  I  G  I  I  G  G  T  G  L  D  D  P  E  24
ATT TTA GAA GGA AGA ACT GAA AAA TAT GTG GAT ACT CCA TTT GGC AAG
25 I  L  E  G  R  T  E  K  Y  V  D  T  P  F  G  K  40
CCA TCT GAT GCC TTA ATT TTG CGG AAG ATA AAA AAT GTT GAT TGC ATC
41 P  S  D  A  L  I  L  G  K  I  K  N  V  D  C  I  56
CTC CTT GCA AGG GAT GGA AGG CAG CAC ACC ATC ATG CCT TCA AAG GTC
57 L  L  A  R  H  G  R  Q  H  T  I  M  P  S  K  V  72
AAC TAC CAG GCG AAC ATC TGG GCT TTG AAG GAA GAG GGC TGT ACA CAT
73 N  Y  Q  A  N  I  W  A  L  K  E  E  G  C  T  H  88
GTC ATA GTG ACC ACA GCT TGT GGC TCC TTG AGG CAG GAG ATT CAG CCC
89 V  I  V  T  T  A  C  G  S  L  R  E  E  I  Q  P 104
GGC GAT ATT GTC ATT ATT GAT CAG TTC ATT GAC AGG ACC ACT ATG AGA
105 G  D  I  V  I  I  D  Q  F  I  D  R  T  T  M  R 120
CCT CAG TCC TTC TAT GAT GGA AGT CAT TCT TGT GCC AGA GGA GTG TGC
121 P  Q  S  F  Y  D  G  S  H  S  C  A  R  G  V  C 136
CAT ATT CCA ATG GCT GAG CCG TTT TGC CCC AAA ACG AGA GAG GTT CTT
137 H  I  P  M  A  E  P  F  C  P  K  T  R  E  V  L 152
ATA GAG ACT GCT AAG AAG CTA GGA CTC CGG TGC CAC TCA AAG GGG ACA
153 I  E  T  A  K  K  L  G  L  R  C  H  S  K  G  T 168
ATG GTC ACA ATC GAG GGA CCT CGT TAT AGC TCC CGG GCA GAA AGC TTC
169 M  V  T  I  E  G  P  R  Y  S  S  R  A  E  S  F 184
ATG TTC CGC ACC TGG GGG GCG GAT GTT ATC AAC ATG ACC ACA GTT CCA
185 M  F  R  T  W  G  A  D  V  I  N  M  T  T  V  P 200
GAG GTG GTT CTT GCT AAG GAG GCT GGA ATT TGT TAC GCA AGT ATC GCC
201 E  V  V  L  A  K  E  A  G  I  C  Y  A  S  I  A 216
ATG GCG ACA GAT TAT GAC TGC TGG AAG GAG CAC GAG GAA GCA GTT TCG
217 M  A  T  D  Y  D  C  W  K  E  H  E  E  A  V  S 232
GAC GAC CGG GTC TTA AAG ACC CTC AAA GAA AAC GCT AAT AAA CCC AAA
233 V  D  R  V  L  K  T  L  K  E  N  A  N  K  A  K 248
AGC TTA CTG CTC ACT AGC ATA CCT CAG ATA GGG TCC ACA GAA TGG TCA
249 S  L  L  L  T  T  I  P  Q  I  G  S  T  E  W  S 264
GAA ACC CTC CAT AAC CTG AAG AAT ATG GCC CAG TTT TCT GTT TTA TTA
265 E  T  L  H  N  L  K  N  M  A  Q  F  S  V  L  L 280
CCA AGA CAT TAA AGTAGCATGGCTGCCCAGGAGAAAAGAAGACATTCTAATTCCAGTCA
281 P  R  H
TTTTGGCAATTCCTGCTTAACTTGAAAAAAATATGGGAAAGACATGCAGCTTTCATGCCCTTGCC
TATCAAAGAGTATGTTGTAAGAAAGACAAGACATTGTGTGTATTAGAGACTCCTGAATGATTTAG
ACAACTTCAAAATACAGAAGAAAAGCAAATGACTAGTAAACATGTGGGAAAAAATATTACATTTT
AAGGGGGAAAAAAAAAAACCCCACCATTCTCTTCTCCCCCTATTAAATTTGCAACAATAAAGGGTG
GAGGGTAATCTCTACTTTCCTATACTGCCAAAGAATGTGAGGAAGAAATGGGACTCTTTGGTTA
TTTATTGAGCGACTGTAAATTGGTACAGTATTCTGGAGGCAATTGGTAAAATGCATCAAAA
GACTTAAAAATACGCACGTCCTTTGGTGCTGGGAACTCTACATCTAGCAATTTCTCTTTAAAACC
ATATCAGAGATGCATACAAGAATTATATATAAGAAAGGGTGTTAATAATGATAGTTATAATA
ATAAATAATTGAAACAATCTGAATCCCTTGCAATTGGAGGTAAATTATGTCTTAGTTATAATCTA
GATTGTGAATCAGCCAACTGAAATCCCTTTTGCATATTTCAATGTCCTAAAAAGACACGGTTG
CTCTATATATGAAGTGAAAAAAGGTATGGTAGCATTTTATAGTACTAGTTTTGCTTTAAAATGC
TATGTAAATATACAAAAAAACTAGAAAGAAATATATATAACCTTGTTATTGTATTTGGGGGAGGG
ATACTGGGATAATTTTTATTTTCTTTGAATCTTTCTGTGTCTTCACATTTTCTACAGTGAATAT
AATCAAATAGTAAAGGGCCGTAAAAATAAAAGTGGATTTAGAAAGATCCAGTTCTTGAAAACACT
GTTTCTGGTAATGAAGCAGAATTTAAGTGGTAATATTAAGGTGAATGTCATTTAAGGGAGTTAC
ATCTTTATTCTGCTAAAGAAGAGATCATTGATTTCTGTACAGTCAGAACAGTACTTGGGTGTGC
AACAGCTTTCTGAGAAAAGCTAGGTGTATAATAGTTTAACTGAAAGTTTAACTATTTAAAAGACT
AAATGCACATTTTATGGTATCTGATATTTTAAAAAGTAATGTGAGCTTCTCCTTTTTATGAGTTA
AATTATTTTATACGAGTTGGTAATTTGTGCCTTTTAATAAAGTGGAAGCTTGCTTTTTAAAAAAA
AAAAAAAAGCGGAATTC
```

b

```
MTAP :   12 IGIIGGTGLDDPEILEGRTEKYVDTPFGKPSDALILGKIKNVDCILLARHGRQHTIMPSK 71
RRUORF:      G.IGG.G..D...LEG.....V..PPG..SD....G.........L.RHGR.H...PS.

MTAP :   72 VNYQANIWALKEVGCTHVIVTTACGSLREEIQPGDIVIIDQFIDRTTMRPQSFYDGSHSC 131
RRUORF:     VNY.ANI.ALK..G.T......A.GSL.E...PG..VI.DQFIDRT..R..SF
HSAPNP:                  G.....VT.A.G.L......GDI..I...I.......Q....G....
MMUPNP:                  G.....VT.A.G.L......GDI..I...I.......Q....G....
SCE8167:                      IVT.A.G......Q..D...I...........Q....G....

MTAP : 132 ARGVCHIPMAEPFCPKTREVLIETAKKLGLRCHSKGTMVTIEGPRFSSRAESFMYRTWGA 191
RRUORF:
HSAPNP:     ..G.....M........R.....T.K..G...  ..GT.V...GP.F...AE.......GA
MMUPNP:     ..GV....M........R.....T.K..G.....GT.V...GP.F...AES......GA
SCE8167:    ..G..............R..L....K.L.......GT.....GF.F..RAES.M.R..G.
BSUPNP:                                      KG......GP.....AE....RT.G.
MLEPNP:                                       G......GP.....AE..M.R..GA

MTAP : 192 DVINMITVPEVVLAKEAGICYASIAMATD 220
RRUORF:                                    (54/114 identities)
HSAPNP:     D...M.TVPEV..A...G.........T   (39/135 identities)
MMUPNP:     D...M.TVPEV..A...G.........T   (40/135 identities)
SCE8167:    D...M.TVPEV..A...G.....I      ( 20/50 identities)
BSUPNP:     D...M.TV.E...A..AG.....I      ( 20/50 identities)
MLEPNP:     D...M.TV.E...A..AG.........T   ( 13/53 identities)
```

FIG. 3. (*a*) Cloning of *MTAP*. The nucleotide sequence of the *MTAP* cDNA is shown along with the deduced amino acid sequence of the MTAP protein. (*b*) Protein sequence comparison of the MTAP protein with the highest scoring protein sequences found in a BLASTP search of the protein databases. The highest homology was detected with RRUORF, which shows 47% (54 of 114) amino acid identity. The function of this protein from *R. rubrum* is not known. The homology detected with other PNPs was lower but extended over a slightly larger region in eukaryotic proteins (HSAPNP, MMUPNP, and SCE8167). Only identical amino acids are shown. Dots denote nonidentical amino acids; no gaps were introduced into the alignment. RRUORF, hypothetical 25.8-kDa protein in cytochrome c_1 (*petC*) 3′ region from *Rhodospirillum rubrum* (Swiss-Prot accession no. P23139); HSAPNP, human PNP (EC 2.4.2.1; GenBank accession no. K02574); MMUPNP, murine PNP (GenBank accession no. L11292); SCE8167, L8167.19 gene product from *S. cerevisiae* (GenBank accession no. U14913);

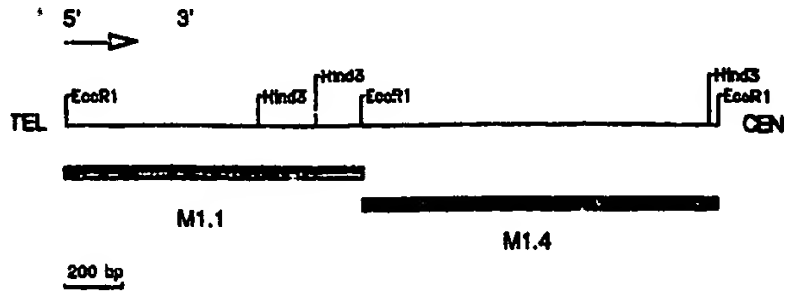

FIG. 4. Map of *MTAP* cDNA clone. Not all restriction sites are indicated.

the 25.8-kDa protein is distinct from the region of homology to the PNPs with only a minor overlap.

We correlated the presence or absence of a 1.4-kb subclone of the cDNA (probe M1.4, Fig. 4) with the presence or absence of MTAP enzyme activity in previously characterized cell lines (4, 5). This 1.4-kb probe is deleted in every cell line that lacks MTAP enzyme activity and is present in all cell lines with MTAP enzyme activity. When the 1.1-kb 5′ fragment of the cDNA probe (M1.1, Fig. 4) was used for Southern blot analysis of *Pst* I-digested human genomic DNA, four bands were seen (data not shown). One of these bands was always seen in cell lines with homozygous deletions of the 9p21 region. The M1.1 probe was then used on a somatic cell hybrid panel and found to hybridize only to human chromosomes 9 and 3. Thus, it appears that another gene or pseudogene homologous to *MTAP* maps to human chromosome 3.

DISCUSSION

The *MTAP* gene was previously localized (8) by using somatic cell hybrids. We refined the location by using information obtained from PFGE and cell lines (2, 15). Because there was no probe available for the *MTAP* gene, we concluded that the putative TSG must lie between the *IFN* gene cluster and the *MTAP* gene. By using similar reasoning, Coleman *et al.* (30) placed the SRO in melanomas centromeric to the *MTAP* gene and suggested that the SRO in melanoma was distinct from the SRO in gliomas, leukemias, and lung cancers. Barring any complex rearrangements in both T98G (glioma) and Hs294T (melanoma), we believe that the position of the TSG should be within the region defined by the homozygous deletions in these two cell lines. This region maps centromeric to *MTAP* and the *IFN* gene cluster but distal to *D9S966* and includes *CDKN2* (Fig. 1). This region corresponds to the only critical region that we have defined by using primary samples from patients with gliomas and leukemias (ref. 31 and unpublished data). The region overlaps the *MLM* locus because it maps in the 2-centimorgan region between *D9S736* and *D9S171* (9, 28). These data are consistent with recent results published by Jen *et al.* (32) who found a high frequency of homozygous deletions of *CDKN2* and *CDKN2B* in primary glioma samples. No point mutations of either gene were observed in primary gliomas.

Our long-range map covers 2.8 Mb including the *IFN* gene locus but does not reach *D9S126* or *D9S171*. There are now two reports (14, 33) of homozygous deletions on 9p that do not extend into the *CDKN2* locus. In fact, these two reports suggest that one of the other 9p TSGs is telomeric to *CDKN2*. To date, all the data available in primary tumors and tumor cell lines suggest that the preferred mechanism for gene inactivation on 9p is homozygous deletion rather than point mutations. We know of no other chromosomal region with such a high frequency of homozygous deletions. It is rather intriguing that all of the genes (the *IFN* gene cluster, *MTAP*, *CDKN2*, and

BSUPNP, *Bacillus subtilis* PNP (Protein Information Resource accession no. A42708); MLEPNP, *Mycobacterium leprae* PNP (GenBank accession no. U00022).

CDKN2B) identified thus far in this region could have some significant biological role in cancer. The most efficient way to inactivate all of these genes if they are biologically important would be by a large enough deletion. Alternatively, these genes may have been deleted as "innocent bystanders" because intrinsic fragility or recombinogenicity around the TSG may make the region a hot spot for illegitimate recombination.

It has been proposed that the inclusion of *MTAP* gene in these deletions may present an opportunity to use this phenomenon in drug development (8, 34, 35). MTAP is involved in the purine salvage pathway in which methylthioadenosine is recycled to the purine nucleotide pool. MTAP deficiency interferes with this salvage pathway. MTAP deficiency in human malignancy may permit the development of chemotherapeutic approaches in which MTAP-negative cancer cells will be selectively killed with drugs causing the depletion of purine nucleotides. This major difference between normal and malignant cells might be used to design more effective chemotherapy approaches in gliomas, lung cancer, and other solid tumors where there are currently no effective therapies. Thus, further characterization of this gene may have both diagnostic and therapeutic implications.

The data presented here support the fact that *CDKN2* is the most frequently homozygously deleted marker within 9p21 in gliomas and leukemias. However, it is apparent that it is not the only clinically relevant gene for every tumor type. Thus, it will be necessary to identify and map other candidate genes in this region. The reagents described herein should be useful in further characterization of the 9p tumor suppressor locus.

This work has benefited from discussions with many colleagues, including Drs. Janet Rowley, John Minna, Michael Lerman, and Manuel Diaz. We are grateful to Drs. Denis Le Paslier and Daniel Cohen for screening the CEPH MegaYac library; to Dr. Cannon-Albright for the *D9S736* primers information prior to publication; to Dr. Joseph Testa for the *D9S171* end-clone information; to Oncor for gridding the chromosome 9 library and for sequencing the *MTAP* cDNA clone; to Dr. Peter De Jong and the Lawrence Livermore Laboratory for the chromosome 9 flow-sorted library; to Dr. Marion Buckwalter for the pICL and pLUS vectors; to Drs. Sandra Bigner, Meenhard Herlyn, and Alan Linnenbach for providing us with tumor cell lines; and to Dr. David Beach for the *CDKN2* and *CDKN2B* cDNA probes. This research was supported by funds from the J. S. McDonnell foundation and the Cancer Center Core Grant from the National Cancer Institute (CA14599-19 to O.I.O.), U.S. Public Health Service Grant CA40046 to M.M.L.B., and Grant CA42557 and Department of Energy Grant DE-FG02-86ER60408 to Janet D. Rowley. S.G. was supported by National Institutes of Health Training Grant 5-T32GMO7183-20. M.H.D. was supported by a training grant from the Deutsche Forschungsgemeinschaft.

1. Mitelman, F. (1994) *Catalog of Chromosome Aberrations in Cancer* (Wiley/Liss, New York), 5th Ed.
2. Díaz, M. O., Zieman, S., Le Beau, M. M., Pitha, P., Smith, S. D., Chilcote, R. R. & Rowley, J. D. (1988) *Proc. Natl. Acad. Sci. USA* 85, 5259–5263.
3. Díaz, M. O., Rubin, C. M., Harden, A., Ziemin, S., Larson, R. A., Le Beau, M. M. & Rowley, J. D. (1990) *New Engl. J. Med.* 322, 77–82.
4. Olopade, O. I., Jenkins, R. B., Ransom, D. T., Malik, K., Pomykala, H., Nobori, T., Cowan, J. M., Rowley, J. D. & Diaz, M. O. (1992) *Cancer Res.* 52, 2523–2529.
5. Olopade, O. I., Buchhagen, D. L., Malik, K., Sherman, J., Nobori, T., Bader, S., Nau, M. M., Gazdar, A. F., Minna, J. D. & Díaz, M. O. (1993) *Cancer Res.* 53, 2410–2415.
6. Nobori, T., Miura, K., Wu, D. J., Lois, A. Takabayashi, K. & Carson, D. A. (1994) *Nature (London)* 368, 753–756.
7. Kamb, A., Gruis, N. A., Weaver-Feldhaus, J., Liu, Q., Harshman, K., Tavtigian, S. V., Stockert, E., Day, R. S. I., Johnson, B. E. & Skolnick, M. H. (1994) *Science* 264, 436–440.
8. Carerra, C. J., Eddy, R. L., Shows, T. B. & Carson, D. A. (1984) *Proc. Natl. Acad. Sci. USA* 81, 2665–2668.
9. Cannon-Albright, L. A., Goldgar, D. E., Meyer, L. J., Lewis, C. M., Anderson, D. E., Fountain, J. W., Hegi, M. E., Wiseman, R. W., Petty, E. M., Bale, A. E., Olopade, O. I., Diaz, M. O., Kwiatkowski, D. J., Piepkorn, M. W., Zone, J. J. & Skolnick, M. H. (1992) *Science* 265, 1148–1152.
10. Serrano, M., Hannon, G. J. & Beach, D. (1993) *Nature (London)* 366, 704–707.
11. Hannon, G. J. & Beach, D. (1994) *Nature (London)* 371, 257–259.
12. Hussussian, C. J., Struewing, J. P., Goldstein, A. M., Higgins, P. A. T., Ally, D. S., Sheahan, M. D., Clark, W. H., Jr., Tucker, M. A. & Dracopoli, N. C. (1994) *Nature Genet.* 8, 15–19.
13. Kamb, A., Shattuck-Eidens, D., Eeles, R., Liu, Q., Gruis, N. A., Ding, W., Hussey, C., Tran, T., Miki, Y., Weaver-Feldhaus, J., McClure, M., Aitken, J. F., Anderson, D. E., Bergman, W., Frants, R., Goldgar, D. E., Green, A., Maclennan, R., Martin, N. G., Meyer, L. J., Youl, P., Zone, J. J., Skonick, M. H. & Cannon-Albright, L. A. (1994) *Nature Genet.* 8, 22–26.
14. Cheng, J. Q., Jhahwar, J. S., Klein, W. M., Bell, D. W., Lee, W.-C., Altomare, D. A., Nobori, T., Olopade, O. I., Buckler, A. J. & Testa, J. R. (1994) *Cancer Res.* 54, 5547–5551.
15. Olopade, O. I., Bohlander, S. K., Pomykala, H., Maltepe, E., Nobori, T., Le Beau, M. M. & Diaz, M. O. (1992) *Genomics* 14, 437–443.
16. Weaver-Feldhaus, J., Gruis, N. A., Neuhausen, S., Le Paslier, D., Stockert, E., Skolnick, M. H. & Kamb, A. (1994) *Proc. Natl. Acad. Sci. USA* 91, 7563–7567.
17. Diaz, M. O., Pomykala, H. M., Bohlander, S. K., Maltepe, E., Malik, K., Brownstein, B. & Olopade, O. I. (1994) *Genomics* 22, 540–552.
18. Kwiatkowski, D. J. & Diaz, M. O. (1992) *Hum. Mol. Genet.* 1, 658.
19. Bohlander, S. K., Dreyling, M. H., Hagos, F., Sveen, L., Olopade, O. I. & Diaz, M. O. (1994) *Genomics* 24, 211–217.
20. Feinberg, A. P. & Vogelstein, B. (1983) *Ann. Biochem.* 132, 6–13.
21. Bohlander, S. K., Espinosa, R., Fernald, A. A., Rowley, J. D., Le Beau, M. M. & Diaz, M. O. (1994) *Cytogenet. Cell Genet.* 65, 108–110.
22. Rowley, J. D., Díaz, M. O., Espinosa, R., Patel, Y. D., van Melle, E., Ziemin, S., Taillon-Miller, P., Lichter, P., Evans, G. A., Kersey, J. H., Ward, D. C., Domer, P. H. & Le Beau, M. M. (1990) *Proc. Natl. Acad. Sci. USA* 97, 9358–9362.
23. Hermanson, G. G., Hoekstra, M. F., McElligot, D. L. & Evans, G. A. (1991) *Nucleic Acids Res.* 19, 4943–4948.
24. Buckler, A. J., Chang, D. D., Graw, S. L., Brook, D. J., Haber, D. A., Sharp, P. A. & Housman, D. E. (1991) *Proc. Natl. Acad. Sci. USA* 88, 4005–4009.
25. Lovett, M., Kere, J. & Hinton, L. M. (1991) *Proc. Natl. Acad. Sci. USA* 88, 9628–9632.
26. Altschul, S. F., Gish, W., Miller, W., Myers, E. W. & Lipman, D. J. (1990) *J. Mol. Biol.* 215, 403–410.
27. Porterfield, B. W., Diaz, M. O., Rowley, J. D. & Olopade, O. I. (1992) *Proc. Am. Assoc. Cancer Res.* 33, 72 (abstr.).
28. Povey, S. & the Utah Genome Center Genetic Marker and Mapping Group (1994) *Ann. Hum. Genet.* 58, 177–250.
29. Fountain, J. W., Karayiogu, M., Taruscio, D., Graw, S. L., Buckler, A. J., Ward, D. C., Dracopoli, N. C. & Housman, D. E. (1992) *Genomics* 14, 105–112.
30. Coleman, A., Fountain, J. W., Nobori, T., Olopade, O. I., Robertson, G. & Housman, D. E. (1994) *Cancer Res.* 54, 344–348.
31. Dreyling, M. H., Bohlander, S. K., Adeyanju, M. C. & Olopade, O. I. (1995) *Cancer Res.* 55, 984–988.
32. Jen, J., Harper, W., Bigner, S. H., Bigner, D. D., Papadoupoulos, N., Markowitz, S., Willson, J. K. V., Kinzler, K. W. & Vogelstein, B. (1994) *Cancer Res.* 54, 6353–6358.
33. Lydiatt, W. A., Murty, V. V. V. S., Davidson, B. J., Xu, L., Dyomina, K., Sacks, P. G., Schantz, S. P. & Chaganti, R. S. K. (1994) *Genes Chromosomes Cancer*, in press.
34. Della Ragione, F., Palumbo, R., Russo, G. L., Gragnaniello, V. & Zappia, V. (1992) *Biochem. J.* 281, 533–538.
35. Nobori, T., Szinai, I., Amox, D., Parker, B., Olopade, O. I., Buchhagen, D. L. & Carson, D. A. (1993) *Cancer Res.* 53, 1098–1101.

Analysis of the p16 gene (*CDKN2*) as a candidate for the chromosome 9p melanoma susceptibility locus

A. Kamb[1], D. Shattuck-Eidens[1], R. Eeles[2,3], Q. Liu[1], N. A. Gruis[1,4], W. Ding[1], C. Hussey[1], T. Tran[1], Y. Miki[2], J. Weaver-Feldhaus[1], M. McClure[1], J. F. Aitken[5], D. E. Anderson[6], W. Bergman[4], R. Frants[4], D. E. Goldgar[2], A. Green[5], R. MacLennan[5], N. G. Martin[5], L. J. Meyer[7,8], P. Youl[5], J. J. Zone[7], M. H. Skolnick[1,2] & L. A. Cannon-Albright[7]

[1]*Myriad Genetics, Inc., 421 Wakara Way, Salt Lake City, Utah 84108, USA*
[2]*Department of Medical Informatics, University of Utah Medical Center, Salt Lake City, Utah 84108, USA*
[3]*CRC Academic Unit of Radiotherapy, Royal Marsden Hospital and Institute for Cancer Research, Sutton, Surrey, SM2 5PT, UK*
[4]*MGC-Department of Human Genetics and Department of Dermatology, Leiden University, Leiden, The Netherlands*
[5]*Queensland Institute of Medical Research, Brisbane, Queensland 4029, Australia*
[6]*Department of Molecular Genetics, The University of Texas M.D. Anderson Cancer Center, Houston, Texas 77030, USA*
[7]*Department of Internal Medicine, University of Utah School of Medicine, Salt Lake City, Utah 84132, USA*
[8]*Geriatric Research Education and Clinical Center, Veteran's Administration Medical Center, Salt Lake City, Utah 84148, USA*

Correspondence should be addressed to A.K.

A locus for familial melanoma, *MLM*, has been mapped within the same interval on chromosome 9p21 as the gene for a putative cell cycle regulator, $p16^{INK4}$ (*CDKN2*) MTS1. This gene is homozygously deleted from many tumour cell lines including melanomas, suggesting that *CDKN2* is a good candidate for *MLM*. We have analysed *CDKN2* coding sequences in pedigrees segregating 9p melanoma susceptibility and 38 other melanoma-prone families. In only two families were potential predisposing mutations identified. No evidence was found for heterozygous deletions of *CDKN2* in the germline of melanoma-prone individuals. The low frequency of potential predisposing mutations detected suggests that either the majority of mutations fall outside the *CDKN2* coding sequence or that *CDKN2* is not *MLM*.

Susceptibility to melanoma has a significant genetic component, apart from skin coloration and melanin composition. A locus responsible for melanoma predisposition, *MLM*, has been mapped to a 2 centiMorgan (cM) interval in chromosome 9p21 between *D9S171* and *D9S736* (refs 1–5). This locus is believed to act as a somatically recessive tumour suppressor gene in the manner originally proposed by Knudson[6]. Inheritance of a single defective *MLM* allele predisposes to melanoma, while somatic loss or mutation of the second allele completes one of the steps necessary for development of malignancy. Based on this two-step model for carcinogenesis, somatic mutations are predicted to occur in neoplastic cells at the location of *MLM*.

Consistent with this view, chromosome 9p21 is the site of frequent somatic chromosomal aberrations in tumour cells and cell lines. Nearly 60% of melanoma tumour cell lines have homozygous deletions in 9p21, a finding that strongly suggests the presence of a tumour suppressor gene in 9p21 (ref. 7). Recently, a gene named *CDKN2* was localized within the deleted region[8–9]. *CDKN2* encodes a protein, p16, previously identified by its ability to bind and inhibit cyclin-dependent kinases (CDKs) *in vitro*[10]. CDKs, along with their associated positive regulatory factors, the cyclins, are principal determinants of the decision to initiate DNA replication and mitosis (for review, see ref. 11). As it encodes a putative inhibitor of cell division, *CDKN2* has the hallmarks of a tumour suppressor gene.

CDKN2 consists of three coding exons: exon 1 (E1) containing 125 bp, exon 2 (E2) 307 bp and exon 3 (E3) just 12 bp[8]. *CDKN2* is deleted homozygously in a wide variety of tumour cell lines, including melanomas[8,9]. In addition, a high percentage of melanoma lines that do not contain homozygous deletions contain smaller hemizygous genetic lesions in either E1 or E2 of *CDKN2* such as frameshift, nonsense and missense mutations[8]. Similar mutations are seen in primary and metastatic melanomas (N.A.G. *et al.*, manuscript submitted). These results suggest that *CDKN2* is involved in formation of melanomas and, as such, is an appealing candidate for *MLM*. To test whether or not *CDKN2* is *MLM*, we have examined *CDKN2* for mutations that segregate with predisposition in melanoma-prone families.

Analysis of *CDKN2* in 9p21-linked families

Individuals belonging to melanoma-prone families that show evidence of 9p21-linked susceptibility were screened for predisposing mutations in *CDKN2* (Table 1). Eight of these families were American (7 from Utah, 1 from Texas[12]), exhibiting a combined multipoint lod score of +12.8 for localization between the 9p21 markers *IFNA* and *D9S126* (ref. 1). Five Dutch families with a combined lod score of +3.52 for *D9S171* were also examined[3]. Although in some kindreds the lod scores are low, or slightly negative, each kindred showed significant haplotype sharing among melanoma cases for the *IFNA–D9S126* region (Table 1), and were thus considered putative 9p-linked kindreds.

For all samples the same screening strategy was used: The entire coding sequence of *CDKN2* including adjacent splice junctions was amplified in three parts corresponding to E1, E2 and E3, using oligonucleotide primers flanking the exons. DNA sequence analysis from the various samples revealed three heterozygous nucleotide substitutions in E2 among the eight American probands. (No *CDKN2*

Table 1 Evidence for 9p linkage in putative 9p-linked kindreds

Nationality	Kindred	Lod score	Cases total (n)	Cases with haplotype (n)
American	3346	5.97	21	21
	1771	3.57	12	12
	3137	1.90	17	16
	1764	1.04	4	4
	3012	0.64	4	4
	3006	0.19	6	3
	3343	–0.53	10	8
	3161	–0.01	10	8
Dutch	4	1.22	6	6
	10	0.97	5	5
	1	0.95	4	4
	6	0.62	4	4
	3	–0.24	5	4

The lod scores were calculated for marker *D9S171* in Dutch families, and between markers *IFNA* and *D9S126* in American families.

sequence differences were detected in the Dutch individuals.) The three mutations detected in the American individuals were single nucleotide, missense mutations. One, in kindred 3012 (Gly93Trp), resulted in the substitution of a small, neutral amino acid by a large hydrophobic residue. Another, in kindred 1771 (Val118Asp), involved the replacement of a small hydrophobic residue by an acidic residue. The third variant, in kindred 3343 (Ala140Thr), involved a more conservative substitution.

Thirty-eight additional affected individuals (28 from Utah, ten from Australia) with a positive family history for melanoma from kindreds that had not been tested for 9p linkage were also screened for *CDKN2* mutations. The 28 Utah kindreds consisted of 26 with an average of more than three melanoma cases per kindred (range 2–10 cases), and two kindreds with one melanoma case and two or more cases of dysplastic nevus syndrome, a condition characterized by frequent occurrence of abnormal skin moles[3]. The ten Australian kindreds were ascertained for a significant excess of melanoma cases and have an average of more than three melanoma cases per kindred (range 3 to 4 cases)[13]. E1 and E2 were amplified from the genomic DNA of these individuals and subjected to DNA sequence analysis. No further polymorphisms were observed.

Population frequency of *CDKN2* substitutions

To test whether or not the missense substitutions observed in the melanoma-prone individuals were common polymorphisms, a population frequency analysis was conducted in unrelated individuals who had married into high risk cancer kindreds studied in Utah, but who themselves had no apparent increased risk of cancer. Genomic DNA from this normal set was used to amplify the E2 fragment from *CDKN2*. These fragments were probed with allele-specific oligonucleotides (ASOs) designed to detect each of the three missense changes. Two of the variants (Gly93Trp, Val118Asp) were not detected in the set of 100 normal samples, while the third (Ala140Thr) was present in 6/163 of the samples. These results suggest that the Ala140Thr missense change is a moderately common polymorphism present in roughly 4% of the Utah population and is unlikely to be a predisposing mutation. The other two missense mutations were rare in the normal population and were, therefore, candidates for predisposing mutations.

To determine whether the Gly93Trp and Val118Asp substitutions were present in other familial melanoma cases and in sporadic melanoma cases, we performed further ASO experiments. Thirty affected individuals (for Val118Asp) and 51 (for Gly93Trp) with positive family histories for melanoma from Australian families in which linkage analysis had not been performed were screened for these mutations. Also, 66 affected individuals (for Val118Asp) and 20 (for Gly93Trp) with unknown family history from Utah and Australia were analysed. No other occurrences of the mutations were detected, suggesting that they are rare in familial and sporadic melanoma cases.

Segregation analysis of *CDKN2* mutations

If the Gly93Trp and Val118Asp mutations are predisposing, they should segregate with melanoma susceptibility in the respective kindreds. To test linkage to the chromosome carrying the melanoma predisposition in kindreds 3012 and 1771, genomic DNA from available related individuals in each kindred was used to amplify E2 sequences for DNA sequence or ASO analysis. In both kindreds, the mutations were present in the *MLM* carrier individuals and not in noncarriers, demonstrating cosegregation of *MLM* with the two mutations (Fig. 1). This finding is consistent with the possibility that these two missense mutations Gly93Trp in family 3012 and Val118Asp in family 1771 may be predisposing *MLM* mutations.

Analysis of *CDKN2* germline deletions

Large germline deletions are the exception rather than the rule in familial cancers. Nevertheless, the prevalence in tumour cell lines of *CDKN2* homozygous deletions, some of which stretch several megabases, suggested that hereditary predisposition to melanoma might involve germline deletions in melanoma-prone families[7,14]. To test this possibility, probands and relatives from seven American 9p21-linked families and 21 unrelated individuals from 18 Utah melanoma kindreds were examined. Southern blots were prepared using genomic DNA digested with *Bam*HI or *Pvu*II. The blots were probed with cosmid c5, a cosmid that includes E1 and E2 of *CDKN2* and E2 from a related gene, *MTS2*. The blots revealed the presence of restriction fragment length polymorphisms (RFLPs) that could distinguish one homologue from the other in this region (Fig. 2 shows *Bam*HI digests). These RFLP patterns were interpreted as allele types and their frequencies determined.

If a significant fraction of the samples contained large heterozygous deletions of this region, the distribution of homozygotes compared to heterozygotes should deviate from the distribution predicted by the Hardy-Weinberg law. The observed gene frequencies for the rarer allele were 0.40 for the *Bam*HI polymorphism and 0.18 for the *Pvu*II polymorphism. In each case, the genotype frequencies fit the Hardy-Weinberg equilibrium (χ^2 $p = 0.98$ and $p = 0.60$, respectively). This suggests that the region does not contain large deletions in a significant fraction of melanoma-prone kindreds. Moreover, no

RFLPs other than the two allelic types were detected. This excludes the possibility of smaller deletions on the order of tens to thousands of base pairs which would have generated novel restriction fragments within the set of fragments detected by cosmid c5.

Discussion

So far, ten familial cancer genes have been cloned and characterized[15]. In each case where the gene has been analysed extensively, it is involved in sporadic cancer, as well as in hereditary cancer. For example, mutant forms of *p53* cause a proportion of the rare familial Li-Fraumeni cancer syndrome, while *p53* is mutated in nearly 50% of sporadic human cancers[16] Similarly, a gene that contributes to hereditary melanoma such as *MLM* is expected to be mutated in some sporadic cancers as well. *MLM* maps to a region that may encompass over a megabase in chromosomal region 9p21. *CDKN2*, deleted homozygously or mutated in nearly 75% of melanoma cell lines, maps within the same interval and is, therefore, an ideal candidate for *MLM*.

In a search for predisposing mutations in 9p-linked melanoma-prone families, we have found two potential *CDKN2* mutations. Both were linked to the carrier chromosome and neither was detected in the normal population. Neither involved a conservative amino acid substitution. Thus, these two mutations satisfy several important criteria for predisposing mutations. In addition, a previous study reported a nonsense mutation in a lymphoblastoid cell line derived from an individual with dysplastic nevus syndrome[9]. However, this finding is based on the analysis of DNA from cultured cells and it is unknown whether or not the mutation was present in the germline of the individual. In our screen of *MLM*-linked pedigrees, no unquestionably disruptive *CDKN2* mutations such as nonsense or frameshift mutations were found. This finding contrasts with the observation of point mutations in melanoma cell lines where 11/18 changes from the wildtype sequence caused premature termination of the p16 protein[8].

Could the two missense mutations detected in kindreds 1771 and 3012 be neutral? The p16 protein encoded by *CDKN2* consists of four tandemly repeated ankyrin motifs that together account for 88% of the total sequence[10]. Both the putative Gly93Trp and Val118Asp mutations disrupt the ankyrin repeat consensus. In contrast, the Ala140Thr substitution (also found in healthy individuals) lies outside the ankyrin domains. This is consistent with the rare mutations affecting p16 function, and the common polymorphism having no effect. On the other hand, the p16 protein is only 148 residues long, which implies a large surface to volume ratio, increasing the probability that an amino-acid change would occur on the exterior of the protein, and hence, be less disruptive to the folded state of the molecule. Therefore, in the absence of biochemical or structural information, the possibility that the two rare missense mutations are neutral cannot be excluded.

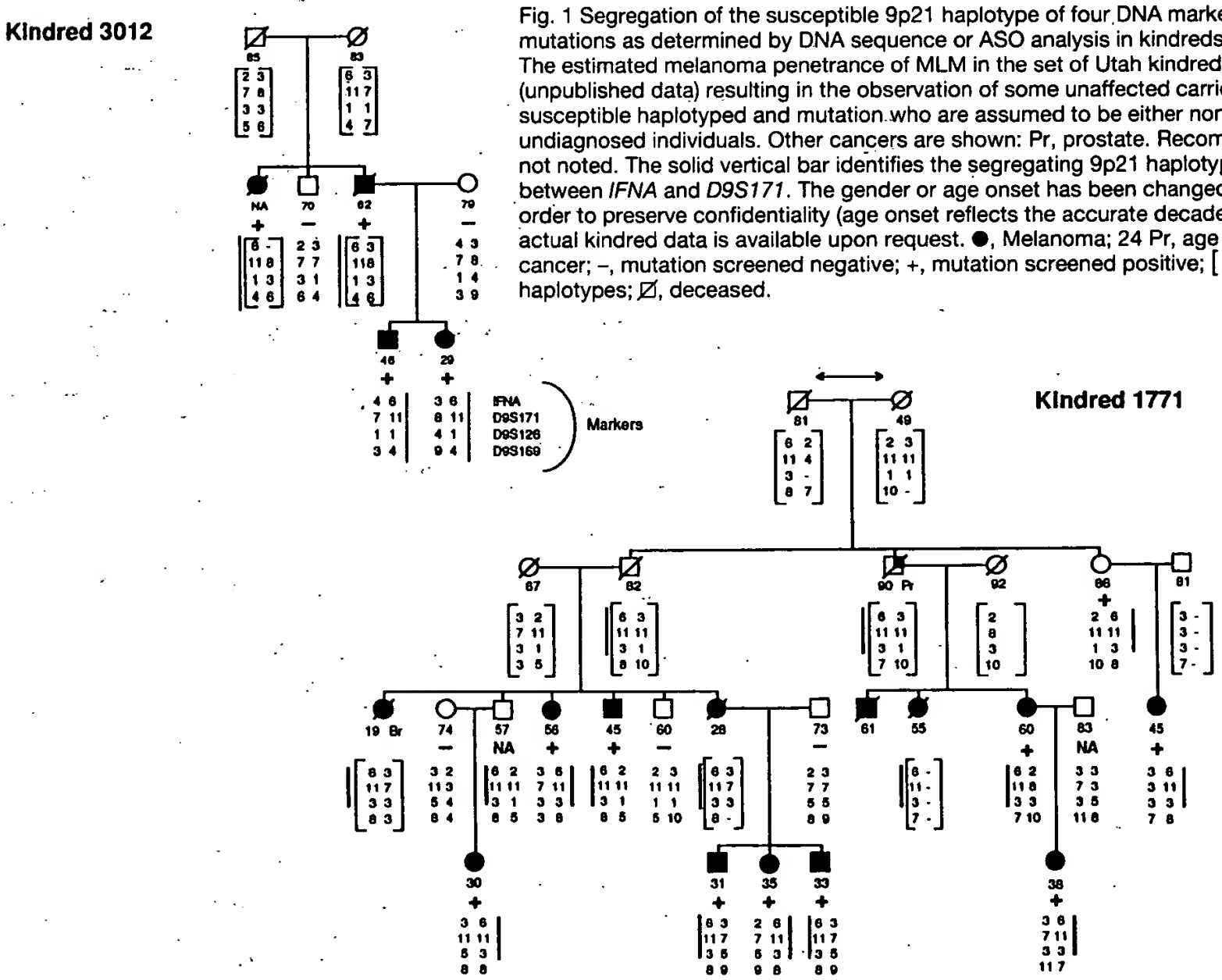

Fig. 1 Segregation of the susceptible 9p21 haplotype of four DNA markers and the *CDKN2* mutations as determined by DNA sequence or ASO analysis in kindreds 3012 and 1771. The estimated melanoma penetrance of MLM in the set of Utah kindreds is 53% by age 80 (unpublished data) resulting in the observation of some unaffected carriers of the susceptible haplotyped and mutation who are assumed to be either non-penetrant or undiagnosed individuals. Other cancers are shown: Pr, prostate. Recombinant events are not noted. The solid vertical bar identifies the segregating 9p21 haplotype; *MLM* maps between *IFNA* and *D9S171*. The gender or age onset has been changed in some cases in order to preserve confidentiality (age onset reflects the accurate decade in all cases). The actual kindred data is available upon request. ●, Melanoma; 24 Pr, age diagnosis, other cancer; –, mutation screened negative; +, mutation screened positive; [ ], inferred haplotypes; ⊘, deceased.

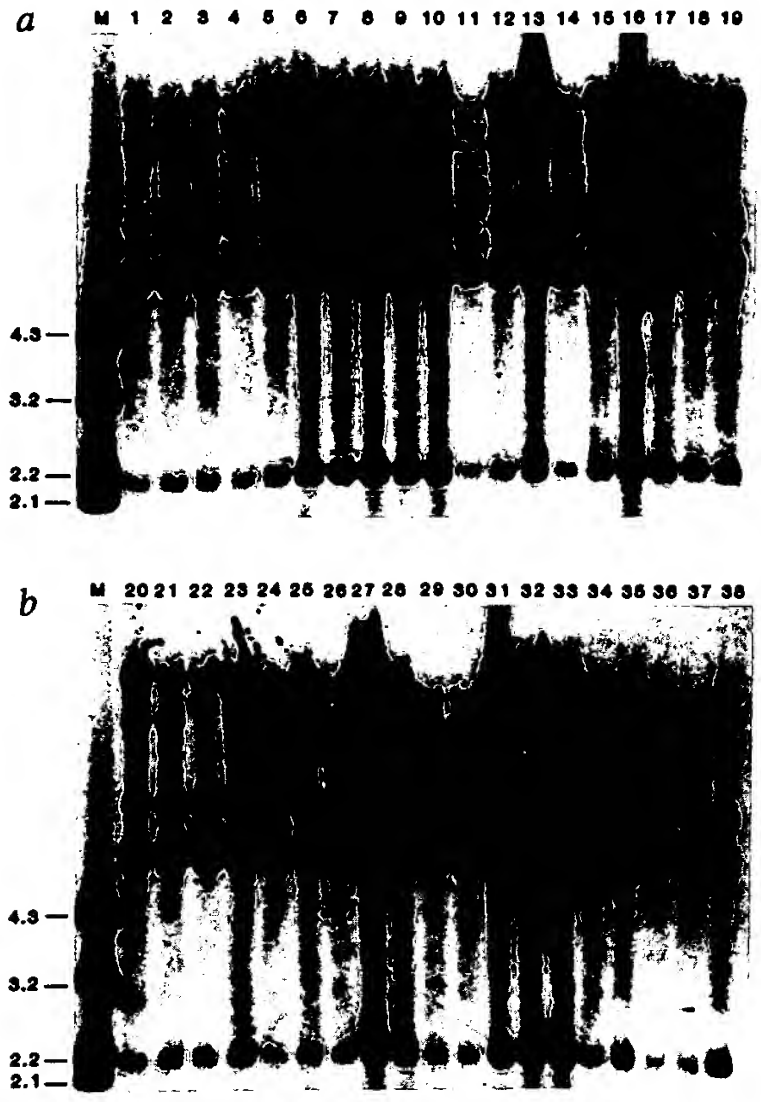

Fig. 2 Autoradiograph of Southern blot probed with cosmid c5. *a*, Lanes 2 and 6 are control DNA samples from noncarriers. *b*, Lanes 3 and 4 are control DNA samples from noncarriers. 5 μg genomic DNA was digested with *Bam*HI and loaded onto a 0.7% agarose gel. Lanes other than the control lanes contain DNA from either 9p-linked, predisposition carriers or from affected individuals from melanoma-prone families. Genotypes were assigned as Aa for lane 1, aa for lane 5, and AA for lane 9, for example; A is the rarer allele.

Regardless of whether or not these changes are neutral, the frequency of *CDKN2* mutations observed in melanoma-prone kindreds was much lower than would be expected if *CDKN2* were *MLM*: 2/13 in 9p21-linked families and 0/38 in familial melanoma cases while it is possible that not all 13 kindreds are linked, several of these kindreds have been shown previously to segregate a locus for melanoma predisposition at 9p21 with a high degree of statistical confidence. For example, kindreds 3346 and 3137 have lod scores in favour of 9p21 linkage of +5.97 and +1.90, respectively[1]. Evidence for genetic heterogeneity in melanoma predisposition involving a 1p locus has been presented[4,17,18]. However, there is no evidence in Utah, Dutch and Australian families for 1p-linkage or genetic heterogeneity in melanoma predisposition[1,19–23]. Even allowing for sporadic melanoma incidence and genetic heterogeneity, the frequency of germline *CDKN2* mutations is low.

There are two possible explanations for the low frequency of *CDKN2* mutations observed: either *CDKN2* and *MLM* are distinct genes or *CDKN2* is *MLM*, but the majority of predisposing mutations occur outside the p16 coding region and adjoining splice junction sequences. The authors of two recent reports argue that a second tumour suppressor gene may lie in 9p21 based on analysis of several non-melanoma primary tumours and that homozygous deletions of *CDKN2* in tumour cell lines may be partly an artifact of growth in culture[24,25]. However, other studies do not support this possibility[26,27]. Because of its *a priori* strength as a candidate, it is difficult to exclude *CDKN2* categorically and conclude that *MLM* is a different gene in 9p21. The precedent is compelling that in transformed cells somatic lesions occur in tumour suppressor genes, some alleles of which predispose to cancer. In the case of *CDKN2*, the homozygous deletion frequencies of individual members of a set of markers from 9p21 peak within the *CDKN2* gene[8]. The only other candidate gene identified so far in the immediate vicinity of *CDKN2* is its relative, *MTS2*. E2 sequences of this gene have been exhaustively screened for mutations in both pedigrees and melanoma lines[8]. The only polymorphisms identified so far were common and fell in a presumptive intron well outside the equivalent of E2 from *MTS2*. Thus, based on homozygous deletions in tumour cell lines and DNA sequence analysis, there is no evidence that *MTS2* or any other gene is involved. In contrast, the high frequency of point mutations and small deletions in *CDKN2* in melanoma primary tumours and cell lines further pinpoints *CDKN2* as a tumour suppressor gene involved in melanoma.

Apart from the present findings, the only indication that *CDKN2* may not correspond to *MLM* is based on the observation that somatic abberations in *CDKN2* are involved in diverse types of cancer cell lines, not only melanoma. Thus, predisposing *CDKN2* mutations might be expected to increase the occurrence of many cancer types in linked families. Indeed, some investigators have reported increased incidence of other tumours in melanoma-prone families[28] and it is unclear at present if 9p21-linked hereditary cancer is solely melanoma, or is truly multifocal.

The other possibility is that *CDKN2* and *MLM* are the same gene, but that predisposing mutations occur primarily outside the p16 coding sequence. This possibility is weakened by the observation of so many *CDKN2* coding sequence mutations in sporadic melanoma cell lines. In the subset of melanoma cell lines that do not contain *CDKN2* homozygous deletions, nearly half (14/34) contain nonsilent changes. If it is assumed that predisposing mutations are distributed in the same manner as somatic mutations, a similar percentage of the kindreds should have displayed mutations in the *p16* coding sequence. On the other hand, there is precedent for germline mutations falling outside the coding sequences of genes. For instance, in the thalassaemias a high percentage of germline mutations occur in noncoding regions that affect either protein translation, mRNA splicing or mRNA stability[29]; and an entire class of genes involved in neuronal development or function contains trinucleotide repeats outside the coding sequence that may predispose to disease[30] Moreover, it is conceivable that heterozygous, inherited, loss-of-function mutations in *CDKN2* might be lethal due to haploinsufficiency. In this case, predisposing *CDKN2* mutations might be expected to cause reduced expression of the gene and, therefore lie more frequently in sequences that regulate the level of *CDKN2* expression.

In summary, despite the appeal of *CDKN2* as a candidate

for *MLM*, we have encountered only two mutations in the p16 coding sequence which may confer susceptibility to melanoma. To prove or disprove the hypothesis that *CDKN2* is *MLM* will require an extensive search for predisposing mutations that lie in noncoding regions of the *CDKN2* gene or in neighbouring genes.

Methodology

MLM pedigrees and DNA samples. Lymphocytes were separated from whole blood using Ficoll-Hypaque (Pharmacia) according to the manufacturer's instructions. Lymphocyte DNA was extracted using standard procedures. Similar procedures were used to extract DNA from blood samples in the Netherlands and Australia.

PCR amplification and mutation screening. All three coding exons of *CDKN2* and their associated splice sites were amplified from tumour or matched normal genomic DNA using PCR[8]. The PCR conditions were: one cycle at 95 °C (5 min); 4 cycles at 95 °C (10 s), $T_{ann.}$ = 68 °C (10 s), 72 °C (10 s); 4 cycles with $T_{ann.}$ = 66 °C; 4 cycles with $T_{ann.}$ = 64 °C; 4 cycles with $T_{ann.}$ = 62 °C; 30 cycles with $T_{ann.}$ = 60 °C. The buffer conditions were as described except that 5% DMSO was added to the reaction[7]. The products were purified from 1.0% agarose gels using Qiaex beads (Qiagen) and analysed by cycle sequencing with α-^{32}p-ATP[31]. Products were run on 6% polyacrylamide gels. All adenosine reactions were loaded side by side, followed by the cytosine reactions, etc. Detection of polymorphisms was by eye with confirmation on the other strand. The DNA sequences of the primers used for *CDKN2* amplification and sequence determination were: exon 1, amplification: 1F – CAG CAC CGG AGG AAG AAA G; 1108R – GCG CTA CCT GAT TCC AAT TC; sequencing: 1108R; exon 2, amplification: 42F – GGA AAT TGG AAA CTG GAA GC; 551R – TCT GAG CTT TGG AAG CTC T; sequencing: 42F and 551R; exon 3, amplification 237F – CCA TTG CGA GAA CTT TAT CC; 654R – TGG ACA TTT ACG GTA GTGGG; sequencing: 237F and 654R.

Allele-specific oligonucleotide (ASO) analysis. PCR products were generated as described above and quantified after electrophoresis through 2% agarose gels plus ethidium bromide by comparison with known amounts of standard DNA. 10 µl PCR product was added to 110 µl of denaturant (7.5 ml, H_2O, 6.0 ml 1 N NaOH, 1.5 ml 0.1% bromophenol blue and 75 µl 0.5m EDTA) and incubated for 10 min at room temperature before blotting 30 µl on to Hybond membrane (Amersham) using a dot-blotting apparatus (GIBCO-BioRad). The DNA was fixed on the membrane by exposure to UV light (Stratagene). Prehybridization was carried out at 45 °C in 5× SSPE and 2% SDS[30]. Wildtype and mutant ASOs were labelled by incubation at 37 °C for 10 min in a reaction that included 50 µC$_i$ γ-^{32}p-ATP, 100 ng ASO, 10 U T4 polynucleotide kinase (New England Biolab), and kinase buffer. 20 ng of labelled ASO was used in an overnight hybridization reaction in the same buffer as for prehybridization. Each blot was washed twice in 5×SSC and 0.1% SDS for 10 min at room temperature, followed by 30 min at progressively higher temperatures until nonspecific hybridization signals were eliminated. Blots were exposed typically for 40 min without an intensifying screen. The ASOs used are shown below. The wild type sequence is listed with the mutant base shown in parentheses following the base that it replaces in the wildtype sequence.

Base change location	Amino acid location	DNA sequence
436	140	AGA TGC CG(A)C GGA AGG
294	93	GGG CCG(T) GGG CGC
371	118	CGA TGT(A) CTC ACG GTA

Southern blots. 5 µg genomic DNA from each individual were digested with *Bam*HI or *Pvu*II and loaded onto a 0.7% agarose gel which was blotted according to standard procedures[31]. Cosmid c5 DNA was labelled by random hexamer priming[31]. Prehybridization, hybridization and filter washing were as described[32], except that 200 ng ml^{-1} total human DNA was added to the prehybridization reaction and incubated overnight.

Acknowledgements

We thank Marguerite Jost, Deborah Harrison and Sue Healey for collection of family data. This work was supported in part by NIH grants CA48711, CA42014, CN 05222, and RR00064; and by National Health and Medical Research council projects grants 870774 and 900536 and a Queensland Cancer Fund research grant.

Received 6 June; accepted 8 August 1994.

1. Cannon-Albright, L.A. *et al.* Assignment of a locus for familial melanoma MLM, to chromosome 9p13–22. *Science* **258**, 1148–1152 (1992).
2. Nancarrow, D.J. *et al.* Confirmation of chromosome 9p linkage in familial melanoma. *Am. J. hum. Genet.* **53**, 936–942 (1993).
3. Gruis, N.A. *et al.* Linkage analysis in Dutch familial atypical multiple mole-melanoma (FAMMM) syndrome families. Effect on naevus count. *Melanoma Res.* **3**, 271–277 (1993).
4. Goldstein, A.M. *et al.* Linkage of cutaneous malignant melanoma/dysplastic nevi to chromosome 9p, and evidence for genetic heterogeneity. *Am. J. hum. Genet.* **54**, 489–496 (1994).
5. Cannon-Albright, L.A. *et al.* Localization of the 9p melanoma susceptibility locus to a 2cM region between D9S736 and D9S171. *Genomics* (in the press).
6. Knudson, A.G. Mutation and cancer: statistical study of Retinoblastoma. *Proc. natn. Acad. Sci. U.S.A.* **68**, 820–823 (1971).
7. Weaver-Feldhaus, J. *et al.* Localization of a putative tumor suppressor gene using homozygous deletion breakpoints in melanomas. *Proc. natn. Acad. Sci. U.S.A.* **91**, 7563–7567 (1994).
8. Kamb, A. *et al.* A cell cycle regulator potentially involved in genesis of many tumor types. *Science* **264**, 436 (1994).
9. Nobori, T. *et al.* Deletions of the cyclin-dependent kinase-4 inhibitor gene in multiple human cancers. *Nature* **368**, 753 (1994).
10. Serrano, M., Hannon, G.J. & Beach, D. A new regulatory motif in cell-cycle control causing specific inhibition of cyclin D/CDK4. *Nature* **366**, 704, (1993).
11. Sherr, C.J. Mammalian G1 cyclins. *Cell* **73**, 1059–1065 (1993).
12. Anderson, D.E. & Badzioch, M.D. Hereditary cutaneous malignant melanoma: A 20-year family update. *Anticancer Res.* **11**, 433–438 (1991).
13. Aitken, J.F. *et al.* Heterogeneity of melanoma risk in families of melanoma patients. *Am. J. Epidem.* (in the press).
14. Fountain, J.W. *et al.* Homozygous deletions within human chromosome band 9p21 in melanoma *Proc. natn. Acad. Sci. U.S.A.* **89**, 10557–10561 (1992).
15. Knudson, A.G. All in the (cancer) family. *Nature Genet.* **5**, 103–104 (1993).
16. Harris, C.C. p53: at the cross roads of molecular carcinogenesis and risk assessment. *Science* **262**, 1980 (1993).
17. Goldstein, A.M. *et al.* Further evidence for a locus for cutaneous malignant melanoma-dysplastic nevus (CMM/DN) on chromosome 1p, and evidence for genetic heterogeneity. *Am. J. hum. Genet.* **52**, 537–550 (1993).
18. Bale, S.J. *et al.* Mapping the gene for hereditary cutaneous malignant melanoma-dysplastic naevus to chromosome 1p. *New Engl. J. Med.* **320**, 1367–1372 (1989).
19. Cannon-Albright, L.A. *et al.* Evidence against the reported linkage to the cutaneous melanoma-dysplastic naevus syndrome locus to chromosome 1p36. *Am. J. hum. Genet.* **46**, 912–918 (1990).
20. Gruis, N.A., Bergman, W. & Frants, R.R. Locus for susceptibility to melanoma on chromosome 1p. *New Engl. J. Med.* **322**, 853–854 (1990).
21. Kefford, R.F., Salmon, J., Shaw, H.M., Donald, J.A. & McCarthy W.H. Hereditary melanoma in Australia: variable association with dysplastic naevi and absence of genetic linkage to chromosome 1p. *Cancer Genet. Cytogenet.* **51**, 45–55 (1991).
22. Nancarrow, D.J. *et al.* Exclusion of the familial melanoma locus (MLM) from the PND/D1S47 and LMYC regions of chromosome arm 1p in 7 Australian pedigrees. *Genomics* **12**, 18–25 (1992).
23. van Haeringen, A. *et al.* Exclusion of the dysplastic naevus syndrome (DNS) locus from the short arm of chromosome 1 by linkage studies in Dutch families. *Genomics* **5**, 61–64 (1989).
24. Cairns, P. *et al.* Rate of p16 (MTS1) mutations found in primary tumors with 9p loss. *Science* **265**, 415–416 (1994).
25. Spruck, C.H. III *et al.* p16 gene in uncultured tumours. *Nature* **370**,183–184 (1994).
26. Takahiro, M. *et al.* Frequent somatic mutation of the MTS1/CDK4I (multiple tumor suppressor/cyclin-dependent kinase 4 inhibitor) gene in esophageal squamous cell carcinoma. *Cancer Res.* **54**, 3396–3397 (1994).
27. Kamb, A. *et al.* Response to rate of p16 (MTS1) "Rate of mutations found in primary tumors with 9p loss". *Science* **265**, 416–417 (1994).
28. Bergman, W., Palan, A. & Went, L.N. Clinical and genetic studies in six Dutch kindreds with Dysplastic Naevus Syndrome. *Ann. hum. Genet.* **50**, 249–258 (1986).
29. Cai, S.P. *et al.* Two novel beta-thalassemia mutations in the 5' and 3' noncoding regions of the beta-globin gene. *Blood* **79**, 1342–1346 (1992).
30. Randall, T. Triplet repeat mutations: amplification within pedigrees generates three human diseases. *J. Am. med. Assoc.* **269**, 558 & 562 (1993).
31. Sambrook, J., Fritsch, E.F., & Maniatis, T. *Molecular cloning: a laboratory manual* (Cold Spring Harbor Laboratory Press, Plainview, New York, 1989).
32. Miki, Y. *et al.* Disruption of the *APC* gene by a retrotransposal insertion of L sequence in a colon cancer. *Cancer Res.* **52**, 643–645 (1992).

US 086743111AP1

Creation date: 09-02-2004
Indexing Officer: AWILSON2 - ANDREA WILSON
Team: OIPEBackFileIndexing
Dossier: 08674311

Legal Date: 06-13-2002

No.	Doccode	Number of pages
1	AP.B	39
2	AF/D	8
3	AF/D	8
4	AF/D	7
5	AF/D	6
6	AF/D	12
7	AF/D	15
8	AF/D	9
9	AF/D	8
10	AF/D	4
11	AF/D	50
12	AF/D	11

Total number of pages: 177

Remarks:

Order of re-scan issued on .....